
NAWI Graz
Natural Sciences


TU
Graz

AFFIDAVIT

I declare that I have authored this thesis independently, that I have not used other than the declared sources/resources, and that I have explicitly indicated all material which has been quoted either literally or by content from the sources used. The text document uploaded to TUGRAZonline is identical to the present master‘s thesis.

Date

Signature

Acknowledgement

As this thesis would never be possible without the help and support from a lot of people, I would like to recognize the invaluable assistance that you all provided during my study.

First of all, I would like to express my gratitude to my supervisors Dr. Alexander Deutsch and Julia Feichtinger, PhD of the Medical University of Graz for their useful comments, remarks and engagement through the learning process of this master thesis, helping me whenever it was necessary and guiding me through each stage of the process.

Furthermore, I would like to acknowledge the members of my working group, whose contribution was a big help. I want to thank Katrin Pansy, Timna Bergmann, Tanja Schukoff, Julia Unterluggauer and Karoline Fechter not only for their professional input and knowledge, but also for the funny conversations and the entertainment between long incubation times.

Additionally, I wish to acknowledge the support of all my friends and master course colleagues, especially Lisa Auinger, Max Schinagl and Jürgen Gindlhuber, who provided me a lot of information and made the master course an intensive time of joyful memories.

Finally, I like to pay my special regards to my family Ingrid, Dieter, Iris and Philipp and my partner Johanna Windisch, who have assisted me throughout the entire process, both by helping me putting pieces together and keeping me going on. Without them this thesis would not have been possible. Thank you.

Abstract

Background: Diffuse large B cell lymphoma and Burkitt lymphoma belong to the group of non-Hodgkin-lymphomas and represent lymphomas with an aggressive clinical course. The fact, that their incidence is increasing and that one third of patients relapses, indicates the need for novel therapeutic intervention. Tested in different types of cancer i.e. glioblastoma, fasting is becoming an efficient combination tool to enhance the sensibility to chemotherapeutics and to reduce side effects according to the differential stress sensibility and resistance theory.

Aims: The aim of this master thesis was to investigate if fasting effects the growth inhibitor activity of the BTK-inhibitor Ibrutinib in aggressive lymphoma cell lines. Furthermore, activation of BCR signalling pathways, especially the NF-κB, PI3K/Akt and MAPK pathway, was studied under fasting conditions.

Methods: We fasted two different ABC-DLBCL cell lines (RI-1 and U2932), two GCB-DLBCL cell lines (SuDHL4 and Karpas-422) and two Burkitt lymphoma cell lines (Raji and BL-2) in media with reduced glucose and reduced protein concentration. After pre-fasting for 24h, the cells were treated in a range from 50μM to 0.25μM with Ibrutinib followed by cell growth assay (EZ4U) after 24h, 48h and 72h. In addition, the expression levels of known NF-κB, MAPK and PI3K target genes were determined by RQ-PCR after 24h pre-fasting. In addition, members of the NF-κB pathway were investigated by Western blot analysis. Unfasted cells served as controls.

Results: Combining fasting with Ibrutinib treatment significantly increased the cell growth inhibition compared to treatment alone of all investigated lymphoma cell lines (RI-1, U2932, SuDHL4, Karpas-422, Raji and BL-2) after 24h, 48h and 72h. The IC_{50} concentration was around 1.5-fold lower for fasted cells compared to controls. Furthermore, more cells were stained positive for Annexin V, when fasting and Ibrutinib treatment were combined. Interestingly, most fasted cell lines exhibited higher expression of NF-κB, MAPK and PI3K target genes in comparison to unfasted controls**.** Finally, Western blot analysis demonstrated that members of the NF-κB pathway were higher induced and/or higher activated by fasting.

Conclusion: Our data indicates that fasting potentiates the anticancer activity of Ibrutinib. Fasting seems to potentially activate several pathways linked to BCR signalling and therefore rendering lymphoma cells, making them more vulnerable targets to specific inhibitors. Based on our finding, the combination of dietary intervention with Ibrutinib treatment should be further taken into consideration and be investigated for anticancer therapy of aggressive lymphomas.

Zusammenfassung

Hintergrund: Diffuse großzellige B-Zell Lymphome und Burkitt Lymphome gehören zu der Gruppe der Non-Hodgkin-Lymphome und repräsentieren hier die Lymphome mit aggressivem klinischem Verlauf. Die ansteigende Inzidenz und die Tatsache, dass ein Drittel der Patienten einen Rückfall erleidet, indizieren die Notwendigkeit eines neuen therapeutischen Ansatzes. Bereits in anderen Krebsentitäten, wie z.B. dem Glioblastom, getestet fungiert Fasten als ein effektiver Kombinationsansatz um die Chemosensitivität von Chemotherapeutika zu erhöhen und Nebenwirkungen, nach den Theorien der „Different stress resistance“(DSR) und „Different stress sensitisation“(DSS), zu reduzieren.

Ziele: Das Ziel dieser Masterarbeit war die detaillierte Untersuchung der Auswirkungen von Fasten auf die wachstumshemmende Aktivität des BTK-Inhibitors Ibrutinib in aggressiven Lymphom Zelllinien. Weiters sollte die Aktivierung von BCR Signalwegen speziell der MAPK, der PI3-K/Akt und der NF-κB Signalweg unter neu etablierten Fastenbedingungen untersucht werden.

Methoden: Hierzu wurden zwei unterschiedliche ABC-DLBCL Zelllinien, RI-1 und U2932, zwei GCB-DLBCL Zelllinien, SuDHL4 und Karpas-422, und zwei Burkitt Lymphom Zelllinien, Raji und BL-2 in Medien mit reduzierte Glukose- und Proteinkonzentrationen gefastet. Nach 24 stündigem Vorfasten wurden die Zellen mit Ibrutinibkonzentrationen im Bereich von 50μM bis 0.25μM behandelt und anschließend nach 24, 48 und 72 Stunden mittels Zellwachstumstest (EZ4U) analysiert. Zusätzlich wurden Expressionslevel von bekannten NF-κB, MAPK und PI3K Zielgenen nach 24 Stunden Vorfasten mittels RQ-PCR quantifiziert. Weiters wurden die Mitglieder des NF- κB Signalweges genauer mittels Westernblot analysiert. Ungefastete Zellen wurden als Kontrollen verwendet.

Resultate: Kombiniertes Fasten mit Ibrutinibtherapie führte zu einer signifikanten Erhöhung der Zellwachstumsinhibierung verglichen mit einer reinen Ibrutinibtherapie in allen untersuchten Lymphom Zelllinien (RI-1, U2932, SuDHL4, Karpas-422, Raji und BL-2) nach 24, 48 und 72 Stunden. Die IC_{50} Konzentration war um einen Faktor 1,5x niedriger in gefasteten Zellen verglichen mit den Kontrollen. Weiters waren mehr Zellen Annexin V positiv markiert, wenn Fasten mit der Ibrutinibtherapie kombiniert wurde. Im Vergleich zu ungefasteten Kontrollen konnte gezeigt werden, dass in den meisten gefasteten Zelllinien eine erhöhte Expression der NF-κB, MAPK und PI3K Zielgene stattfindet. Schlussendlich konnte im Westerblot dargestellt werden, dass Mitglieder des NF-κB Signalweges unter Fastenbedingungen stärker aktiviert und stärker induziert werden.

Zusammenfassung: Unser Daten stellen einen Zusammenhang zwischen Fasten und der erhöhten Antikrebsaktivität von Ibrutinib fest. Es scheint das Fasten verschiedene Signalwege aktiviert und dadurch die Lymphomzellen zu einem besseren Ziel für spezifische Inhibitoren macht. Basierend auf den erhaltenen Daten sollte die Kombination von diätologischen Interventionen und einer Ibrutinibtherapie für die Therapie von aggressiven Lymphomen genauer verifiziert und analysiert werden.

Table of Contents

List of Tables

List of figures

Abbreviation

ABC	activated B-cell like
AID	activation-induced cytidine deaminase
Akt	AKT serine/threonine kinase 1
AMPK	AMP-activated protein kinase
ASHM	aberrant somatic hypermutations
ATMK	Ataxia Telangiectasia Mutated kinase
ATR	Ataxia telangiectasia and Rad3 related protein
BAFF	B-cell activating factor
Bax	BCL2 Associated X, Apoptosis Regulator
BCL2A1	BCL2 related protein A1
BCL-6,2	B-cell lymphoma
BCR	B-cell receptor
Btk	Bruton tyrosine kinase
BUB1	BUB1 mitotic checkpoint serine/threonine kinase
CCL3	C-C Motif Chemokine Ligand 3
CCL4	C-C Motif Chemokine Ligand 4
CCND2	cyclin D2
CD 19,25,40,45	cluster of differentiation 19,25,40,45
CHK1	checkpoint kinase 1
CLL	chronic lymphocytic leukemia
CLP	common lymphoid progenitor
CSR	class-switch recombination
CXCR 4,5	chemokine receptor 4,5
CXCL 12	chemokine receptor ligand 12, 13
CYP450	cytochrome P450
C-FOS	Fos Proto-Oncogene, AP-1 transcription factor subunit
c-Kit	KIT Proto-Oncogene, receptor tyrosine kinase
DAG	1,2-diacylglycerine
DC	dendritic cells
DLBCL	diffuse-large-B-cell-lymphoma
DNA	deoxyribonucleic acid
DSR	differential stress resistance
DSS	differential stress sensitization
DUSP1	dual Specificity Phosphatase 1
E2A	TCF3, transcription factor E2-alpha
Ebf	early B-cell factor
EBV	Epstein-Barr virus
EGR1	early Growth Response 1
EGR3	early Growth Response 3
ELP	early lymphoid progenitor
ERK	extracellular-signal-regulated kinase
ETP	early T-cell precursor
ETV5	ETS Variant 5
FBS	Fetal Bovine Serum
FDC	follicular dendritic cell
FMD	fasting mimicking diet

GAPDH	glyceraldehyde-3-phosphate dehydrogenase
GC	germinal center
GCB	germinal genter-cell like subtype
GPCR	G-protein coupled receptor
Grb2	growth factor receptor bound protein 2
GTP	guanosine-5'-triphosphate
HBSS	“Hank's Balanced Salt Solution”
HDAC	histon deacetylase
HL	Hodgkin-Lymphomas
HPRT	hypoxanthine Phosphoribosyltransferase 1
HPSC	pluripotent hematopoietic stem cells
HRP	horseradish peroxidase
HSC	hematopoietic stem cells
HTLV-1	human T-cell lymphotropic virus type 1
IGF1	insuline-like-growth factor
IgH	immunoglobulin-heavy chain
IK α,β,ε	NF-κB inhibitor α, β, ε
IκB α,β	NF-κB transcription factor inhibitor α, β
IKK α,β,γ	NF-κB inhibitor kinase
IL-7	interleukin 7
IP3	Inositol-1,4,5-trisphosphat
IRF 4,8	interferon-regulatory factor 4,8
ITAM	immunoreceptor-tyrosine-receptor-based-motif
JNK	Jun-amino-terminal kinase
JunB	JunB Proto-Oncogene, AP-1 transcription factor subunit
JunC	Jun Proto-Oncogene, AP-1 transcription factor subunit
KLF10	Kruppel Like Factor 10
MAPK	mitogen-activated protein kinase
MAPKK	mitogen-activated protein kinase kinase
MAPKKK	mitogen-activated protein kinase kinase kinase
MDM-2	murine double minute 2
MEF2B&C	myocyte-specific enhancer factor 2B
MHC	major histocompatibility complex
MPP	multipotent (myeloid/lymphoid) progenitors
mTOR	mechanistic target of Rapamycin kinase
MXD1	MAX Dimerization Protein 1
MYC	myelocytomatosis oncogene cellular homolog
NF-KB	nuclear factor KB
NHL	Non-Hodgkin-Lymphomas
NK	neutral killer cell
OAS3	2'-5'-Oligoadenylate Synthetase 3
Pax5	paired box 5
PDVF	polyvinylidene fluoride
PIP2	phosphatidylinositol-4,5-bisphosphate
PI3-K	phosphoinositide-3-kinase
PKA	protein kinase A
PLC- γ2	phospholipase γ2
PPIA	peptidylprolyl Isomerase A

PTK	protein tyrosine kinase
PU-1	hematopoietic transcription factor PU-1
P53	tumour suppressor protein p53
Raf	rapidly accelerated fibrosarcoma
RAG 1 & 2	recombination activating gene 1/2
R-CHOP	rituximab, cyclophosphamide, doxorubicin hydrochloride (hydroxydaunorubicin), vincristine sulfate (Oncovin), and prednisone
Rel A & B	REL-associated protein A & B
RGS1	regulator of G Protein Signalling 1
RHD	rel-homolgy domain
RNA	ribonucleic acid
ROS	reactive oxygen species
RPMI	“Roswell Park Memorial Institute”
RTK	receptor tyrosine kinase
SAPK	stress-activated protein kinase
SCF	stem cell factor
Src	“sarcoma” tyrosine kinase
Shc	Src homology 2 domain containing
SHM	somatic hypermutations
SH2	Src-homology 2
TBS	tris-buffered saline
TCR	T-cell receptor
TKI	tyrosine kinase inhibitor
TNF	tumour necrose factor
V, D, J	variable, diversity, joining
WHO	World health organisation

1.Introduction

1.1. B-Cell Development

As the main part of the adaptive immune system, B-cells play a major role in immunologic processes in the body. Beside their main function in the production of antibodies they produce cytokines and interact with other cells of the immune system. The developmental process from the hematopoietic stem cell (HPSC) to the fully functional B-cell or plasma cell can be separated in different stages as described below [1-4].

1.1.1. Differentiation in the bone marrow

Next to a wide range of other transcription factors, the main transcription factors that induce the early differentiation from HSC to the common lymphoid precursor are *PU-1* transcription factor family, a member of the *Ets* family, and *Ikaros* [3,5]. *PU-1* deficiency could be associated with a significant loss of T-cells, B-cells and NK-cells, as shown in different mouse experiments [6] (figure 1). The differentiation from HSC to the multipotent progenitor (MPP) cell is activated by *c-Kit* and *Flt3*. Both factors play also an important role in the development of the early lymphoid progenitor (ELP). In the ELP, the heavy chain gene rearrangement at the immunoglobulin-heavy chain (IgH) locus starts, induced by the factors *RAG 1* and *2*. However, the main part of this process takes place in later stages [7]. The ELP is able to differentiate either into the early T-cell precursor (ETP), this step is preferred in the thymus to involve into T-cells, or into the common lymphoid progenitor (CLP), the progenitor of T, B, NK and dendritic cells. Cells often get arrested in the next differentiation step to the early-pro-B-cell [6,7,9].
Three important transcription factors and their downstream target are necessary for differentiation to the early-pro-B-cell: *E2A, EBF* and *EBF´*s downstream target *Pax5* force the cell to express CD19 on the surface and play an important role in the heavy chain genes rearrangement. Therefore, they regulate the *RAG 1* and *2* gene [7], which are necessary for the cell to become an early-pro-B-cell [5,6]. Furthermore, *RAG1* and *2* initiate the pre-BCR signalling setup – not all of them are synthesised in this stage – by regulating synthesis of the pre-BCR components (λ5, VpreB, Igα, Igβ and Igμ). As an additional factor *IL-7* does not only lead to the differentiation to the early-pro-B-cell but acts as an essential signal in pro-B-cell survival. As they develop to the late pro-B-cell the cells start with the V_H-DJ_H rearrangement. If that process is successful, the cell express Igμ, which is an important checkpoint in the B-cell pathway [7,8].

Wnt and *LEF1*, which are controlled by *Pax5*, intensify the differentiation in that stage, however they were repressed, after the pre-BCR signalling starts its response. After that the cells become pre-B-cells, CD25 gets expressed and the rearrangement of the light chain genes occurs [6,9]. The two factors, *IRF4* and *IRF8*, are mandatory for that rearrangement [10]. After

a successful light chain rearrangement, the cells reach the last step of their early development in the bone marrow and become immature B-cells, expressing IgM on their surface [6,9].

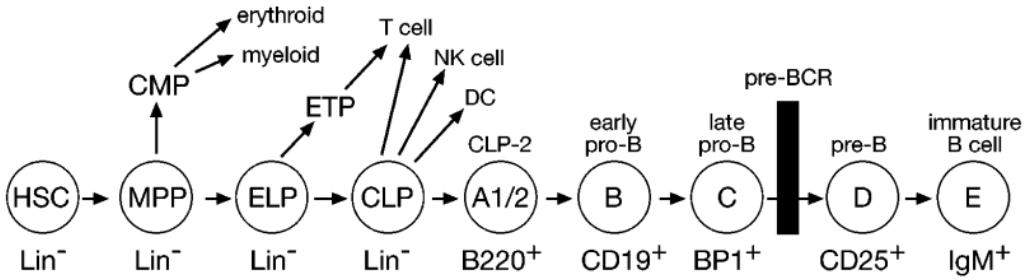

c-Kit	high	high	high	low	low	low	low	-	-
Flt3	-	+	+	+	+	-	-	-	-
IL-7Rα	-	-	-	+	+	+	+	-	-
D_H-J_H	-	-	(+)	+	+	+	+	+	+
V_H-DJ_H	-	-	-	-	-	(+)	+	+	+
V_L-J_L	-	-	-	-	-	-	-	+	+

Figure 1 Early development of the immature B-cell from its progenitor HSC.
Specific regulation ensures that a B-cell is able to develop only under the right conditions and at the right time. While *c-Kit, Flt3* and *IL-7Rα* are necessary in different stages the recombination of the heavy and light chains occurs step by step throughout the development. Derived from Busslinger, M. (2004) [6].

1.1.2. Differentiation in the lymph nodes

As the immature B-cell leaves the bone marrow, it emigrates into secondary lymphoid tissue forming primary lymph follicle. The structure of this follicle is given by a network of follicular dendritic cells (DC). Before B-cells are activated, T-cells of the T-cell zone – that is next to the interfollicular region – are activated. As a result, both activated cells interact in the interfollicular region outside the primary follicle. For a full B-cell activation, T-cell involvement mediated by TCR and MHC-surface molecules as well as CD40/ CD40 ligand interaction is needed. While some of the B-cells leave the tissue as early plasma blasts, the T-cells migrate into the primary follicle. These T-cells build together with the rest of the B cells and the follicular dendritic cells (FDCs) the early germinal centre (GC) [11,12]. In the GC, the activated B-cells proliferate at a high rate. The non-activated B-cells around the GC build the mantle zone. While the proliferation takes place, the immunoglobulin variant region genes undergo somatic hypermutations (SHM) [6], achieving a high variety of immunoglobulin genes caused by base pair changes. The GC can morphological be separated into the light (FDCs and T-cells, partly B-cells) and dark zone (proliferating B-cells). In the dark zone, the SHM takes place and the B-cells immigrate to the light zone [11]. Selected by affinity the B-cells have four faiths [12] (figure 2): (1) If there is low or no affinity to the used antigen, the B-cell is eliminated by induction of apoptosis. (2) Achieving middle or high affinity they either are sent back to the dark zone to undergo the SHM and proliferation for another circle to enhance the affinity level. (3 & 4) The other option is the differentiation to a plasmoblast, which later becomes a plasma

cell - or a memory B-cell precursor – both leave the GC and change the tissue. Some B-cells use an extra step and have to pass an immunoglobulin class-switch recombination (CSR). This step is regulated by *AID* [6,11,12].

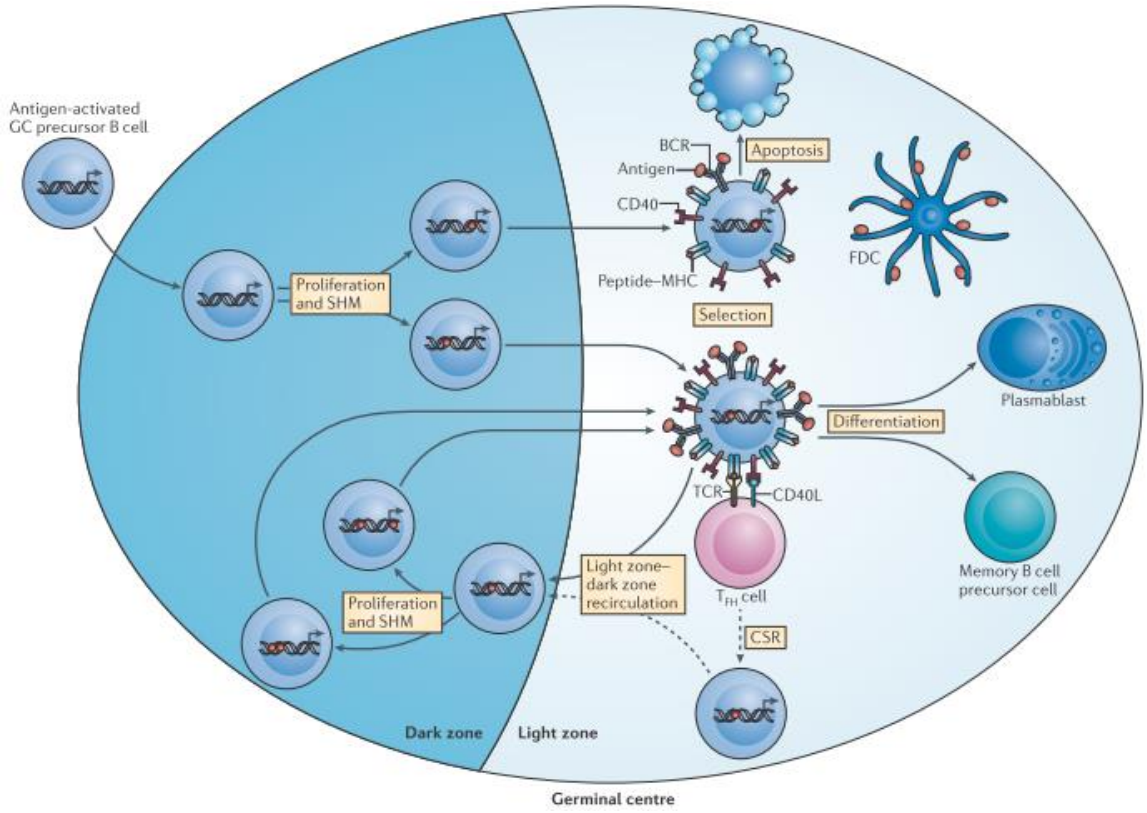

Figure 2 Late stages of B-cell development.
In the germinal centre the final differentiation of the B-cell takes place. While the dark zone is the location for proliferation and SHM, the light zone is for segregation and sorting of the B-cells. That can lead to the re-entry into the dark zone, apoptosis or development and differentiation into plasma cells or memory B-cell precursors. Derived from Nilushi, S. (2015) [12].

Using high proliferation rates and intended mutations, for this system a wide range of expression factors and a big, variable set of regulatory genes are necessary. Selected regulatory genes are shown below (figure 3) [12].

For the emigration and reimmigration processes of T- and B-cells, multiple chemokines are expressed, as there are *CXCR 4* and *5* and their corresponding ligands (i.e. *CXCL12* and *13*), in both cell types and in the FDC [11,12]. *NF-κB* is important for the activation of this process. However, this pathway is described in detail in chapter 1.4. “NF- κB pathway”. For proliferation in general and especially for the proliferation in the dark zone of the GC, the transcription factor *MYC* plays an important role. The factor *IRF4* is essential for the formation of the GC, however it occurs only in the early stage of the GC development. Furthermore, *BCL-6* activates the complete late GC development and becomes higher expressed itself, regulated by the factor *MEF2B*, while *MEF2C* initiates early B-cell proliferation after antigen contact [9,12,13].

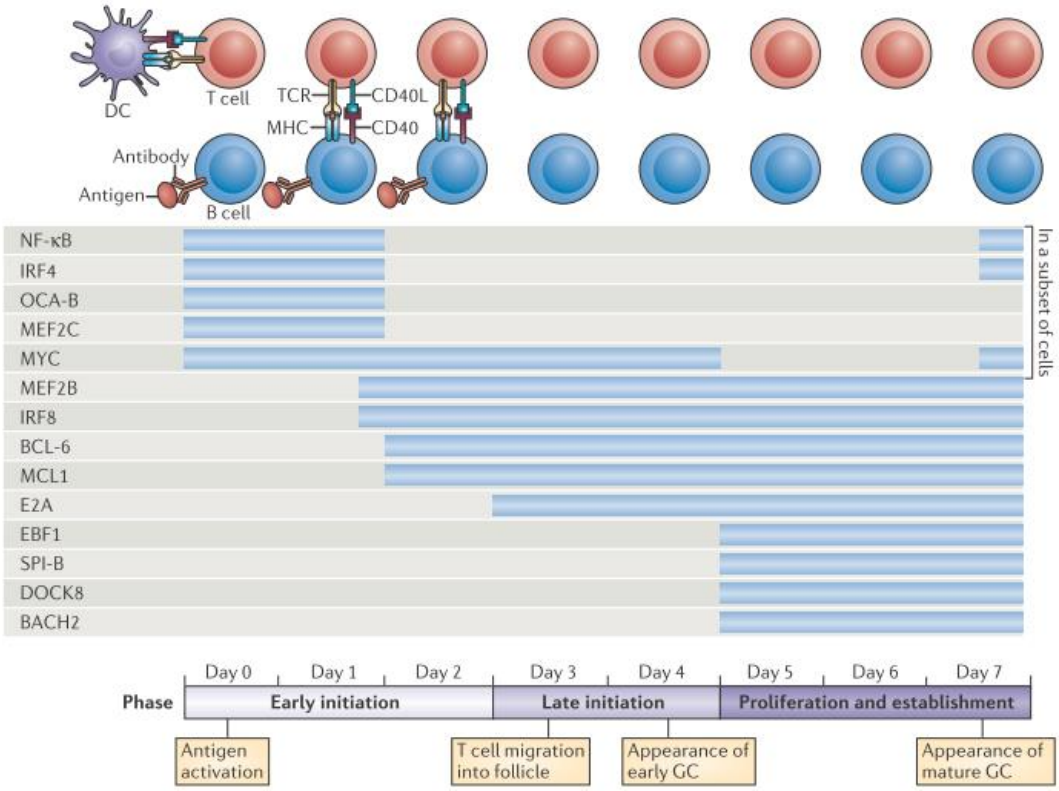

Figure 3 Gene expression in the late B-cell development.
Similar to the proliferation and differentiation in the early stages, also the late stages are driven by the expression of regulatory genes. For each step, a variety of genes has to be present, for an example *NF-κB* in early development in the GC or the *MYC* gene that is also known for its oncogenic character in the early and middle stages. Derived from Nilushi, S. (2015) [12].

1.2. Lymphomagenesis

Lymphomas are defined as neoplastic proliferations of lymphoid cells that derive from different B- and T-cell compartments from the primary or secondary lymphoid tissues. They are categorized into two major entities: the Hodgkin-lymphomas (HL) and the Non-Hodgkin-Lymphomas (NHL). The second group is heterogenous, containing multiple distinct lymphoma types, and comprise more than 60% of the lymphomas in Europe [14]. The NHLs can also be further categorized into B-cell derived (80-85%, B-NHL) and T-cell derived (15-20%, T-NHL) lymphoma and the rarely occurring NK-cell derived lymphoma. The percentage differs depending on the geographic localisation. As it is known that lymphomas are enhanced in immune suppressive entities, in Africa the enhanced appearance of the later described Burkitt lymphoma correlates with the infected area of the Epstein-Barr-Virus (EBV) and chronic EBV infections. Also, in Japan a correlation between HTLV-1 and a higher incidence of T-cell lymphomas could be confirmed [13,14].

From the variety of B-NHL three major subtypes make up around 80% of this entity. Diffuse large B-cell lymphoma (DLBCL), Burkitt lymphoma and follicular lymphoma derive from the GC cells, in contrast to lymphomas, like the plasmablastic lymphoma, deriving from fully differentiated plasma cells [13,14]. While follicular lymphoma has his origin from light zone B-cells, DLBCL can be divided into two subtypes deriving from cells of different regions. The GC-

cell like subtype (GCB) originates from the light zone as well and the activated B-cell like one (ABC) proliferates out of the early post-GC plasmablasts [15]. In contrast, the Burkitt lymphoma originates from the dark zone in the GC. Similar to other malignant tumours, these lymphomas show a variety of genetic alterations, such as amplifications and point mutations. Additionally, alterations in the lymphomas are caused by the aberrant SHMs (ASHMs) and chromosomal translocations, deriving from the CSR and the immunoglobulin rearrangement mechanism [15-17].

The DLBCL is the most common and aggressive B-cell lymphoma entity and has different response rates to therapy according to its molecular subtypes, namely ABC- and GCB-DLBCL [18]. Even though deriving from different cell stages, they have some pathogenic features and alterations in common [19]. Next to the well-known *p53* mutation, inactivating the tumour suppressor, *BCL-6* is rather specific to DLBCL [13]. Additionally, they often lack MHC-complexes on their surface, making them invisible to cytotoxic T-cells. The GCB subtype is more similar to Burkitt lymphoma and often develops *MYC* and *BCL-2* alterations, while ABC cells start to constitutively activate the *NF-κB* pathway and stop the further differentiation into plasma cells [15]. The outcome for ABC-DLBCL under the standard chemotherapy (R-CHOP), is associated with poor clinical course [13,20]. In addition, in GCB-DLBCL a significant lower relapse frequency occurs. This data indicates that a more specific therapy is needed for ABC-DLBCL [20, 21].

Burkitt lymphoma, deriving from the dark zone of the GC, is not as aggressive as the DLBCL, however more than half of the patients is under the age of 40, and in combination with high relapse percentages, the urge for improvement in this field is high [20]. In one-third of the patients an EBV could be detected and this causality is discussed. An unusual feature is the activation of the *PI3*-Kinase pathway, which is normally not active in dark zone cells, leading to a strong BCR signalling. The most common mutations in this subtype are *MYC* alterations, resulting in dysregulation of DNA replication and cell cycle [13]. The standard therapy is a short-intensive chemotherapy with R-CHOP achieving up to 90% cure rate [21-23].

1.3. *p53* pathway

The *p53* pathway contains several gene networks that depend on or activate the p53 protein. Different extrinsic and intrinsic stress factors could activate this pathway and lead to a variety of cellular response. Upon stress signals or DNA damage the p53 protein is post-translational modified, such as phosphorylation or acetylation [24,25]. For example, UV-radiation activates *ATR, CHK1* and *casein kinase-2*, while gamma-radiation induces the *ATM* kinase. As a consequence, from this stimulation, p53 gets phosphorylated on different amino sequences, leading to different responses, e.g. DNA repair or apoptosis [26].

As shown in figure 4, there are four major responses upon *p53* activation. Next to DNA repair and cell cycle arrest, in which *p21* also plays a major role [26,27], the pathway leads to apoptosis and inhibition of angiogenesis and metastasis [28,29]. In the cell cycle arrest, inhibition mainly targets the cyclin protein family, leading to arrest in different cell stages, mainly G1 or G2. If the DNA damage is irreparable, p53 accumulates in higher concentrations and starts to enhance the apoptotic pathway. The main p53 target genes are *BCL-2, Bax* and the *Caspase* family, example given *Caspase 3* and *9*. Due to its necessity, *p53* is highly regulated. Ten feedback loops are known for that purpose (three positive and seven negative ones). *MDM-2* as a direct downregulating antagonist [30] is direct or indirect targeted in more than three feedback loops [28,29]. Despite its high regulation *p53* is one of the highest mutated genes, because it is one of the strongest tumour suppressor proteins existing in eukaryotes [31,32].

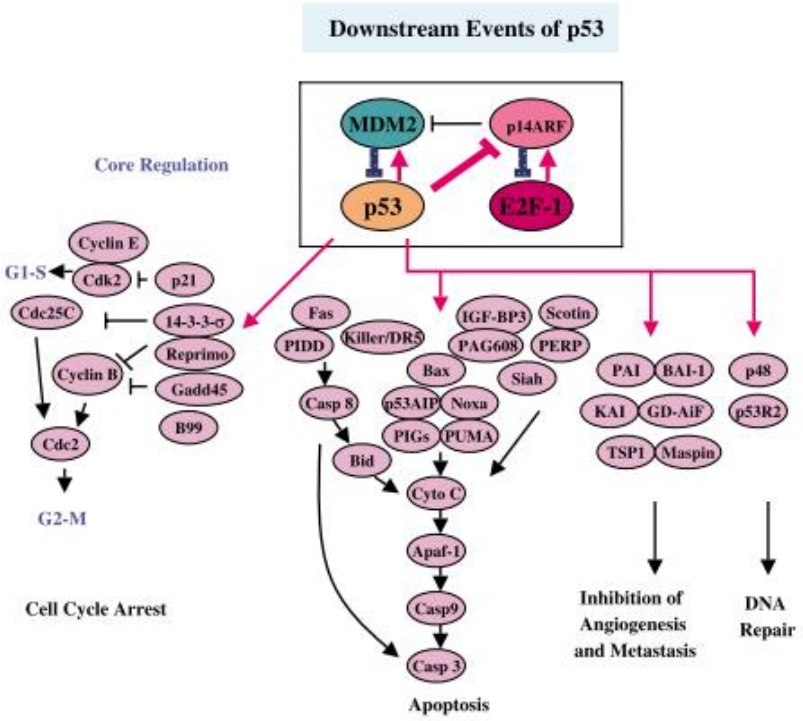

Figure 4 *p53* and his downstream targets.
Receiving multiple different activation signals, there is no surprise that the *p53* pathway also has a large variety of effects. As known as one of the strongest anti-cancer signalling pathway, *p53* leads to immediate repair of damaged DNA. If no repair is possible the cell is sent into apoptosis or sentenced to cell cycle arrest. Furthermore, *p53* activates downstream targets that inhibit angiogenesis and metastasis, both necessary for tumour growth. Derived from Harris, S (2005) [29].

1.4. *NF-κB* pathway

Named by its ability to bind to the enhancer element of immunoglobulin κ light chain gene in the activated B cell, the *NF-κB* pathway is a main part of the cell´s metabolism. However due to its wide range of effects, a lot of them are not fully understood until now. *NF-κB* takes part in immune response, inflammation, proliferation, apoptosis and also in self-regulatory processes [33]. The *NF-κB* pathway is activated through cytokines, antigen receptors,

infections and stress signals leading to the expression of a variety of immune response and inflammation proteins (figure 5). While the genes of this pathway are expressed in nearly every cell type, they furthermore can be constitutive expressed, for example in mature B-cells. In mammals, the *NF-κB* family consists of five main members, namely *p65* (*RelA*), *RelB, c-Rel, NF-κB 1* (*p105/p50*) and *NF-κB 2* (*p100/p52*) [34,35]. In the cell they conduct hetero- and homodimerization potentially producing nearly 15 possible dimers, however, there are no physical evidences of all of them yet. Sharing a 300 amino acid long rel-homology domain (RHD) sequence, this amino-configuration includes not only the necessary sequence for dimerization but also contains requirable parts for DNA binding [36,37], IκB interaction and nuclear translocation [35].

As this pathway has to be fast in responding, these active proteins are already produced before the stimulus occurs but are inhibited by binding the *IK-B* family, which consists of *IKα, IKβ* and *IKε* [36,37]. Furthermore, the precursor p100 and p105 can also lead to inhibition by participating in a dimerization. As they are precursors, the dimer is not active until the phosphorylation of p100 takes place [38].

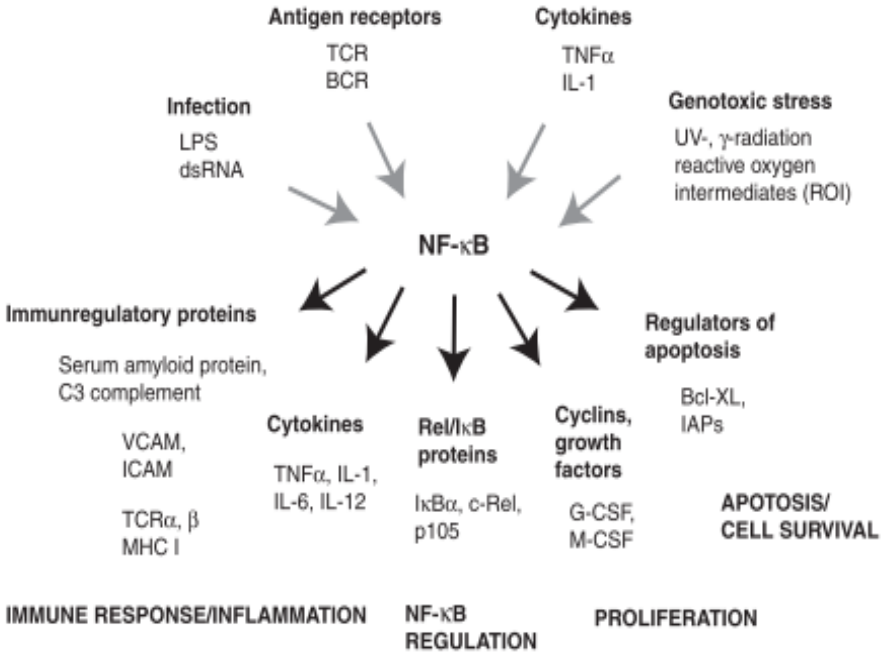

Figure 5 *NF-κB* pathway.
The *NF-κB* receives strong activation signals through cytokines and antigen receptors leading to the expression of a wide range of immune response and inflammation proteins. For the B-cell this signal also induces proliferation and anti-apoptotic effects and leads to cell growth. Derived from Oeckinghaus (2009) [37].

As shown in figure 6, the activation can occur over two different mechanism: the canonical and non-canonical signalling [37]:

(1) Canonical activation: Induced by inflammatory cytokines, antigen receptors and pathogen-associated molecules, the canonical pathway leads to an activation of the kinase IKKβ and the regulatory protein IKKγ (NEMO). This active IKK complex phosphorylates IκBα or IκBβ followed by the ubiquitination of these IκBs [34,39]. Without the inhibitor, the protein dimers for

example p50/p65, which can transfer to the nucleus, bind to the DNA and activate transcription factors.

2) Non-canonical activation: Through activation by specific TNF cytokine family members, such as BAFF, lymphotoxin-b and CD40 ligand, the non-canonical pathway is induced. IKKα phosphorylates p100, linked to RelB, and leads to a partly destruction from p100 receiving p52 as a rest. Additionally, the NF-κB - inducing Kinase (NIK) has a major role in activating IKKα and connecting it to p100 for the following phosphorylation. After p100 is proteolytically processed to p52, the dimer – p52 and RelB – is now active, translates into the nucleus and starts the transcription of target genes [37,38].

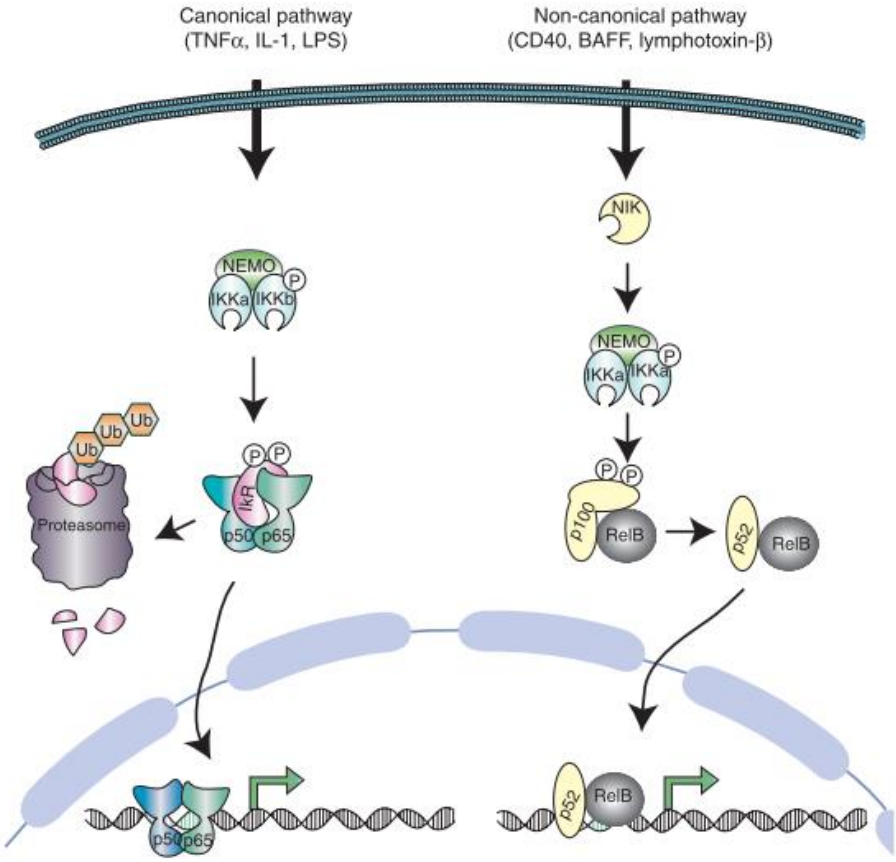

Figure 6 The canonical and non-canonical pathway.
The canonical pathway is activated through inflammatory cytokines, antigen receptors and pathogen-associated molecules, causing a phosphorylation of IκBα and IκBβ and the regulator protein can force the ubiquitination of mentioned proteins. Then the dimers (e.g. p50/p65) transfer into the nucleus and activate transcription factors. In the non-canonical pathway, NIK activation occurs by specific TNF cytokine family members, resulting over NEMO to a phosphorylation and destruction of p100, allowing the complex to enter the nucleus. Derived from Oeckinghaus (2009) [37].

As mentioned above, *NF-κB* also has a high impact on the cell proliferation thus it has to be specifically regulated, otherwise it has negative impact on cell development, for example in mantel cell lymphoma or multiple myeloma [40,41].

In addition to a variety of different side signals from other pathways, the *NF-κB* pathway has also self-inhibiting functions. Not only the inactivity of p100 and p105 dimers and feedback loops by transcription factors, but also the enhanced concentration of NF-κB leads to an

increasing production of its own inhibiting protein IK-Bα [30,31]. Leading to a non-apoptotic and cell proliferating signal this pathway is often known to be upregulated in different tumour types, as known in ABC-DLBCL. However, it is known that there is no upregulation in others, like the GCB-DLBCL [42]. Furthermore *NF-κB* upregulates *MDM2* by activation of the *PI3K* pathway and therefore activates anti-apoptotic effects and cancer migration properties [43].

1.5. *MAPK* pathway

The *MAPK* pathway is highly evolutionary-conserved, necessary for cell proliferation and differentiation. Its upstream proteins like Raf or Ras are favoured targets for tumour mutations [44]. Important for this pathway are three kinases: Mitogen-activated protein kinase (MAPK), Mitogen-activated protein kinase kinase (MAPKK) and Mitogen-activated protein kinase kinase kinase (MAPKKK) [45-47]. Three families can be subdivided as there are the extracellular-signal-regulated kinase (*ERK*) [48], the Jun-amino-terminal kinase (*JNK*) [49] and the p38/stress-activated protein kinase (*SAPK*) family [50,51] as shown in detail in figure 7.

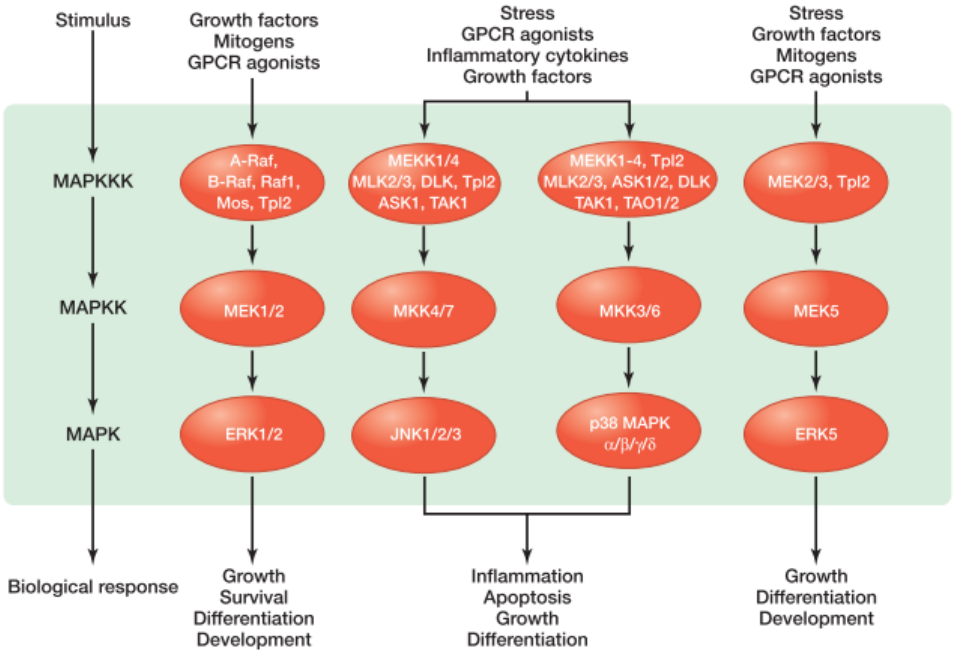

Figure 7 *MAPK* pathway.
The *MAPK* pathway is known as a well-conserved pathway in eukaryotes and is necessary for cell growth, proliferation and differentiation. There are three main families. Therefore, *MAPK* can be divided into the extracellular-signal-regulated kinase (*ERK*), the Jun-amino-terminal kinase (*JNK*) and the p38/stress-activated protein kinase (*SAPK*) family. All of them include the basic MAPKKK-MAPKK-MAPK linage. Derived from Morrison, D [44].

The *ERK* family again is split into two subgroups, the classic *ERK* - *ERK1* and *ERK2* - consisting mainly of a kinase domain and *ERK5* as the large ERK´s subgroup, including also a long carboxy-terminal sequence [38]. After activation per extracellular factors, that interact with receptor tyrosine kinases (RTK), G-protein coupled receptors (GPCR) and integrins, small GTP-binding proteins, mainly Ras, are induced over adaptor proteins, like Shc or GRB2. At the next step the MAPKKK, here mostly the Raf family members, are phosphorylated by Ras

[45,47]. On a downstream phosphorylation the MAPKK MEK1 or 2 and afterwards the MAPK ERK1 or 2 are phosphorylated and turned into their active form. Afterwards various downstream targets in the cytosol or the nucleus are phosphorylated leading to activation of proliferation, differentiation and survival processes. In this cascade a lot of side factors induce upregulation or downregulation in cross-linked pathways or the *MAPK* itself. The other two families contain another variety of MAPKKK, MAPKK and MAPK, however the mechanism does not differentiate [45,46]. For the *JNK* family there were *MEKK1, MEKK4, ASK1, Tpl2, TAK1, MLK2* and *MLK3* (MAPKKK), *MKK4* and *7* (MAPKK) and *JNK 1, 2* and *3* (MAPK) [44]. For the *SAPK* family there were the same MAPKKK as in the *JNK* family with additional *MAPKKK TAO1* and *2*. Other members of this family were *MKK3* and *MKK6* (MAPKK) and *p38* (MAPK) [44].

1.6. B-cell receptor signalling

Next to its major role in efficient development and survival of B-cells, the BCR signalling activates several pathways as shown in detail in figure 8. The multiple protein structure called B-cell receptor (BCR), consists of an antigen-binding subunit, an Immunoglobin bedded in the membrane (mIg) and the two proteins Igα and Igβ, forming together the heterodimeric signalling subunit. Both of them contain a special sequence called immunoreceptor-tyrosine-receptor-based-motif (ITAM), involving a specific binding side for effectors with SH2-domains, as for example the protein tyrosine kinases (PTK). After a stimulus at the antigen-binding subunit takes place, the formation of dimers occurs. The PTK´s phosphorylate the ITAM regions [52,53]. The most well-known PTK family for this interaction is the src-family. Main members of this group are the Lyn, Fyn, Blk or Lek. Only the phosphorylation of both, Igα and Igβ, causes a recruitment of the cytosolic tyrosine kinase Syk, that again phosphorylates the Bruton tyrosine kinase (Btk). The CD45, a surface glycoprotein, ensures the availability of the PTK´s Lyn, Syk and Btk and furthermore the possibility for activation of them, by holding them in a controlled dephosphorylated/phosphorylated ratio, thus providing an enhanced sensibility of the BCR signalling [52-54]. The Btk recruits the phospholipase-γ2 (PLC-γ2) that leads to a conformation change from phosphatidylinositol 4,5-bisphosphate (PIP2) to inositol trisphosphate (IP3) and diacylglycerol (DAG). Additionally, a second protein is necessary for the recruitment. BLNK is known to link the PLC-γ2 to the membrane complex and enables the interaction. Also, the linkage of the earlier mentioned PTK Syk is associated with BLNK [54]. The produced IP3 triggers the increase of the intracellular Ca^{2+} concentration leading to the activation of different pathways, like the *MAPK* pathway or the *NF-κB* pathway (figure 8).

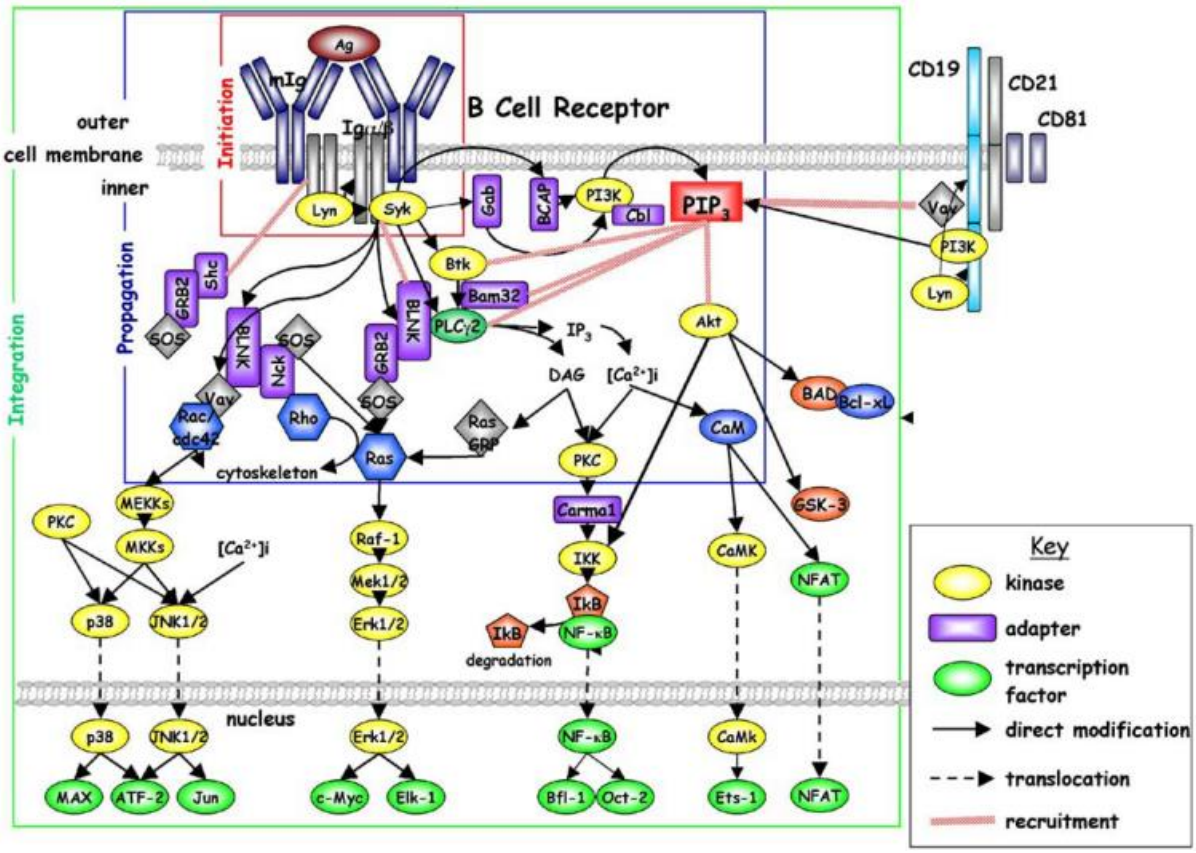

Figure 8 BCR signalling.
Activated over incoming signals, like insulin, the B-cell receptor forms a dimer, followed by autophosphorylation. Additional tyrosine receptor kinases adapt to the BCR leading to signal transduction. The BCR assembles some of the most important pathways in his signal transduction, like *NF-κB, MAPK* or *PI3K/Akt*, being responsible for a big variety of tasks, as their major targets effect cell proliferation, differentiation, regulation of apoptosis and immune response. Derived from Joseph M. Dal Porto (2004) [52].

Even though this process leads to an activation of the mentioned pathway, the limiting step in the BTK activation is connected to an active present PI-3Kinase [55,56]. Another surface glycoprotein, the CD19 is known for regulating the PI3K in its function. By the dimerization of the BCR complex CD19 is initialized and the PI3K produces PIP2, necessary for the following steps. Even though CD19 is the main regulator of *PI3K*, experiments with CD19 deficient mice [57] lead to a normal, yet strong decreased, B-cell development [52,55-58]. Further tests with *PI3K* deficient mice show complete arrestment of immature B-cells. Therefore, other *PI3K* inducing proteins are predicted and physically determined [55-58]. The BCR is well known to be constitutively activated caused by mutations during malignant transformation in a variety of NHLs as i.e. in DLBCL [59] but also in the CLL [60]. That is why treatments of B-cell lymphomas targeting this pathway are commonly used.

1.7. Ibrutinib

Ibrutinib is a small-molecule inhibitor that targets the Btk, known for its irreplaceable function in *NF-κB, MAPK* activation and B-cell development [62,63,64]. Ibrutinib binds specific and covalently to the active side of Btk, inhibiting his enzymatic function [61,62]. As used by oral intake, a fast resorption takes place, leading to a plasma maximum concentration after one to

two hours. After the terminal half-life of four to six hours, metabolization in the liver, by the CYP450 enzyme CYP3A4, is the main elimination component. Ibrutinib is clinically applied in CLL patients resulting in overall response rates up to 60% [64-66]. It was also tested in subtypes of the DLBCL in clinical trials [63]. Due to its lack of mutations and activations in BCR signalling, the GCB-DLBCLs do not seem as a useable target group, confirmed by several studies in which the response rate was just around 5%. In contrast the ABC-DLBCLs exhibit a variety of mutations occurs. Therefore, overall response rate of Ibrutinib treatment in this subtype is up to 37%. As there were no observed side effects at higher concentrations and no contraindications reported, it appears as a well-usable tool in specific patient cohorts [67,68].

1.8. Fasting

Fasting in general is not a modern strategy, it is known for a long time. Therefore, many different studies have been conducted and also novel diets are presented each day, resulting in a high range of misinformation [69].

On a systemic level fasting overall leads to a reduced level of glucose, induced by restricted glucose intake, insulin, that is directly linked to the glucose concentration, leptin and insulin like growth factor 1 (*IGF1*). *IGF1* is indicated to enhance cancer growth, not only *IGF1*-production is decreased but also its counterplayer the insulin like growth factor binding protein 1 (IGFBP1) is generated. In contrast to that a higher level of glucagon and ketone bodies occur in fasted subjects [70,71].

On cellular level in healthy cell samples, the decreased levels of *IGF1* and Insulin lead to lesser activation of the tyrosine receptor again resulting in decreased downstream pathways. Two of main pathways are the *MAPK/mTOR* and the *NF-κB* pathway all linked to the *PI-3K* and also to Akt. Furthermore, the lower glucose concentration inactivated the protein kinase A (PKA). Through this interception AMP activated protein kinase (AMPK) production is not inhibited by the PKA, thus leading to an increased early growth response protein 1 (EGR1) concentration. *EGR1* is known as a stress resistance transcription factor [70-72].

Fasting can be divided into three subgroups according to the intake ratio and fasting conditions. Ketonic diet, chronic caloric restriction and a more modern combined fasting method with or without fasting mimicking diet (FMD). All three of them lack the effectivity as single cancer treatment compared to the average cancer therapies, however depending on the diet, they show a rise of anticancer activity in combination therapy [70,72,73]. The ketonic diet is defined by a high fat, low protein and low carbohydrate intake (normally 4:1) without caloric restriction. As observed in previous studies [70] this diet could lead to a decrease in *IGF1* and insulin concentration [74]. Furthermore, higher ketone body levels inhibit the histone deacetylases (HDACs), which downregulate the DNA transcription by histone conformation, resulting in reduced tumour growth. Compared to the other approaches the ketonic diet has no statistically significant effect, except for some types of tumour like glioma blastoma [70].

Chronic caloric restriction is the most commonly known subtype and includes energy reduction around 25% from the standard caloric intake. As shown in previous experiments by using mouse models and primates it does not only reduce the cardiovascular risk factor but also lead to a reduced cancer appearance in different cancer types. However, the chronic caloric restriction also has a wide variety of side effects, depending on the loss of energy as there are for example metrorrhagia, reduced strength, osteoporosis, increased cold-sensitivity, slower wound healing and depression. Additionally, it can induce malnutrition and its effects [70,75].
As a modern approach non-chronical fasting (up to 72 hours) or water-only fasting and the usage of so-called fasting mimicking diets (FMDs) are established. FMDs are special designed diets with very low caloric intake (300-1100kcal per day) and reduced sugar and proteins. These diets on the one hand simulate main parts of the water-only fasting but on the other hand minimize the side effects of fasting, especially malnutrition [70].
Two effects of fasting can be distinguished, as there are differential stress resistance (DSR) and differential stress sensitization (DSS). With no fasting normal cells and cancer cells are equally targeted by chemotherapy. Unmutated cells are forced into a self-maintenance state and activate protective response. With lower cell dividing rate, the normal cells became difficult to target by chemotherapy using cytostatics and proliferation targeting substances [76]. While normal cells can respond in that way, the activation of stress resistance is blocked by the oncogenes and/or the constitutive activation of pathway like *PI3K* in cancer cells. Thus, cancer cells are easier to target (figure 9) [77]. Furthermore, high glucose and *IGF1* concentrations, enabling a higher toxicity for healthy cells in mice experiments (especially mouse karyocytes), can be reversed by fasting. This occurs by a downregulation of cAMP and PKA activity and inducing *EGR1*. Thus, leading to an increased differential stress resistance caused by the promoted expression of cardioprotective ANP or BNP through *EGR1* [70,77,78].

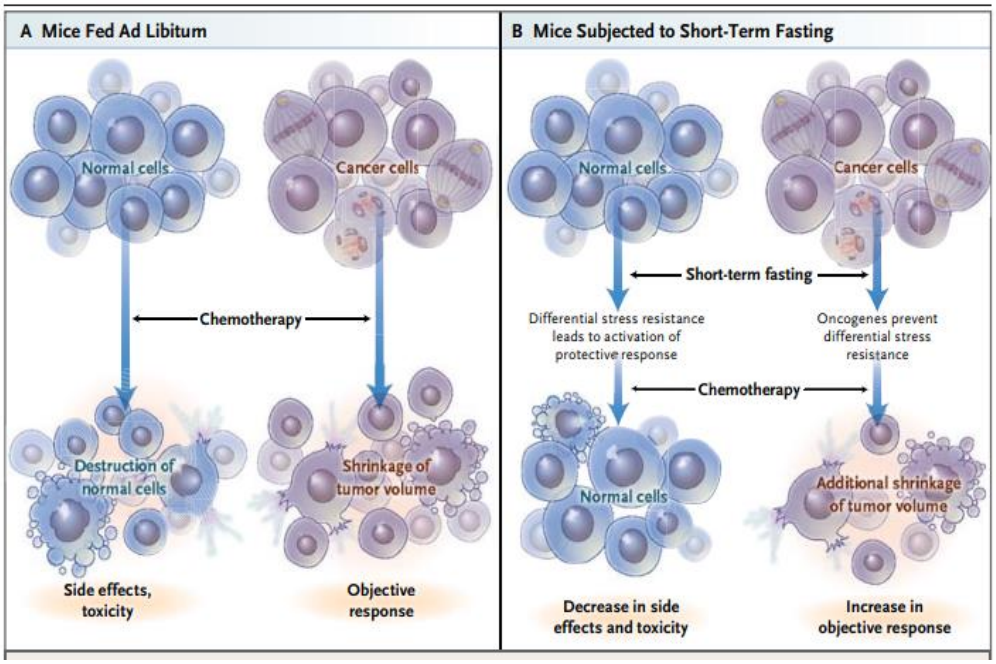

Figure 9 Differential stress resistance (DSR).
Under normal conditions normal cells become targeted by chemotherapeutics similar to cancer cells as there is often no specific anti-cancer treatment available. As a consequence this results in toxicity and variable side effects. Experiments with short-term fasted mice achieve reduced side effects and toxicity, following the DSR theory. While normal cells activate their protective response and become less attractive to chemotherapy and stress factors, the oncogenes in the cancer cells prevent this effect resulting in fewer side effects and toxicity next to increased tumour cell death. Derived from Laviano, A (2012) [77].

In addition, fasting causes a higher sensitivity of cancer cells to chemotherapeutic agents. Apoptosis, which is normally inhibited by IGF1, is increasing, caused by the lack of IGF1. Furthermore, it regulates down a variety of transcription and proliferation factors as, for example, the cellular proliferation factor *IRS2*. The second major effect of fasting in cancer cells is the increased chemotherapy induced DNA damage. Even though it also has the DNA damaging effect by itself, the combination therapy with chemotherapeutics results in an increase of that damage up to twentyfold for example in breast cancer and melanoma cells. Starvation/fasting conditions further promotes oxygen stress leading to a higher amount of reactive oxygen species (ROS). As oxygen stress is linked to apoptosis, the caspase levels, especially *caspase 3*, are upregulated [70,77,78].

As mentioned earlier side effects of toxicity during chemotherapy are heavily reduced by fasted patients compared to the unfasted control group. Effected by the DSR and DSS theory normal cells should achieve a stronger protection response [70,77-79] (figure 10). As the fast dividing cell types in gastrointestinal and hair tissue are send into a self-maintenance state the survival of this tissue leads to less hair loss and less gastrointestinal complications. Furthermore, neuropathic-motoric side effects and weakness are reported less frequently in fasted probands. Overall, all known side effects of chemotherapy seem to be reduced under fasting conditions. However, these studies only include small number of patients and studies with higher participant numbers are necessary for validation [75].

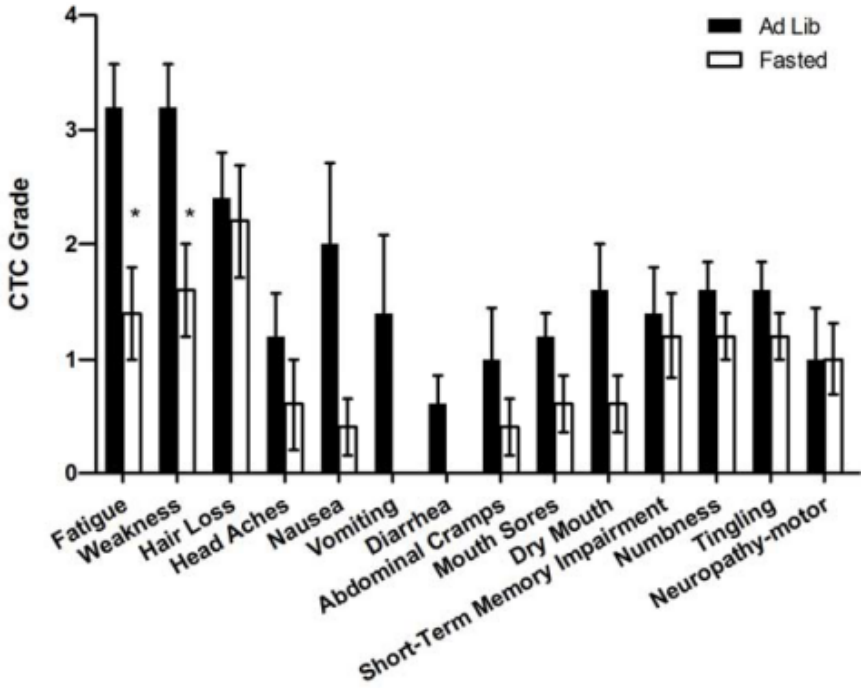

Figure 10 Side effect reduction in human patients.
According to the previous mentioned DSS and DSR the clinical studies also result in reduced toxicity and side effects. The most impact is achieved in normally fast dividing cells resulting in reduced GI complications and hair loss. Derived from Safdie, F (2009) [75].

The often-discussed topic of cancer prevention via fasting is highly debatable, as fasting has a variety of different effects in different cancer types and only a well-planned diet leads to an improvement in cancer prevention [69,75].

2. Aims

The aim of this master thesis was to comprehensively study the effects of fasting conditions on the activation of BCR signalling pathways, especially the *NF-κB, PI3K/Akt* and *MAPK* pathway and to investigate whether fasting influences the growth inhibitor activity of the BTK-inhibitor ibrutinib in aggressive lymphoma cell lines.

Aim 1: Growth inhibitor effects of the BTK-inhibitor Ibrutinib in lymphoma cell lines

The first aim of this thesis was to investigate the sensitivity of aggressive lymphoma cell lines (ABC-DLBCL, GCB-DLBCL and Burkitt lymphoma cell lines), towards BCR inhibition by using Ibrutinib under fasting conditions.

Aim 2: Effects of fasting on signalling pathways in aggressive lymphoma cells

The second aim was to determine the effects of fasting/starvation on the activation of BCR signalling related pathways. Therefore, the *NF-κB* pathway was investigated on RNA and protein levels. In addition, expression analysis of *MAPK* and *PI3K/Akt* target genes under fasting/starving condition was performed.

3. Material & Methods

3.1. Cell cultivation

Seven different cell lines were used in the experiments: RI-1 and U2932 as ABC-DLBCL models, SuDHL4 & Karpas-422 as GCB-DLBCL models and Raji & BL-2 as Burkitt lymphoma models. Under normal condition all cells were maintained in RPMI 1640 Medium (Thermo Scientific; Waltham, MA) supplemented with 10% Fetal Bovine Serum (FBS, Thermo Scientific; Waltham, MA) for RI-1, U2932, SuDHL4 and Raji and 20% FBS for Karpas-422 and BL-2. In some experiments, a T-cell lymphoma model (Jurkat cell line) was included as an additional control. For prevention of bacterial and fungal contamination Antibiotic-Antimycotic (Thermo Scientific; Waltham, MA) was added.

The ideal cultivation conditions for the used lymphoma cell lines are listed in table 1 below.

Table 1 Cultivation conditions for the established lymphoma cells

cell line (subtype)	Medium	split number
RI-1 (ABC)	RPMI (1640) + 10% FBS + 1 % Antibiotic-Antimycotic	$1*10^6$
U2932 (ABC)	RPMI (1640) + 10% FBS + 1 % Antibiotic-Antimycotic	$1*10^6$
SuDHL4 (GCB)	RPMI (1640) + 10% FBS + 1 % Antibiotic-Antimycotic	$0,5*10^6$
Karpas-422 (GCB)	RPMI (1640) + 10% FBS + 1 % Antibiotic-Antimycotic	$0,5*10^6$
Raji (Burkitt)	RPMI (1640) + 10% FBS + 1 % Antibiotic-Antimycotic	$0,5*10^6$
BL-2 (Burkitt)	RPMI (1640) + 20% FBS + 1 % Antibiotic-Antimycotic	$0,5*10^6$
Jurkat (T-cell lymphoma)	RPMI (1640) + 20% FBS + 1 % Antibiotic-Antimycotic	$0,5*10^6$

To optimize the starving conditions the lymphoma cell lines were cultivated in RPMI media, to which different glucose (2.5; 5g/L), FBS (0;1; 2.5; 5; 10%) levels as well as insulin were added. In addition, in second experiment varying glucose (0; 0.2; 0.4; 0.6; 0.8; 1; 1.2; 1.4; 1.6; 1.8g/L) and FBS (0;1; 2.5; 5; 10%) concentrations were tested under the same fasting conditions. All conditions were followed by cell growth measurements (24, 48, 72 hours) and a 3-(4,5-dimethylthiazol-2-yl)-5-(3-carboxymethoxyphenyl)-2-(4-sulfophenyl)-2H-tetrazolium (MTS) cell proliferation assay (EZ4U kit Biomedica; Vienna, Austria) as described in detail in 3.3.

3.2. Ibrutinib treatment

Experiments with the BTK inhibitor Ibrutinib® (0; 0.25; 0.5; 1; 2.5; 5; 7.5; 10; 20; 30; 40; 50µM) (PCI 32765, Selleck Chemicals, Houston, TX) were performed in combination with fasting to determine growth inhibitory effects and to determine the IC_{50}. As described before the cells were fasted for 24 hours double fasting conditions (0.4; 0.6; 0.8; 2g/L glucose; 2.5; 5; 10% FBS) before adding the Ibrutinib. For this experiment unfasted cells functioned as controls (2g/L glucose, 10% FBS). After 24, 48 and 72 hour the cell growth was assessed by using MTS proliferation assay, as described in 3.3.

3.3. Assessment of cell growth

The cells were fasted at 37°C for 24, 48 and 72 hours and a MTS cell proliferation assay was performed by using the EZ4U kit (Biomedica; Vienna, Austria). With the SPECTROstar® Omega Microplate Spectrophotometer (BMG LABTECH; Ortenberg, Germany) the absorption was measured at 492nm and 620nm for reference after four to five hours after MTS treatment, depending on the experiments.

3.4. mRNA expression analysis

To determine the effect of fasting on transcription levels, the lymphoma cell lines were incubated in RPMI with glucose (5g/L) and FBS (0; 1; 2.5; 10%) at 37° for 24h. Afterwards $1x10^6$ cells were processed for RNA using the RNeasy mini kit (Qiagen; Hilden, Germany) or the ReliaPrep™ RNA Cell Miniprep System (Promega; Madison, WI) according to the manufacturer protocol. cDNA synthesis was performed by using RevertAid RT Kit (Thermo Scientific; Waltham, MA).

Finally, the RT-qPCR was conducted by using the GoTaq® qPCR Master Mix for Dye-Based Detection (Promega; Madison, WI). The PCR reaction were carried out in duplets or triplets in a Bio-Rad CFX364 TouchTM Real-Time PCR Detection System (Bio-Rad, Hercules, CA, USA). Peptidylprolyl Isomerase A (PPIA), Hypoxanthine Phosphoribosyltransferase 1 (HPRT) and Glyceraldehyde-3-Phosphate Dehydrogenase (GAPDH) served as housekeeping genes. For the 17 analysed genes (table 2) commercially available primer assays from Qiagen (Qiagen, Hilden, Germany) were used.

Table 2 Analysed downstream target genes of the NF-κB, MAPK and PI3K/Akt pathways

genes	alternative name	gene function	target gene of the following pathway & GeneID
CCL3	C-C Motif Chemokine Ligand 3	monokine with inflammatory and chemokinetic properties	NF-κB 6348
CCL4	C-C Motif Chemokine Ligand 4	monokine with inflammatory and chemokinetic properties	NF-κB 6351
TNF1	Tumour necrosis factor	induce cell death of certain tumour cell lines, cell proliferation & differentiation	NF-κB 7124
BCL2A1	BCL2 Related Protein A1	retards apoptosis induced by IL-3 deprivation	NF-κB 597
RGS1	Regulator of G Protein Signalling 1	regulates G protein-coupled receptor signalling cascades	NF-κB 5996
EGR1	Early Growth Response 1	transcriptional regulator, important role in regulating the response to growth factors, DNA damage, and ischemia	MAPK 1958
EGR3	Early Growth Response 3	immediate early growth response	MAPK 1960
OAS3	2'-5'-Oligoadenylate Synthetase 3	interferon-induced, dsRNA-activated antiviral enzyme	MAPK 4940
KLF10	Kruppel Like Factor 10	plays a role in the regulation of the circadian clock	MAPK 7071
cFOS	Fos Proto-Oncogene, AP-1 Transcription Factor Subunit	signal transduction, cell proliferation and differentiation	PI3K/Akt 2353
BUB1	BUB1 Mitotic Checkpoint Serine/Threonine Kinase	essential for spindle-assembly checkpoint signalling and for correct chromosome alignment	PI3K/Akt 699
MXD1	MAX Dimerization Protein 1	transcriptional repressor, binds to MAX to form a DNA binding complex	PI3K/Akt 4084
JunC	Jun Proto-Oncogene, AP-1 Transcription Factor Subunit	increased steroidogenic gene expression through cAMP signalling	PI3K/Akt 3725
JunB	JunB Proto-Oncogene, AP-1 Transcription Factor Subunit	transcription factor involved in regulating gene activity following the primary growth factor response	PI3K/Akt 3726
ETV5	ETS Variant 5	involved in development	PI3K/Akt 2119
DUSP1	Dual Specificity Phosphatase 1	dual specificity phosphatase that dephosphorylates MAP kinase MAPK1/ERK2	PI3K/Akt 1843
CCND2	Cyclin D2	Regulatory component of the cyclin D2-CDK4 (DC) complex	PI3K/Akt 894

For the RT-qPCR experiments, the cycling protocol, as shown in table 3, was used. Melt curve analysis was performed to detect possible unspecific side products.

Table 3 RT-qPCR protocol established for the promega GoTaq-assay

stage	Temperature [°C]	time	Performed cycles
1 activation	95	2 min	1
2 denaturation	95	3 sec	39
3 annealing/extension	60	30 sec	
4 final denaturation	95	5 min	1
5 melting curve analysis	65	5 sec	1
	95	5 sec	1

3.5. $2^{-\Delta\Delta CT}$ method

This method is based on the following equations:

$$2^{-\Delta\Delta\mathrm{CT}} = 2^{-(\Delta\mathrm{CT\ treated\ sample} - \Delta\mathrm{CT\ untreated\ control})}$$

ΔC_T treated sample = C_T gene of interest – C_T internal control

ΔC_T untreated control = C_T gene of interest – C_T internal control

The C_T value – also known as threshold cycle – defines the cycle number at which the signal of the reaction reaches the threshold [81].

3.6. Western blot

RI-1, U2932, SuDHL4, Karpas-422, Raji and BL-2 cell lines were fasted with 0,4g/l glucose and 1% FBS and further processed for Western blot analysis. By adding 100µL RIPA buffer (Sigma-Aldrich, Germany) containing Protease inhibitor (100x; Thermo Fisher Scientific, Waltham, MA, USA) and phosphatase inhibitors and freezing/thawing the sample in liquid nitrogen for three times the lysate was prepared. Protein concentrations were determined by using the Lowry Protein Assay using the DC™ protein assay kit (Bio-Rad; Hercules, CA) according to manufacturer's protocol.

20µg/10µL of samples Precision Plus Protein Dual Color Standard (Bio-Rad, Hercules, CA, USA) were loaded on 8% or 10% polyacrylamide gel and separated at 90V for 90 minutes. Afterwards the transfer to PDVF (Bio-Rad, Hercules, CA, USA) membranes, which were activated in methanol for 1 minute, was performed with 400mA for 90min at 4°C.

Blocking of the membrane was performed by using 5% non-fat dry milk, solved in TBST (TBS (Bio-Rad, Hercules, CA, USA) with 1% Tween 20 (Croda International PLC, Snaith, UK), for one hour to prevent unspecific binding of the antibodies. The antibodies bought from Cell Signalling Technology (Danvers, MA) were diluted and attached similar to the manufacture's instruction.

Table 4 Used primary antibodies in western blot analysis

1st antibody	molecular weight [kDa]	5% BSA or non-fat dry milk	Dilution	2nd antibody
NF-κB p65 (C22B4)	45	5% BSA	1:1000	Anti-rabbit
Phospho-NF-κB p65 (Ser536)	65	5% BSA	1:1000	Anti-rabbit
NF-κB2 p100/p52 (D7A9K)	120; 52	5% BSA	1:1000	Anti-rabbit
Phospho-NF-κB2 p100 (Ser866/870)	110	5% BSA	1:1000	Anti-rabbit
NIK	125	5% BSA	1:1000	Anti-rabbit
p53 (7F5)	53	5% BSA	1:1000	Anti-rabbit

Primary antibody incubation was performed over night at 4°C. As second antibody the HRP-linked anti-rabbit IgG antibody (Cell Signalling Technology; Danvers, MA) was used, incubating the membrane for one hour at room temperature. Finally, the detection was performed by using WesternBright ECL- HRP substrate (Advansta, Menlo Park, CA, USA), measured by the ChemiDoc Imaging System (Bio-Rad, Hercules, CA, USA). The ImageJ software (Bio-Rad; Hercules, CA, USA) was used to quantify the signals.

3.7. Annexin V staining

RI-1 and U2932 were treated with Ibrutinib after 24 hours prefasting with 37°C under same fasting conditions (0,4g/L glucose and 1% FBS). After 24- and 48-hours of treatment, a $2x10^5$ cell suspension were further processed for Annexin V and 7AAD staining by using FACS LSR II device (Becton Dickinson, Franklin Lakes, NJ, USA) and the FACSDiva software.

3.8. Statistical analysis

The statistical analysis was performed with Microsoft Excel version 1902 (Microsoft, Redmond, Washington, USA) and GraphPad Prism version 5.01 for Windows (GraphPad Software, La Jolla, California, USA). T-test and Mann-Whitney-U Test were applied on the RT-qPCR data to define significant differences in expression. IC_{50} values were determined using the four-parameter logistic curve.

4. Results

4.1. Optimization of fasting conditions for GCB-DLBCL, ABC-DLBCL subtypes and Burkitt lymphoma

4.1.1. Optimizing glucose fasting conditions

To develop an optimal fasting condition, ABC-DLBCL (RI-1, U2932), GCB-DLBCL (SuDHL4, Karpas-422) and Burkitt lymphoma (Raji, BL-2) cell lines were cultured in varying glucose levels (0; 0.2; 0.4; 0.6; 0.8; 1; 1.2; 1.4; 1.6; 1.8g/L) and FBS concentrations (1; 2.5; 5; 10%) in presence of insulin. After 24 hours of fasting MTS assays were performed to assess cell growth.

As shown in figure 11 and 12, reduced FBS levels caused reduced cell growth for all cell lines (Whitney-U-Test; $p < 0.001$) compared to cells cultured in 10% FBS. In contrast, the investigated cell lines were not influenced in that extend by reduced glucose levels compared to the cells cultured in 1.8g/L glucose. As a result, for further experiments a glucose concentration between 0.4g/L to 1g/L glucose and a protein concentration of 2.5% - 5% FBS have been chosen. At these concentration levels the cell lines obtain a good reproducing number and fasting effects show the highest difference compared with the control.

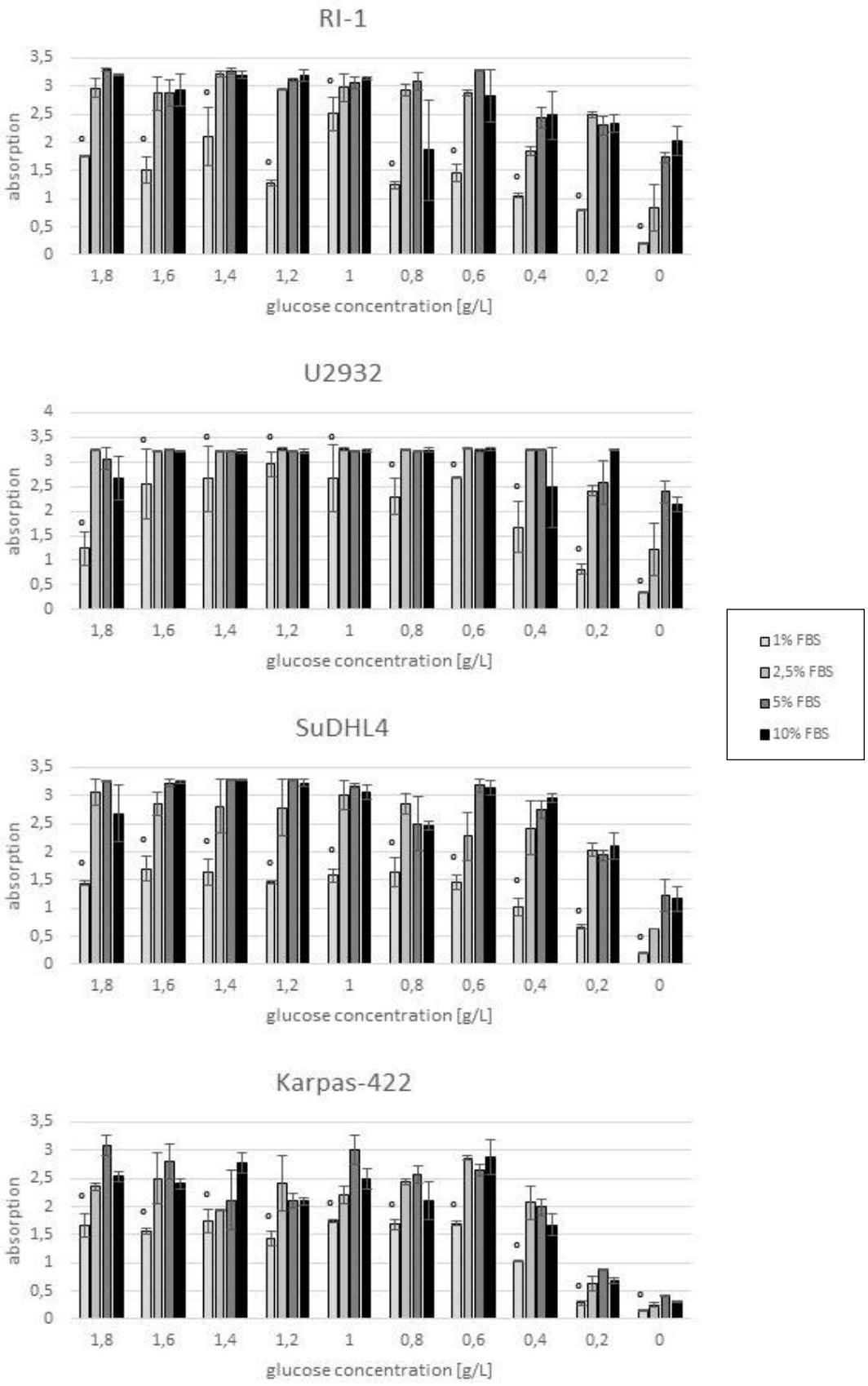

Figure 11 Comparison of cell lines under different glucose fasting conditions 1.
Cell growth of RI-1 and U2932 (as ABC-DLBCL model) and SuDHL4 and Karpas-422 (as GCB-DLBCL model) cell lines under different fasting conditions (1; 2.5; 5; 10% FBS) and reduced glucose levels (0; 0.2; 0.4; 0.6; 0.8; 1; 1.2; 1.4; 1.6; 1.8g/L glucose) as determined by the EZ4U proliferation assay and depicted as absorption at 492nm after 24 hours. ° = p-value < 0,001 compared to the control (10% FBS). Each bar represents the mean ± standard of the mean.

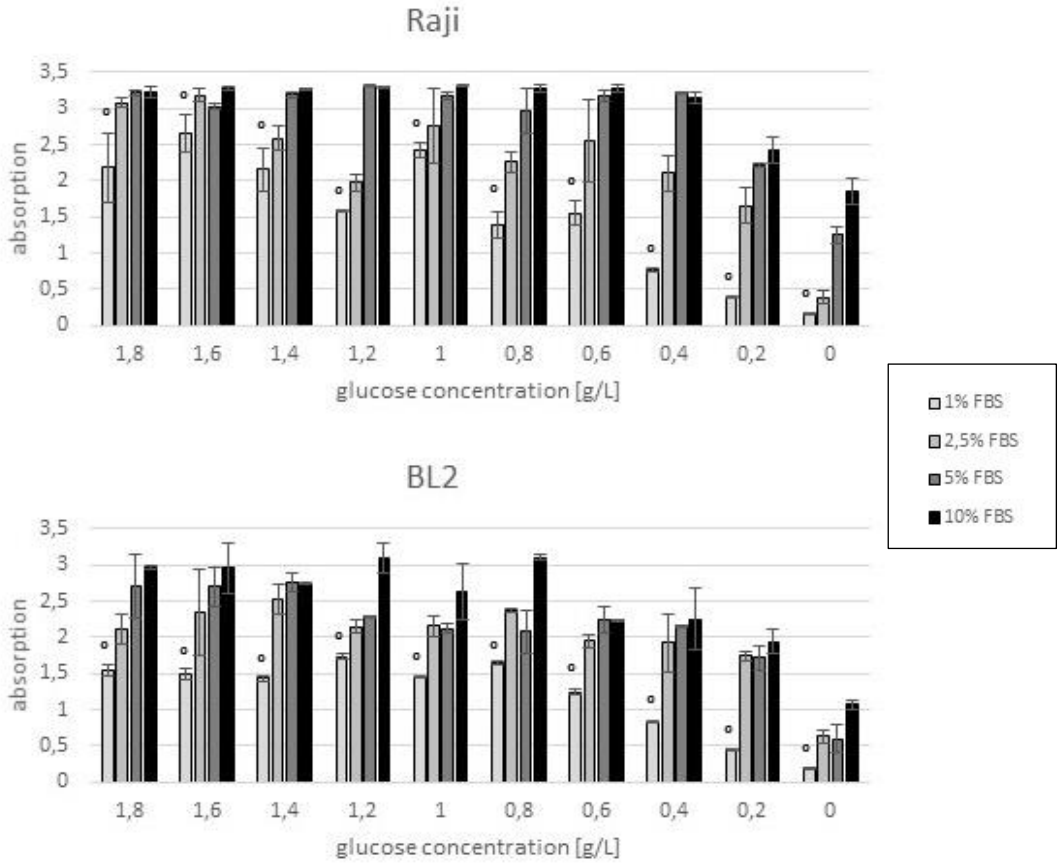

Figure 12 Comparison of cell lines under different glucose fasting conditions 2.
Cell growth of Raji and BL-2 (as Burkitt lymphoma model) cell lines under different fasting conditions (1; 2.5; 5; 10% FBS) and reduced glucose levels (0; 0.2; 0.4; 0.6; 0.8; 1; 1.2; 1.4; 1.6; 1.8g/L glucose) as determined by the EZ4U proliferation assay and depicted as absorption at 492nm after 24 hours. ° = p-value < 0.001 compared to the control (10% FBS). Each bar represents the mean ± standard of the mean.

4.1.2. Ibrutinib-treatment

To determine cell growth inhibitors effects of Ibrutinib-treatment under unfasted conditions, ABC-DLBCL (RI-1, U2932), GCB-DLBCL (SuDHL4, Karpas-422), Burkitt lymphoma (Raji, BL-2) and T-cell lymphoma (Jurkat) were treated with Ibrutinib concentrations (0; 0.25; 0.5; 1; 2.5; 5; 7.5; 10; 20; 30; 40; 50µM) under normal conditions (2g/L glucose, 10% FBS) followed by MTS assay to assess cell growth after 72h of treatment.

ABC-DLBCL cell lines - RI-1 and U2932 - (figure 13a) were more resistant than the GCB-DLBCL -SuDHL4 and Karpas422 - (figure 13b) and the Burkitt cell lines - Raji and BL-2 – (figure 13c). Interestingly, Ibrutinib treatment had growth inhibitory effects on Jurkat cell line, originated from the T cell lymphoma cells (figure 13c).

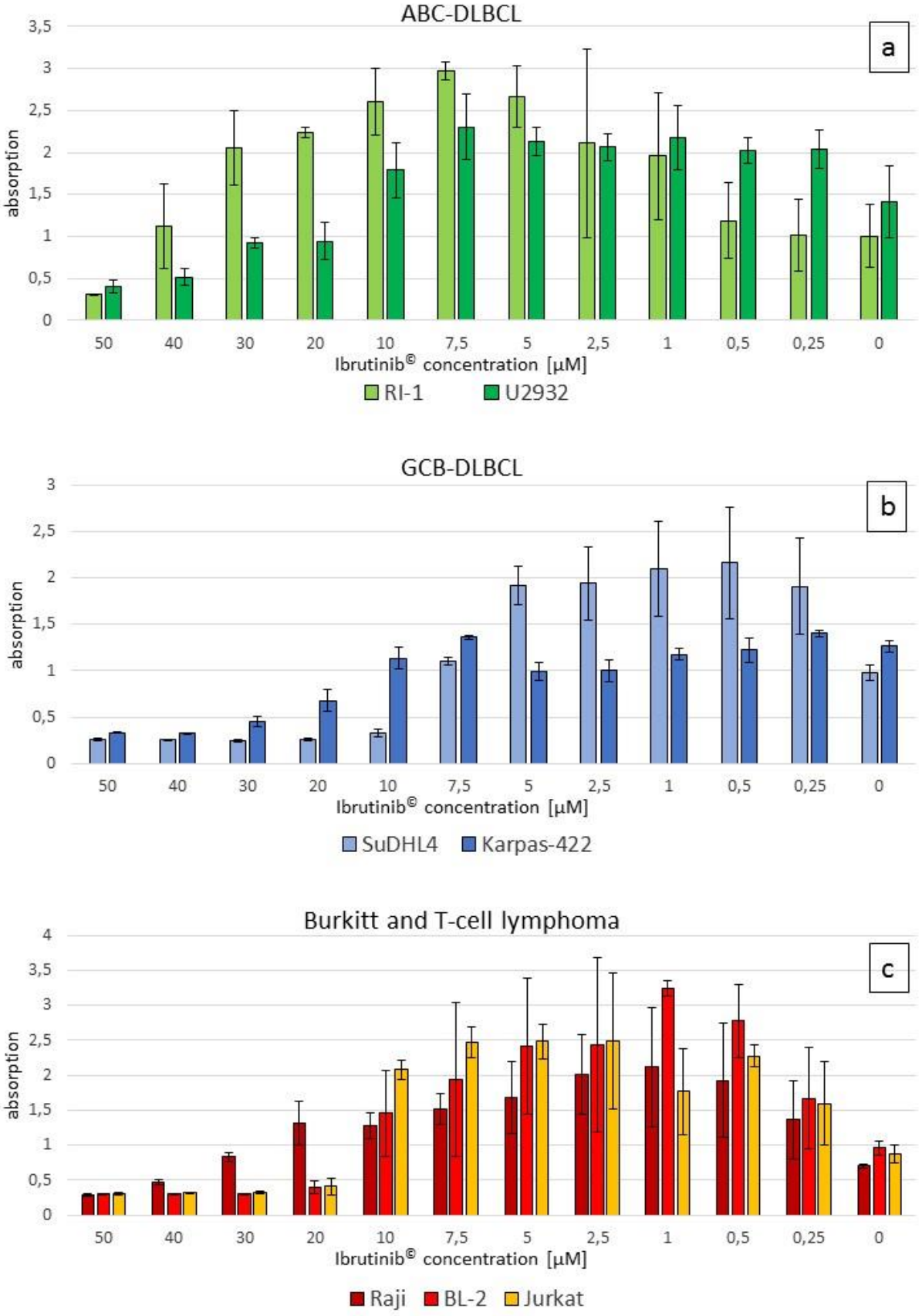

Figure 13 Viability analysis under Ibrutinib-treatment.
Cell growth of RI-1 and U2932 (as ABC-DLBCL model; a), SuDHL4 and Karpa422 (as GCB-DLBCL model; b), Raji and BL-2 (as Burkitt lymphoma model; c) and Jurkat (as T-cell lymphoma model; c) cell lines under Ibrutinib treatment (0; 0.25; 0.5; 1; 2.5; 5; 7.5; 10; 20; 30; 40; 50µM) as determined by the EZ4U proliferation assay and depicted as absorption at 492nm after 72 hours. Each bar represents the mean ± standard of the mean.

4.2. Ibrutinib-treatment under protein fasting conditions

To determine the impact of protein reduction on the cell growth inhibitory effects of Ibrutinib, ABC-DLBCL (RI-1, U2932), GCB-DLBCL (SuDHL4, Karpas-422) and Burkitt lymphoma (Raji, BL-2) cell lines were prefasted in a media containing normal glucose levels (2g/L) and reduced protein concentration (0; 1; 2.5; 10% FBS). After 24h the prefasted cell lines were treated with different concentration of Ibrutinib (0; 0.25; 0.5; 1; 2.5; 5; 7.5; 10; 20; 30; 40; 50µM) followed by MTS assays after 24, 48 and 72h to assess the cell growth.

Under FBS reduction, the growth inhibitory effects of Ibrutinib were particularly elevated for all investigated lymphoma cells, as shown in Table 5 (RI-1, SuDHL4, Raji: figure 14 – 16) and the attachment (U2932, Karpas-422, BL-2), except for Karpas-422. In this cell line cell growth was reduced under FBS fasting.

Table 5 Comparison of IC_{50} of unfasted vs protein-fasted cell lines
The data represents the IC_{50} of the tested 6 lymphoma entities comparing fasted (2g/L glucose, 0% FBS) conditions against unfasted (2g/L glucose, 10% FBS – for Karpas-422 and BL-2 20% FBS were applied) ones after 24 hours.

Cell line	IC_{50} unfasted [µM]	IC_{50} fasted [µM]
RI-1	24,19	17,80
U2932	20,34	13,02
SuDHL4	14,77	9,77
Karpas-422	9,56	N/A
Raji	24,51	13,00
BL-2	22,61	14,58

N/A denotes not applicable because the cell growth under reduce protein concentrations was overall reduced in the fasted Karpas-422 cell line.

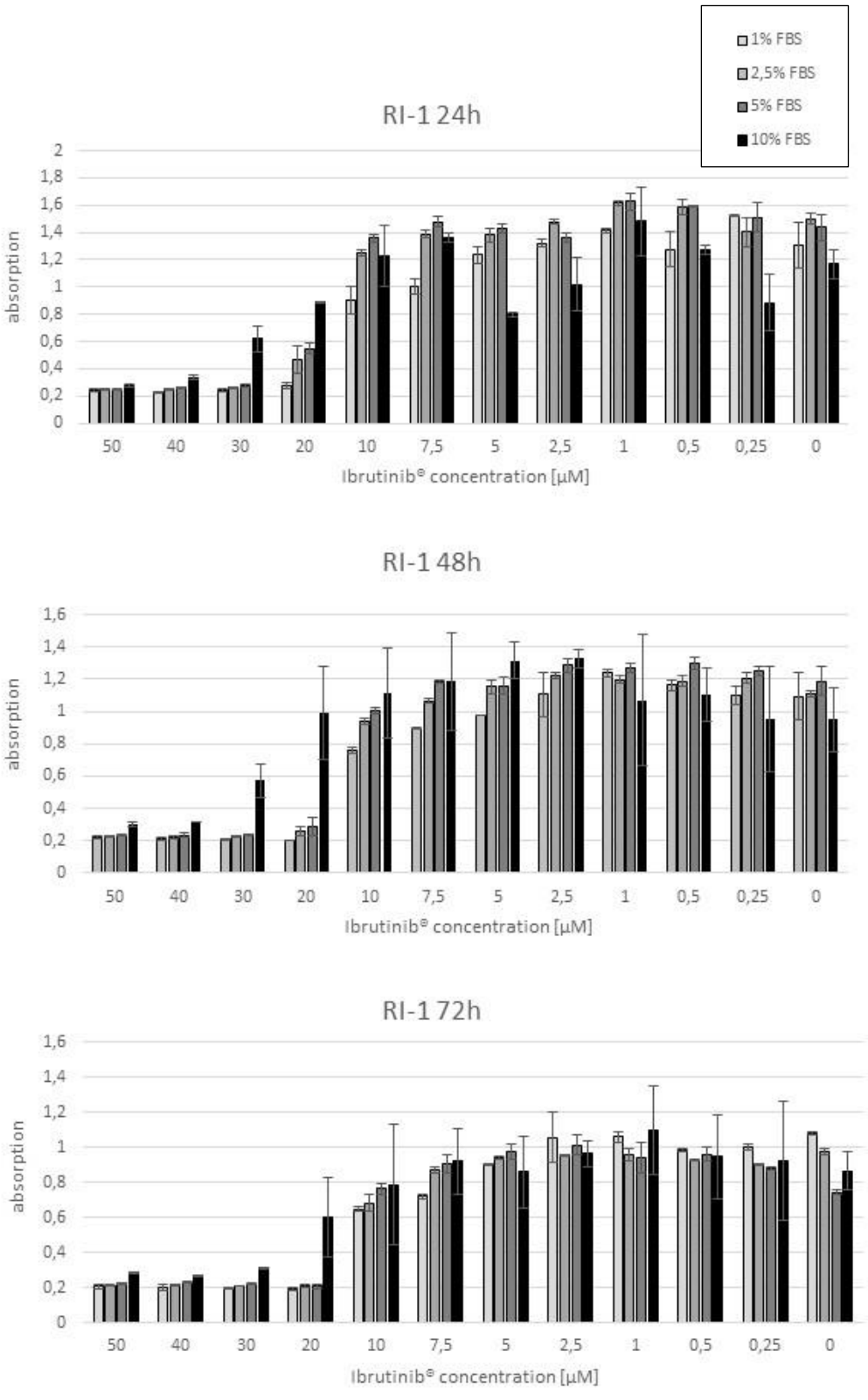

Figure 14 Cell growth of ABC-DLBCL cell line RI-1 under Ibrutinib and protein fasting conditions.
Cell growth of RI-1 (as ABC-DLBCL model) cell line under different FBS fasting conditions (1; 2.5; 5; 10% FBS) and Ibrutinib treatment (0; 0.25; 0.5; 1; 2.5; 5; 7.5; 10; 20; 30; 40; 50µM) as determined by the EZ4U proliferation assay and depicted as absorption at 492nm after 24, 48 and 72 hours. Each bar represents the mean ± standard of the mean.

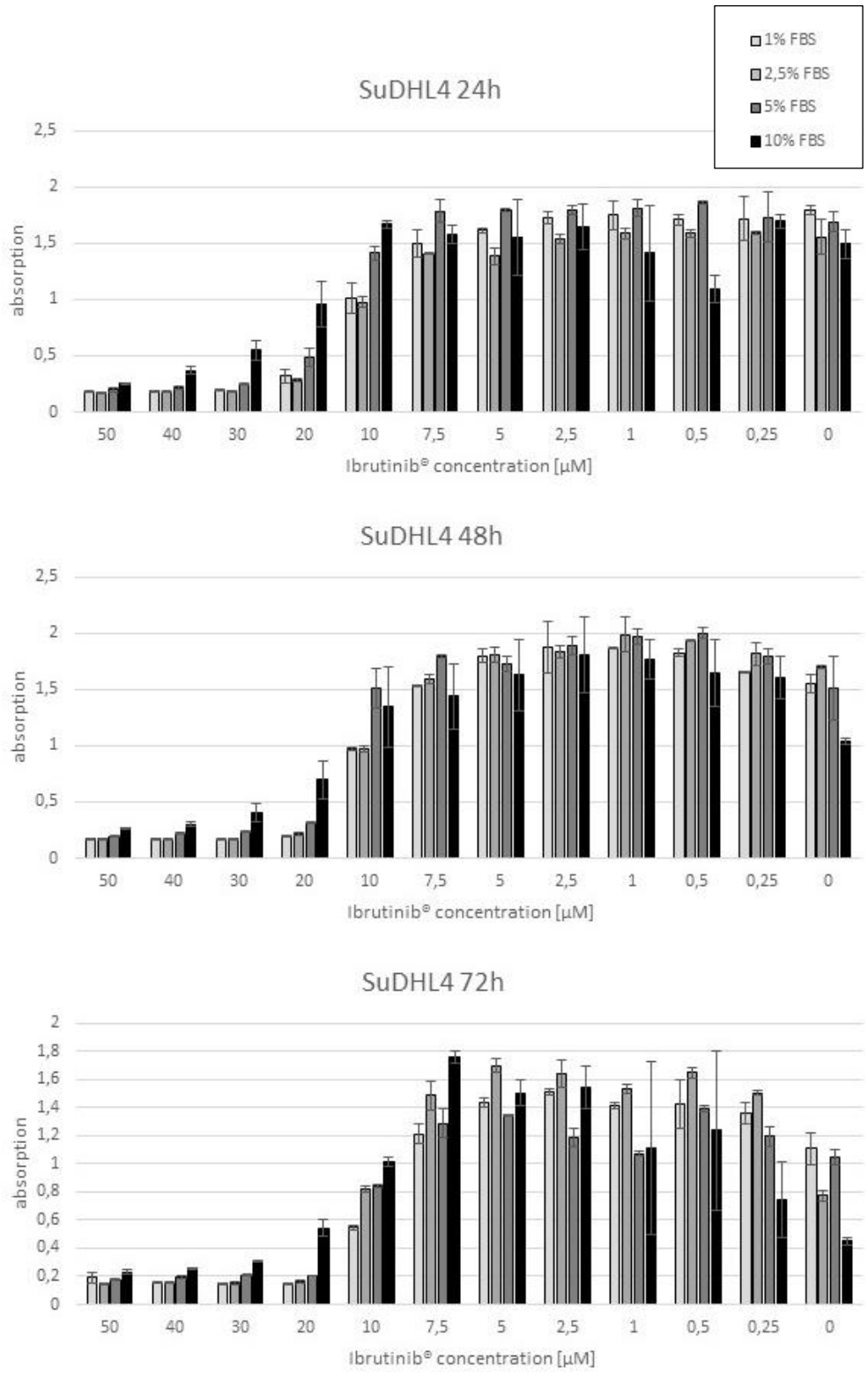

Figure 15 Cell growth of GCB-DLBCL cell line SuDHL4 under Ibrutinib and protein fasting conditions.
Cell growth of SuDHL4 (as GCB-DLBCL model) cell line under different FBS fasting conditions (1; 2.5; 5; 10% FBS) and Ibrutinib treatment (0; 0.25; 0.5; 1; 2.5; 5; 7.5; 10; 20; 30; 40; 50µM) as determined by the EZ4U proliferation assay and depicted as absorption at 492nm after 24, 48 and 72 hours. Each bar represents the mean ± standard of the mean.

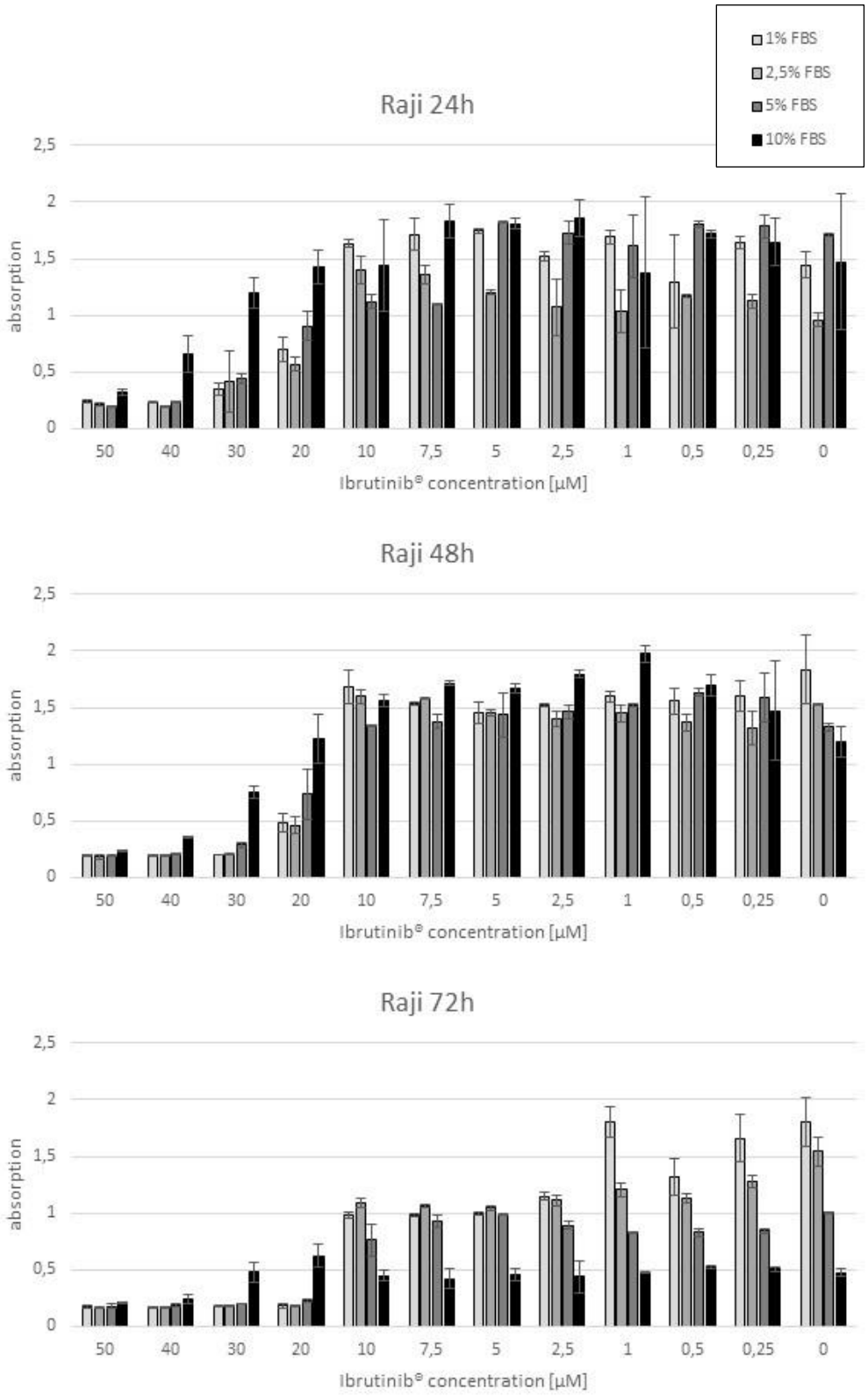

Figure 16 Cell growth of Burkitt lymphoma cell line Raji under Ibrutinib and protein fasting conditions. Cell growth of Raji (as Burkitt lymphoma model) cell line under different FBS fasting conditions (1; 2.5; 5; 10% FBS) and Ibrutinib treatment (0; 0.25; 0.5; 1; 2.5; 5; 7.5; 10; 20; 30; 40; 50µM) as determined by the EZ4U proliferation assay and depicted as absorption at 492nm after 24, 48 and 72 hours. Each bar represents the mean ± standard of the mean.

4.3. Ibrutinib under glucose and protein fasting

To investigate whether the combination of glucose and protein fasting impacts on effects of Ibrutinib, RI-1 cell line was prefasted with reduced FBS concentrations (2.5% FBS) and glucose levels (0.4; 0.6; 0.8g/L). After 24h the prefasted cell line was treated with different concentration of Ibrutinib (0; 0.25; 0.5; 1; 2.5; 5; 7.5; 10; 20; 30; 40; 50µM) followed by MTS assays after 24h to assess the cell growth.

Protein and glucose fasted RI-1 cells were more sensitive to Ibrutinib treatment as shown by the reduced cell growth rates (figure 17; Whitney-U-Test; $p < 0{,}001$). Interestingly, under these conditions the cell growth of the RI-1 cell line was significantly inhibited by the lowest tested Ibrutinib concentration.

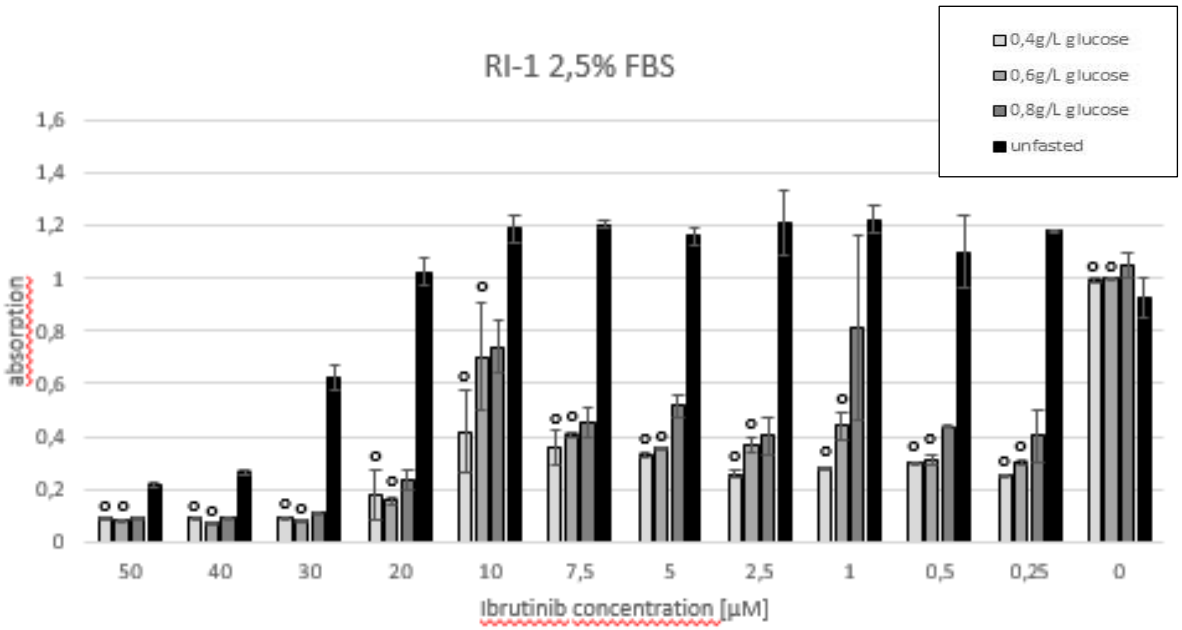

Figure 17 Analysis of changing viability status due to double-fasting treatment.
Cell growth of RI-1 (as ABC-DLBCL model) cell line under reduced FBS (2.5% FBS) and glucose concentrations (0.4; 0.6; 0.8g/L glucose) and Ibrutinib treatment (0; 0.25; 0.5; 1; 2.5; 5; 7.5; 10; 20; 30; 40; 50µM) as determined by the MTS proliferation assay and depicted as absorption at 492nm after 24 hours. Each bar represents the mean ± standard of the mean. The black bar describes the untreated control group (2g/L glucose 10% FBS). ° = p-value < 0.001 compared to the control (2g/L glucose).

4.4. Fasting in combination with Ibrutinib treatment induces higher apoptosis rates

To investigate the apoptotic effect of fasting in combination with Ibrutinib treatment, an Annexin V and 7AAD staining was conducted. The ABC-DLBCL cell lines RI-1 and U2932, both possessing low response rate towards Ibrutinib (based on the experiments above), were fasted for 24 and 48 hours with 0.4g/L glucose and 5% FBS. After 24 hours of Ibrutinib treatment a significant higher percentage of RI-1 cells stained positively for Annexin V under fasted condition compared to unfasted controls (40µM, 30.5% vs 13.6%, $p < 0.002$), while there was no detectable effect in lower Ibrutinib concentrations (0.25µM, 17.8% vs 21.4%, $p < 0.09$; figure

18). Remarkable, after 48h of treatment the effects were even more pronounced (40µM, 30.3% vs 3.9% $p < 0.009$; 0.25µM, 36.1% vs 15.4%, $p < 0.03$; figure 18).

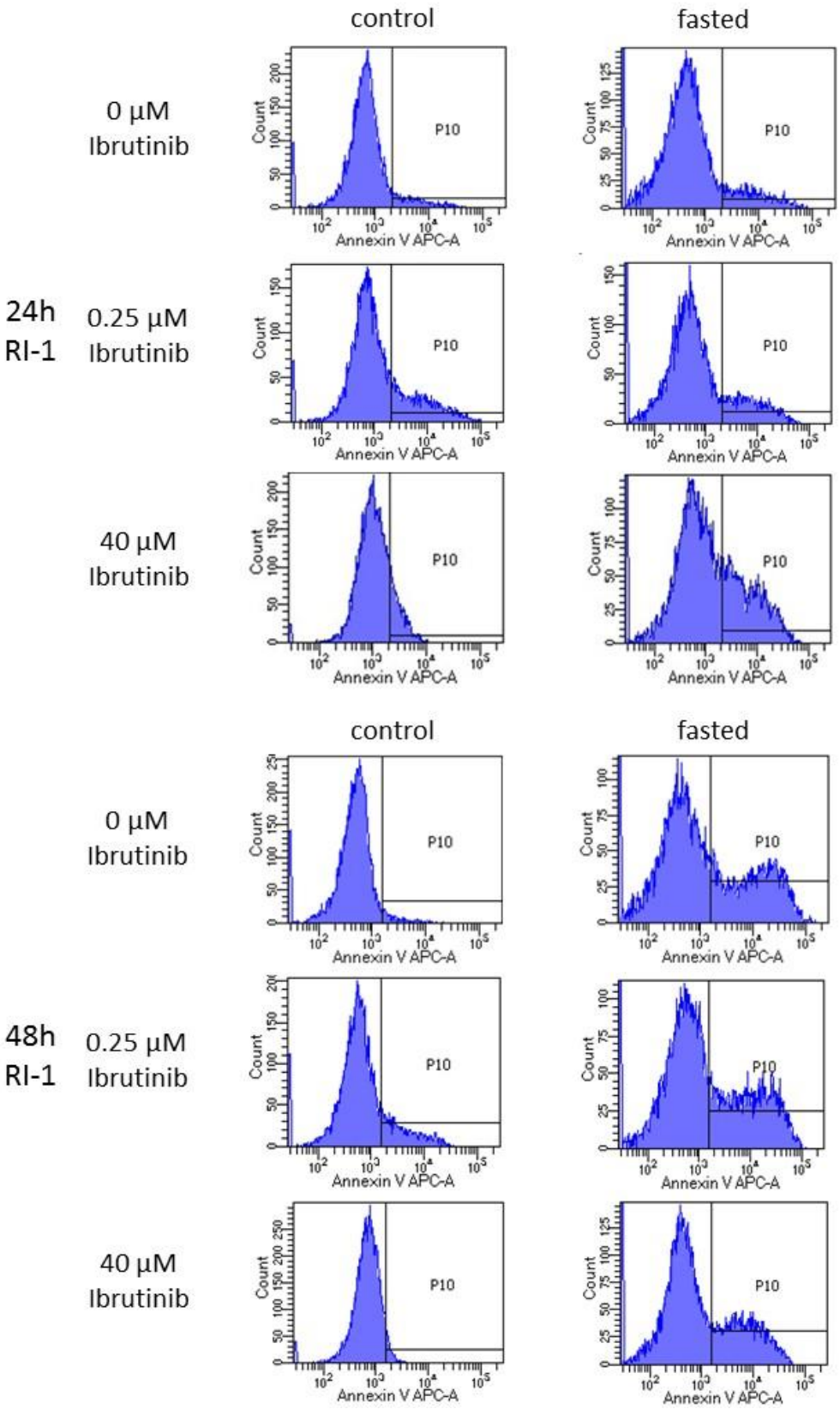

Figure 18 Quantitative comparison of apoptosis rates in different Ibrutinib treated RI-1 ABC-DLBCL.
After 24- and 48-hours prefasting RI-1 samples (0.4g/L glucose; 5% FBS) and an unfasted control RI-1 (2g/L glucose, 10% FBS) received Ibrutinib treatment (0; 0.25; 40µM).

Similar findings were observed for the U2932 cell line: After 24 hours a higher percentage of cells stained positively for Annexin V under glucose and protein fasting condition upon Ibrutinib concentrations compared to unfasted controls (0.25µM, 26.7% vs 7.2%, p = 0.002, and 40µM, 44.5% vs 39.3% p < 0.39, figure 19). After 48 hours similar to RI-1 fasting led to a higher rate of Annexin V staining in low (0.25µM, 33.6% vs 3.8% p < 0.007) and high Ibrutinib concentrations (40µM, 39.4% vs 23% p < 0.03, figure 19).

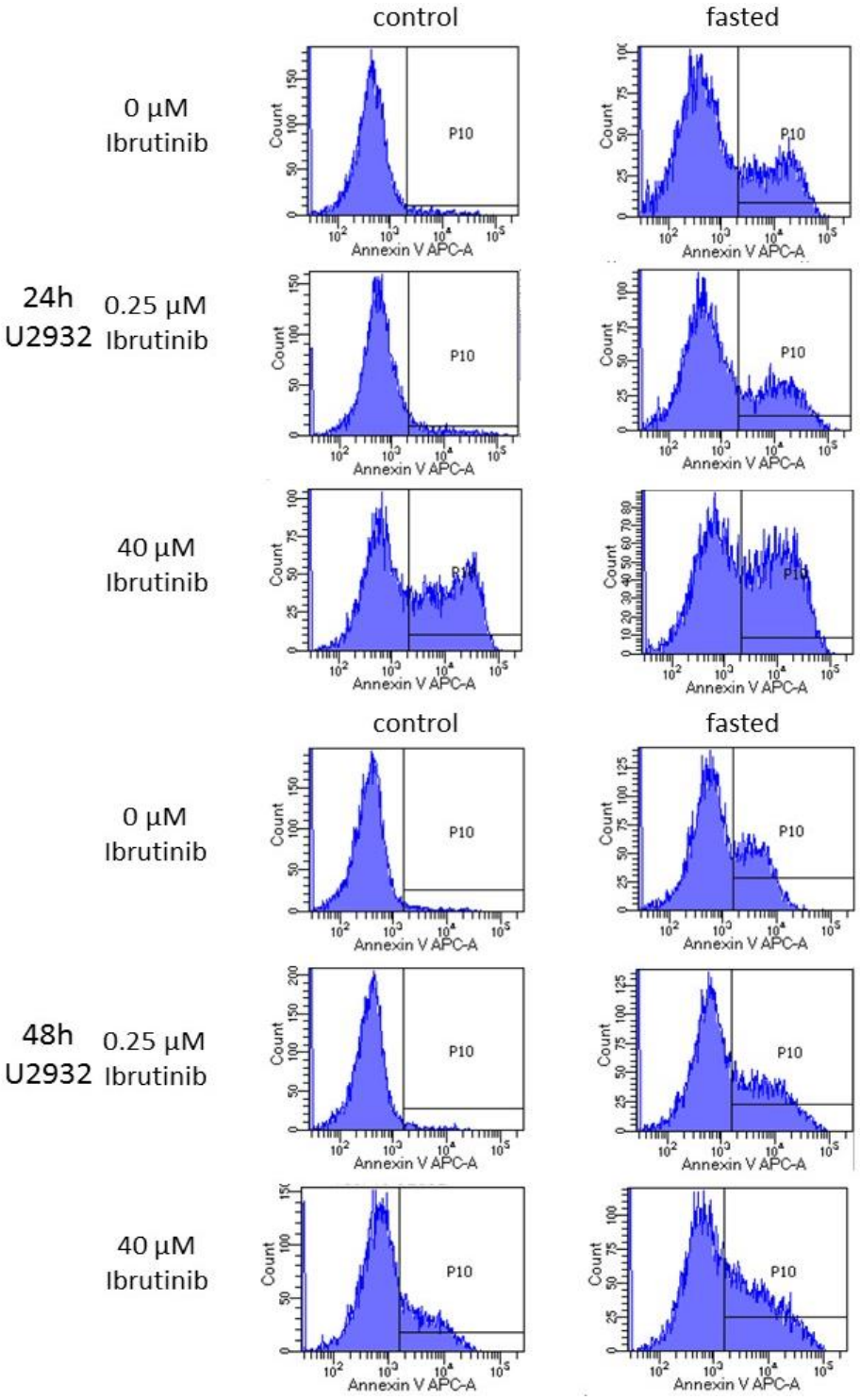

Figure 19 Quantitative comparison of apoptosis rates in different Ibrutinib treated U2932 ABC-DLBCL. After 24 and 48 hours prefasting U2932 samples (0.4g/L glucose; 5% FBS) and an unfasted control U2932 (2g/L glucose, 10% FBS) received Ibrutinib treatment (0; 0.25; 40 µM).

4.5. mRNA expression analysis of oncogenic/apoptotic pathways in nutrients-fasted cell lines

To gain knowledge whether fasting effects the oncogenic and/or apoptotic pathways, mRNA expression of known target genes of the NF-κB pathway (n=5), the MAPK pathway (n=4) and the PI3-Kinase/Akt pathway (n=8) were analysed by RT-qPCR. In table 6, 17 genes related to these pathways are listed. The ABC-DLBCL (RI-1, U2932), GCB-DLBCL (SuDHL4, Karpas 422) and Burkitt lymphoma (Raji, BL-2) cell lines were fasted for 24h with different glucose levels (0.4; 0.6; 0.8; 1g/L) and protein concentrations (2.5% and 5% FBS).

Table 6 In the RT-qPCR analysed target genes and pathways

	Target genes
NF-κB pathway	CCL3, CCL4, TNF1, RGS1, BCL2A1
MAPK pathway	OAS3, EGR1, EGR3, KLF10
PI3-Kinase/Akt pathway	cFOS, Bub1, MxD1, JunB, JunC, DUSP1, ETV5, CCND2

4.5.1. NF-κB pathway

In the RI-1 cell line (ABC-DLBCL) protein and glucose fasting led to an upregulation of *CCL3* (4.8-fold, $p < 0.01$; T-test), *CCL4* (5.0-fold, $p < 0.05$) and *RGS1* (6-fold, $p < 0.05$). In contrast, no change in expression of *TNF1* and *BCL2A1* was detectable (figure 20).

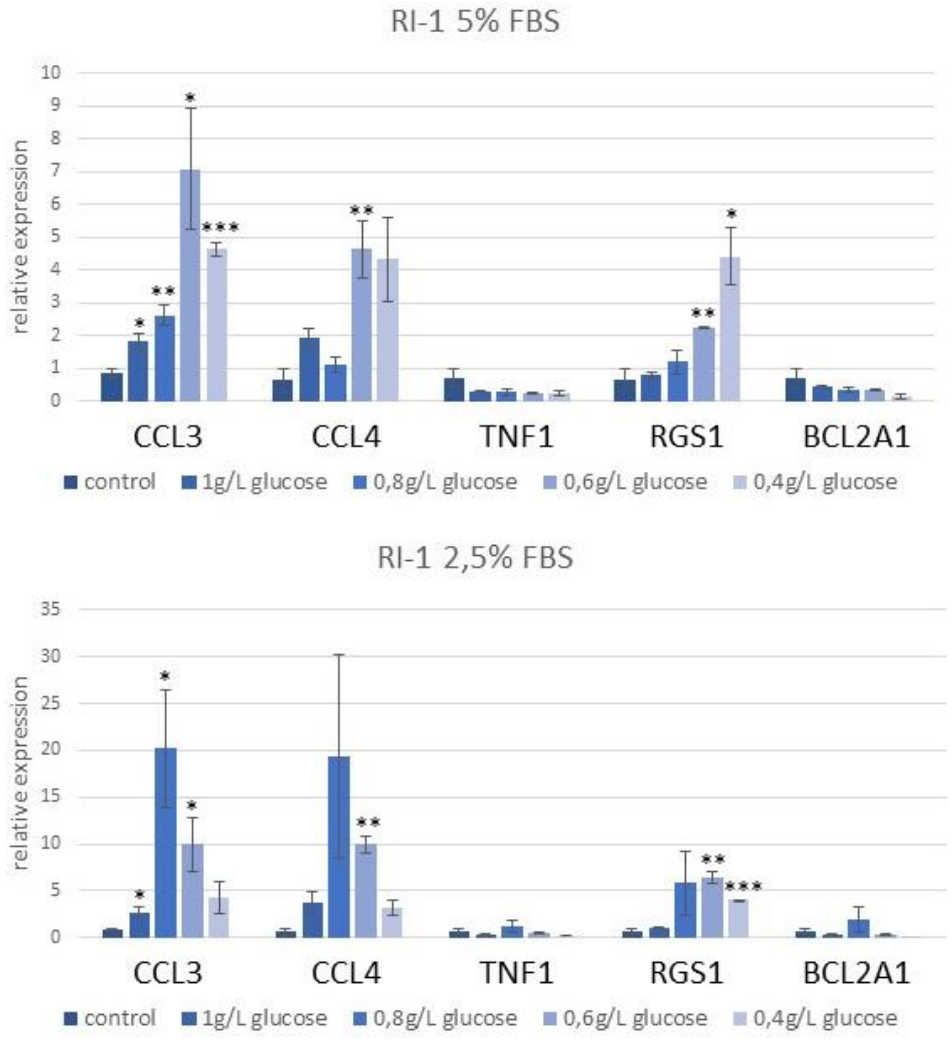

Figure 20 Analysis of significant upregulated target genes (*CCL3, CCL4, RGS1, TNF1* and *BCL2A1)* of the NF-κB pathway under fasting conditions in the ABC-DLBCL RI-1.
Each bar represents the mean median of the relative mRNA expression plus/minus standard error of the mean. The glucose and protein fasted samples were compared with the untreated controls (10% FBS; 2g/L glucose). * = p-value < 0.1; ** = p-value < 0.05; *** = p-value < 0.01. The different colours indicate different glucose fasting conditions (0.4; 0.6; 0.8; 1g/L glucose). In addition, the % in the title define the FBS concentration (either 2.5% or 5% FBS).

In the ABC-DLBCL U2932 protein and glucose fasting also caused higher mRNA levels. *CCL3* (15.8-fold, $p < 0.01$) and *CCL4* (11.6-fold, $p < 0.01$) were upregulated. In contrast, *RGS1* (1.8-fold, $p < 0.05$) was down-regulated and *BCL2A1* expression levels were unaffected (figure 21).

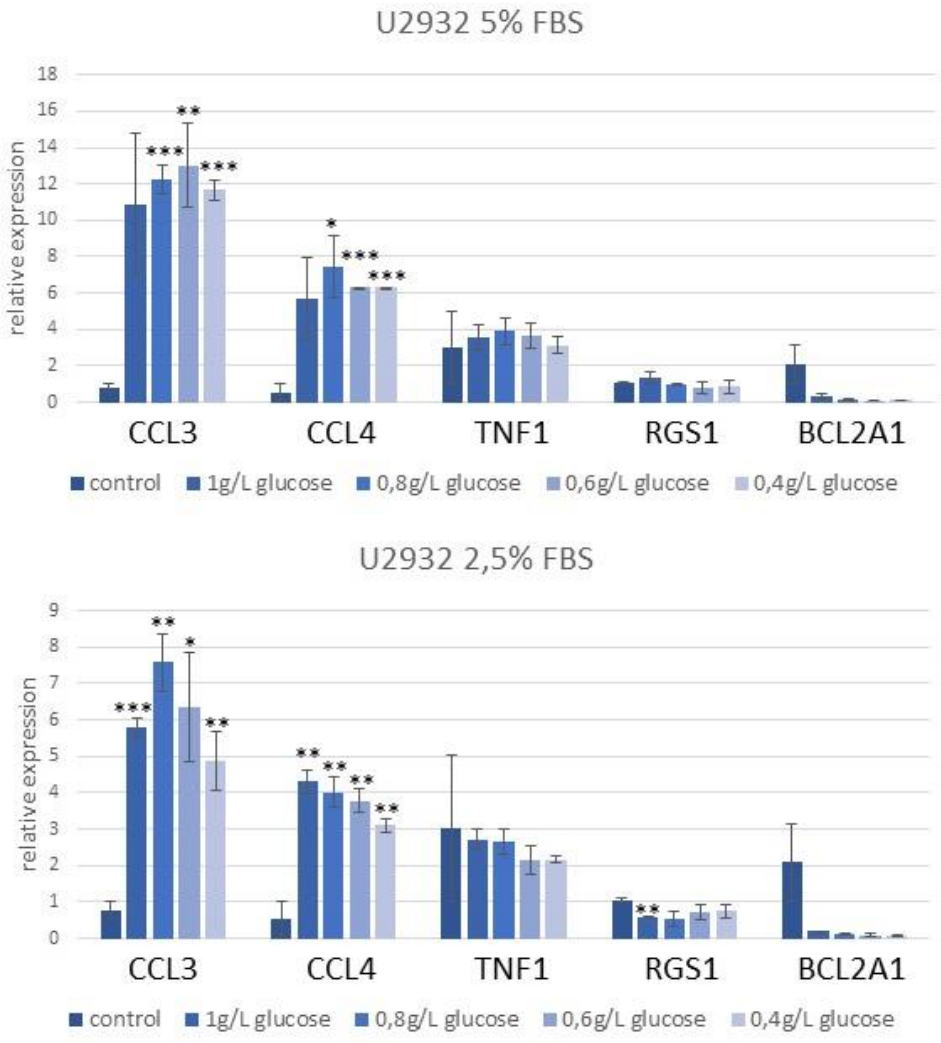

Figure 21 Analysis of significant upregulated target genes (*CCL3, CCL4, RGS1, TNF1* and *BCL2A1)* of the NF-κB pathway under fasting conditions in the ABC-DLBCL U2932.
Each bar represents the mean median of the relative mRNA expression plus/minus standard error of the mean. The glucose and protein fasted samples were compared with the untreated controls (10% FBS; 2g/L glucose). * = p-value < 0.1; ** = p-value < 0.05; *** = p-value < 0.01. The different colours indicate different glucose fasting conditions (0.4; 0.6; 0.8; 1g/L glucose). In addition, the % in the title define the FBS concentration (either 2.5% or 5% FBS).

In the GCB-DLBCL SuDHL4 cell line reduction of glucose and protein led to an upregulation in four of the five investigated genes - *CCL3* (2.6-fold, $p < 0.05$), *CCL4* (3.6-fold, $p < 0.05$), *RGS1* (11.9-fold, $p < 0.05$) and *BCL2A1* (7.1 -fold, $p < 0.1$; figure 22).

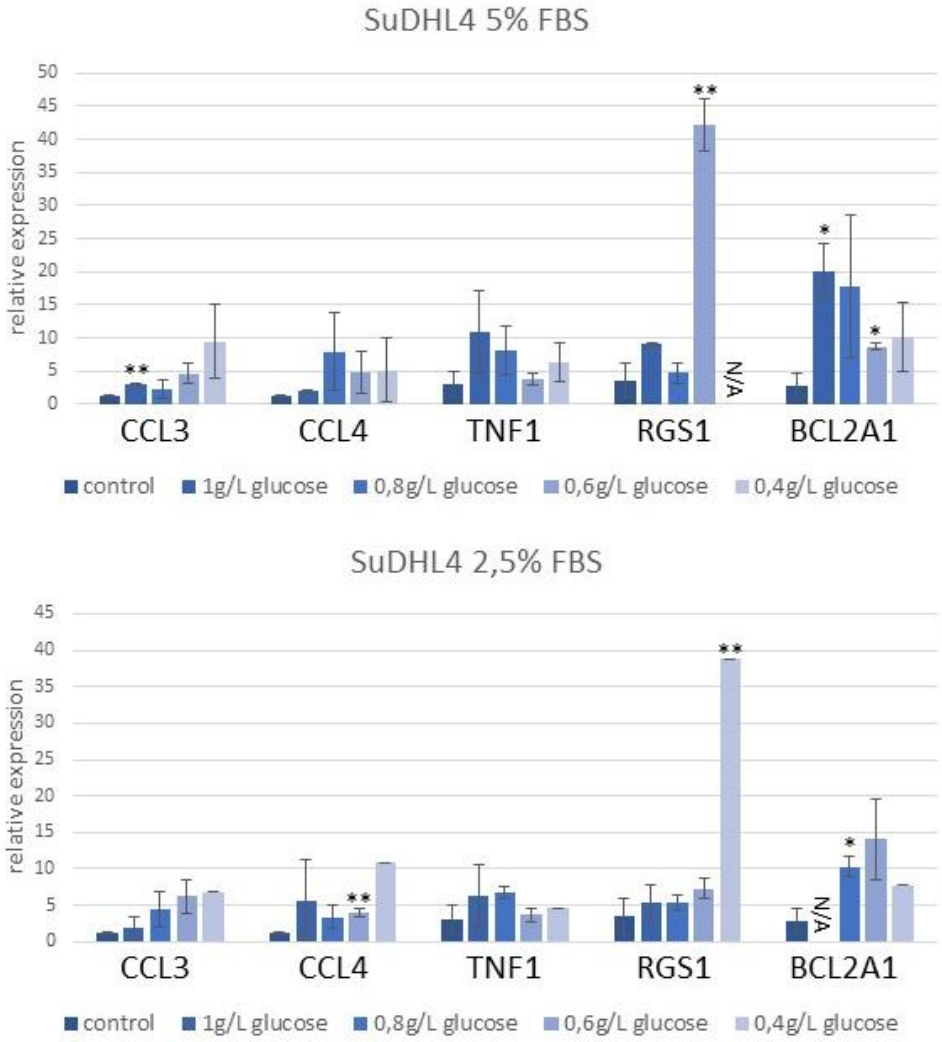

Figure 22 Analysis of significant upregulated target genes (*CCL3, CCL4, RGS1, TNF1* and *BCL2A1)* of the NF-κB pathway under fasting conditions in the GCB-DLBCL SuDHL4.
Each bar represents the mean median of the relative mRNA expression plus/minus standard error of the mean. The glucose and protein fasted samples were compared with the untreated controls (10% FBS; 2g/L glucose). * = p-value < 0.1; ** = p-value < 0.05; *** = p-value < 0.01. The different colours indicate different glucose fasting conditions (0.4; 0.6; 0.8; 1g/L glucose). In addition, the % in the title define the FBS concentration (either 2.5% or 5% FBS). N/A indicates concentrations under the detection level.

In glucose and protein fasted GCB-DLBCL Karpas-422 cell line *CCL3* (6.2-fold, $p < 0.01$) and *CCL4* (16.2-fold, $p < 0.05$) were upregulated up to 17-fold. *TNF1* (1.6-fold, $p < 0.1$) possessed an increased mRNA expression too (figure 23).

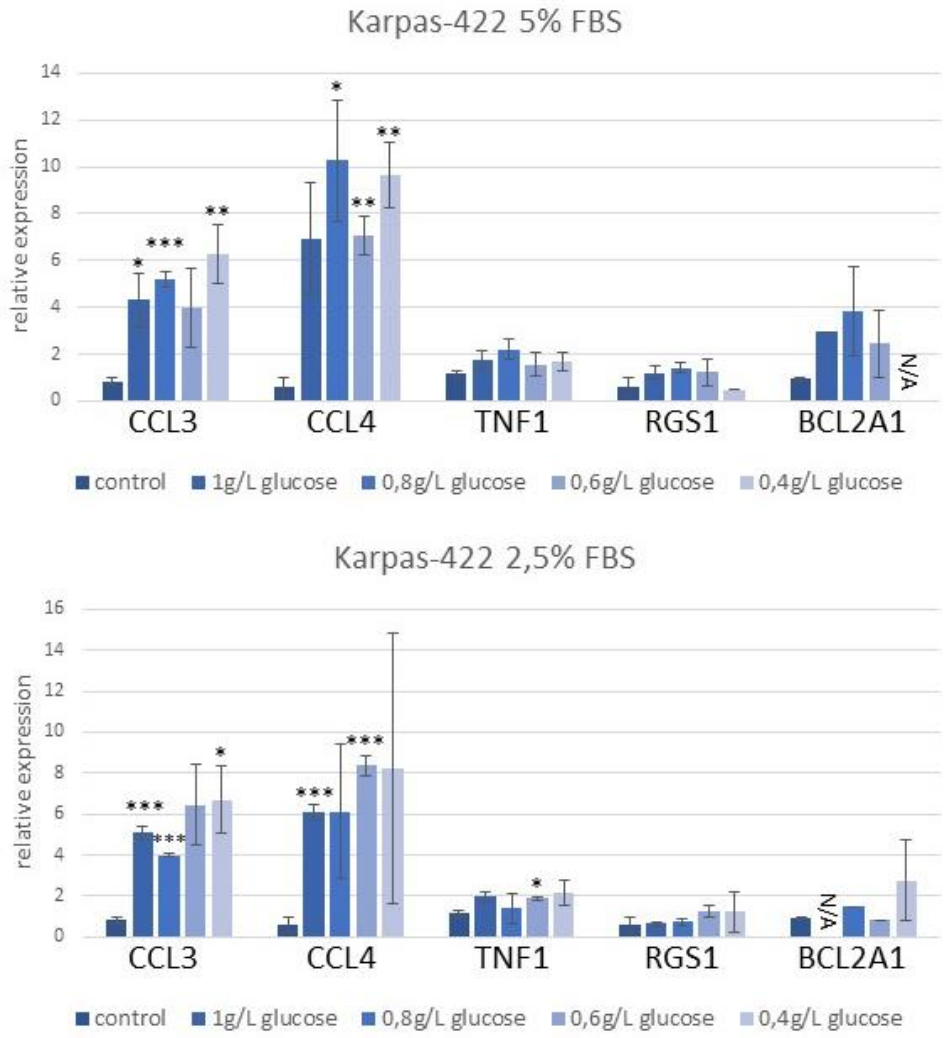

Figure 23 Analysis of significant upregulated target genes (*CCL3, CCL4, RGS1, TNF1* and *BCL2A1)* of the NF-κB pathway under fasting conditions in the GCB-DLBCL Karpas-422.
Each bar represents the mean median of the relative mRNA expression plus/minus standard error of the mean. The glucose and protein fasted samples were compared with the untreated controls (10% FBS; 2g/L glucose). * = p-value < 0.1; ** = p-value < 0.05; *** = p-value < 0.01. The different colours indicate different glucose fasting conditions (0.4; 0.6; 0.8; 1g/L glucose). In addition, the % in the title define the FBS concentration (either 2.5% or 5% FBS). N/A indicates concentrations under the detection level.

In contrast to the other cell lines, no significant deregulation of the investigated genes was observed in the Burkitt lymphoma cell line Raji under glucose and protein restriction (figure 24).

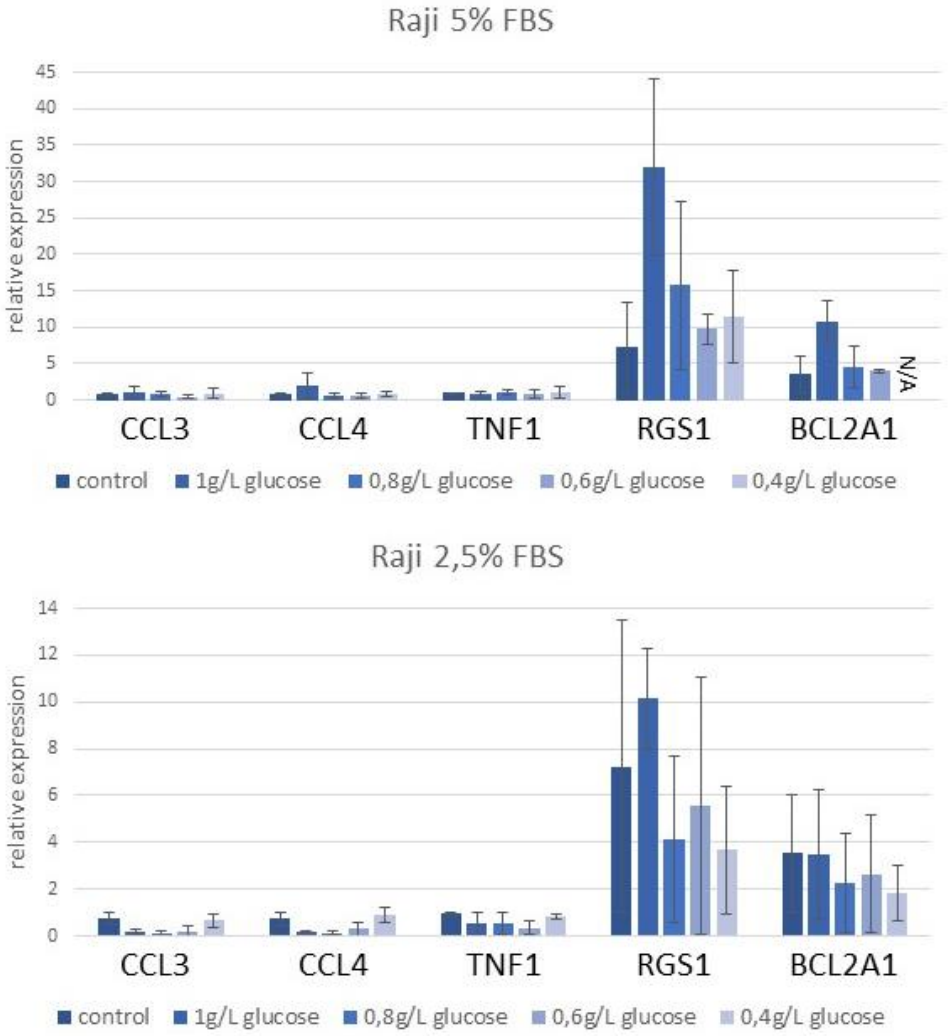

Figure 24 Analysis of significant upregulated target genes (*CCL3, CCL4, RGS1, TNF1* and *BCL2A1)* of the NF-κB pathway under fasting conditions in the Burkitt lymphoma Raji.
Each bar represents the mean median of the relative mRNA expression plus/minus standard error of the mean. The glucose and protein fasted samples were compared with the untreated controls (10% FBS; 2g/L glucose). * = p-value < 0.1; ** = p-value < 0.05; *** = p-value < 0.01. The different colours indicate different glucose fasting conditions (0.4; 0.6; 0.8; 1g/L glucose). In addition, the % in the title define the FBS concentration (either 2.5% or 5% FBS). N/A indicates concentrations under the detection level.

The Burkitt lymphoma cell line BL-2 exhibited an upregulation in four of five investigated genes under glucose and protein fasting conditions - *CCL3* (16.3-fold, $p < 0.05$), *CCL4* (4.9-fold, $p < 0.05$), *RGS1* (108-fold, $p < 0.05$) and *BCL2A1* (10.7-fold, $p < 0.01$; figure 25).

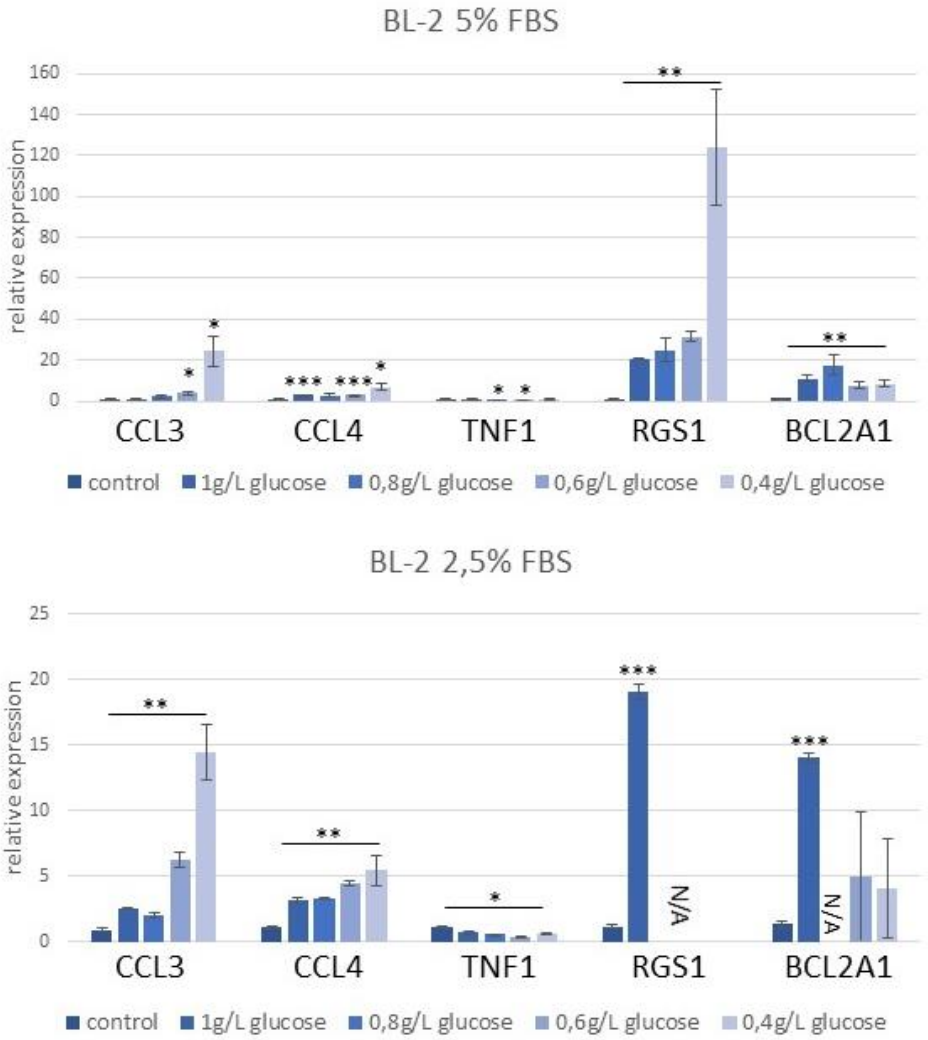

Figure 25 Analysis of significant upregulated target genes (*CCL3, CCL4, RGS1, TNF1* and *BCL2A1)* of the NF-κB pathway under fasting conditions in the Burkitt lymphoma BL-2.
Each bar represents the mean median of the relative mRNA expression plus/minus standard error of the mean. The glucose and protein fasted samples were compared with the untreated controls (10% FBS; 2g/L glucose). * = p-value < 0.1; ** = p-value < 0.05; *** = p-value < 0.01. The different colours indicate different glucose fasting conditions (0.4; 0.6; 0.8; 1g/L glucose). In addition, the % in the title define the FBS concentration (either 2.5% or 5% FBS). N/A indicates concentrations under the detection level.

4.5.2. MAPK pathway

Nutrition restriction led to an upregulation of *OAS3* (17.4-fold, $p < 0.05$), *EGR1* (5.3-fold, $p < 0.05$) and *EGR3* (14.1-fold, $p < 0.01$) in the ABC-DLBCL RI-1 (figure 26). In *KLF10* no deregulation occurred under given conditions.

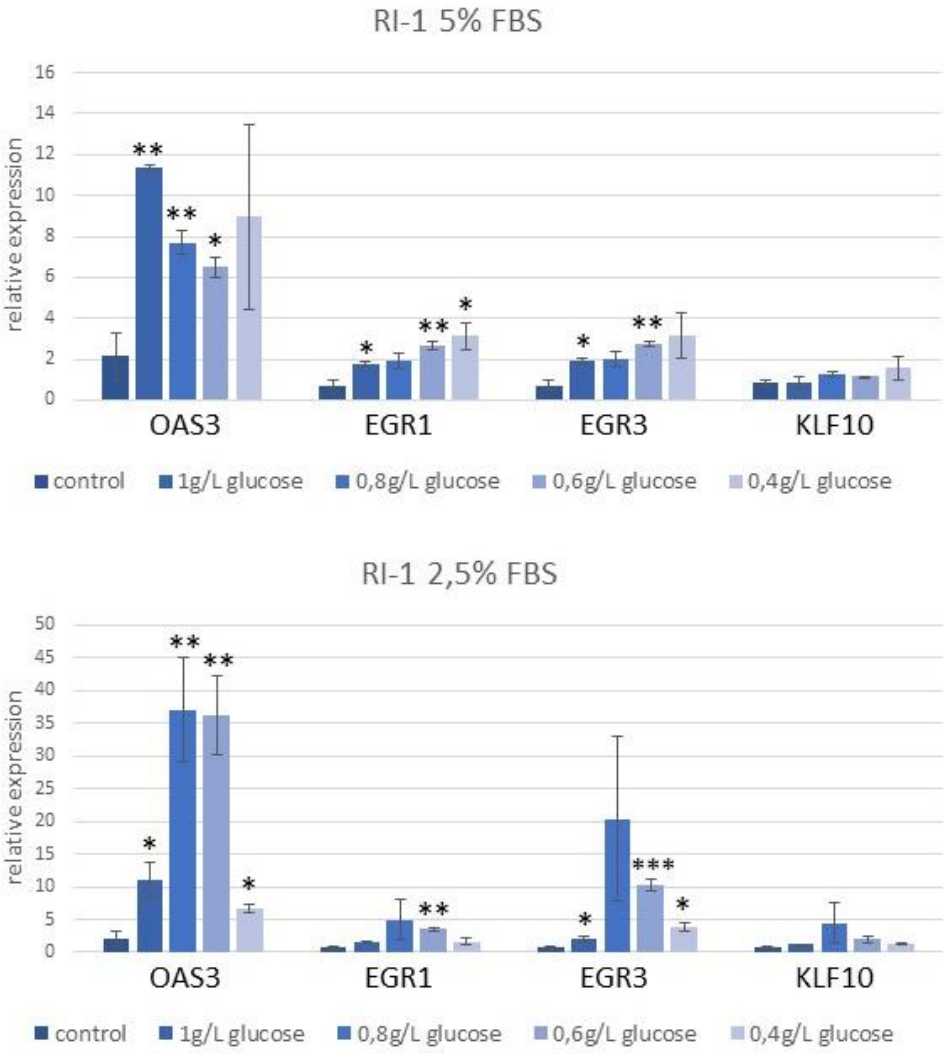

Figure 26 Analysis of significant upregulated target genes (*OAS3, EGR1, EGR3* and *KLF10*) of the MAPK pathway under fasting conditions in the ABC-DLBCL RI-1.
Each bar represents the mean median of the relative mRNA expression plus/minus standard error of the mean. The glucose and protein fasted samples were compared with the untreated controls (10% FBS; 2g/L glucose). * = p-value < 0.1; ** = p-value < 0.05; *** = p-value < 0.01. The different colours indicate different glucose fasting conditions (0.4; 0.6; 0.8; 1g/L glucose). In addition, the % in the title define the FBS concentration (either 2.5% or 5% FBS).

In the second ABC-DLBCL U2932 the protein and glucose fasting conditions revealed an upregulation in *OAS3* (30.6-fold, $p < 0.05$), *EGR1* (17.8-fold, $p < 0.05$) and *EGR3* (14.4-fold, $p < 0.01$). Expression levels of *KLF10* were unaffected under this treatment too (figure 27).

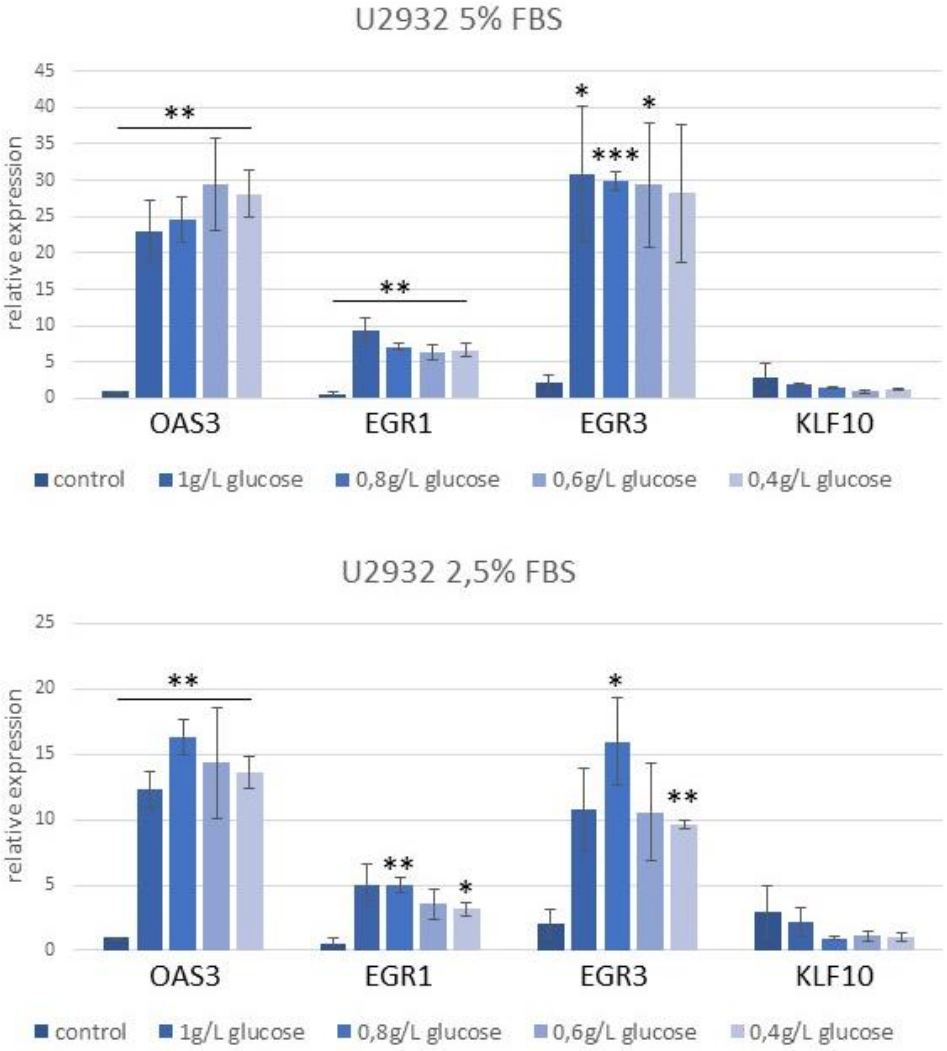

Figure 27 Analysis of significant upregulated target genes (*OAS3, EGR1, EGR3* and *KLF10*) of the MAPK pathway under fasting conditions in the ABC-DLBCL U2932.
Each bar represents the mean median of the relative mRNA expression plus/minus standard error of the mean. The glucose and protein fasted samples were compared with the untreated controls (10% FBS; 2g/L glucose). * = p-value < 0.1; ** = p-value < 0.05; *** = p-value < 0.01. The different colours indicate different glucose fasting conditions (0.4; 0.6; 0.8; 1g/L glucose). In addition, the % in the title define the FBS concentration (either 2.5% or 5% FBS).

Interestingly, in the GCB-DLBCL SuDHL4 the double fasting conditions had no affection on the expression level of neither *OAS3, EGR1, EGR3 and KLF10* (figure 28).

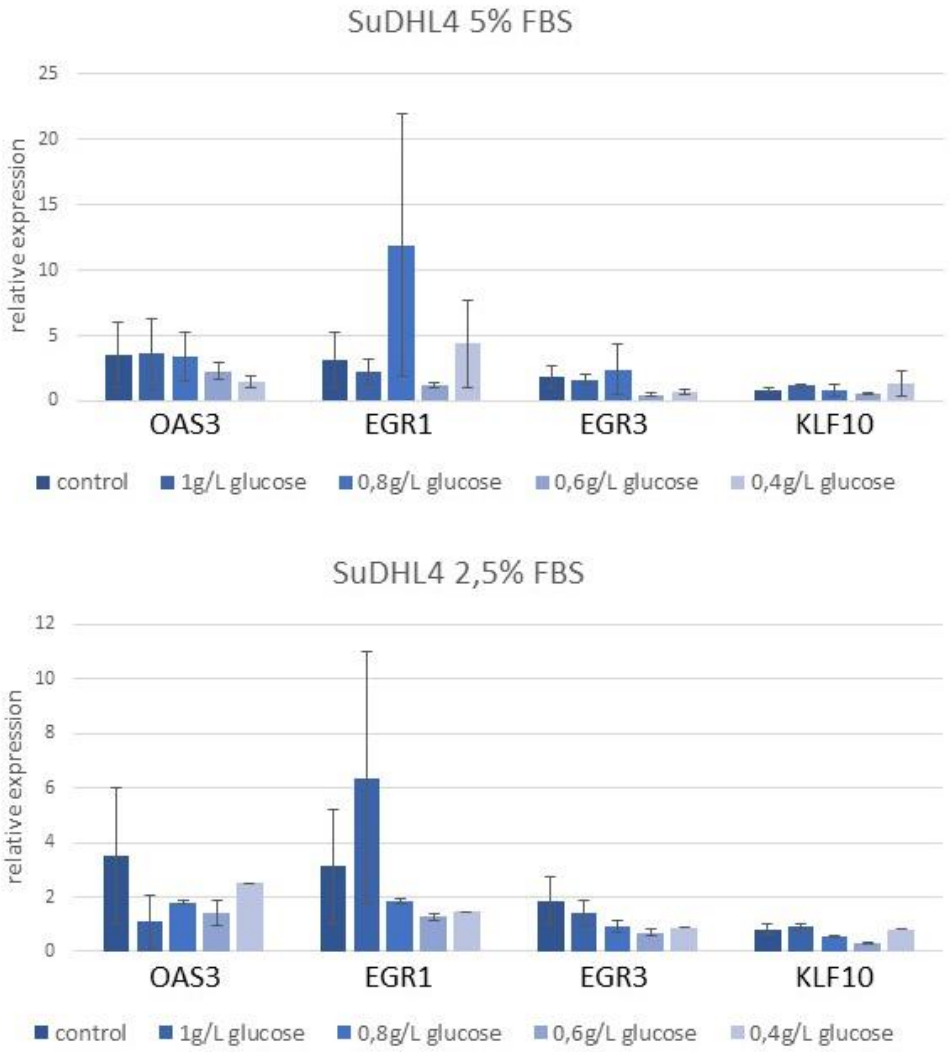

Figure 28 Analysis of significant upregulated target genes (*OAS3, EGR1, EGR3* and *KLF10*) of the MAPK pathway under fasting conditions in the GCB-DLBCL SuDHL4.
Each bar represents the mean median of the relative mRNA expression plus/minus standard error of the mean. The glucose and protein fasted samples were compared with the untreated controls (10% FBS; 2g/L glucose). * = p-value < 0.1; ** = p-value < 0.05; *** = p-value < 0.01. The different colours indicate different glucose fasting conditions (0.4; 0.6; 0.8; 1g/L glucose). In addition, the % in the title define the FBS concentration (either 2.5% or 5% FBS).

The second GCB-DLBCL Karpas-422 revealed higher mRNA expression of *OAS3* (1.5-fold, $p < 0.1$) and *EGR1* (5.2-fold, $p < 0.05$) under protein and glucose restriction. However, no significant deregulation occurred in *EGR3* and *KLF10* under these conditions (figure 29).

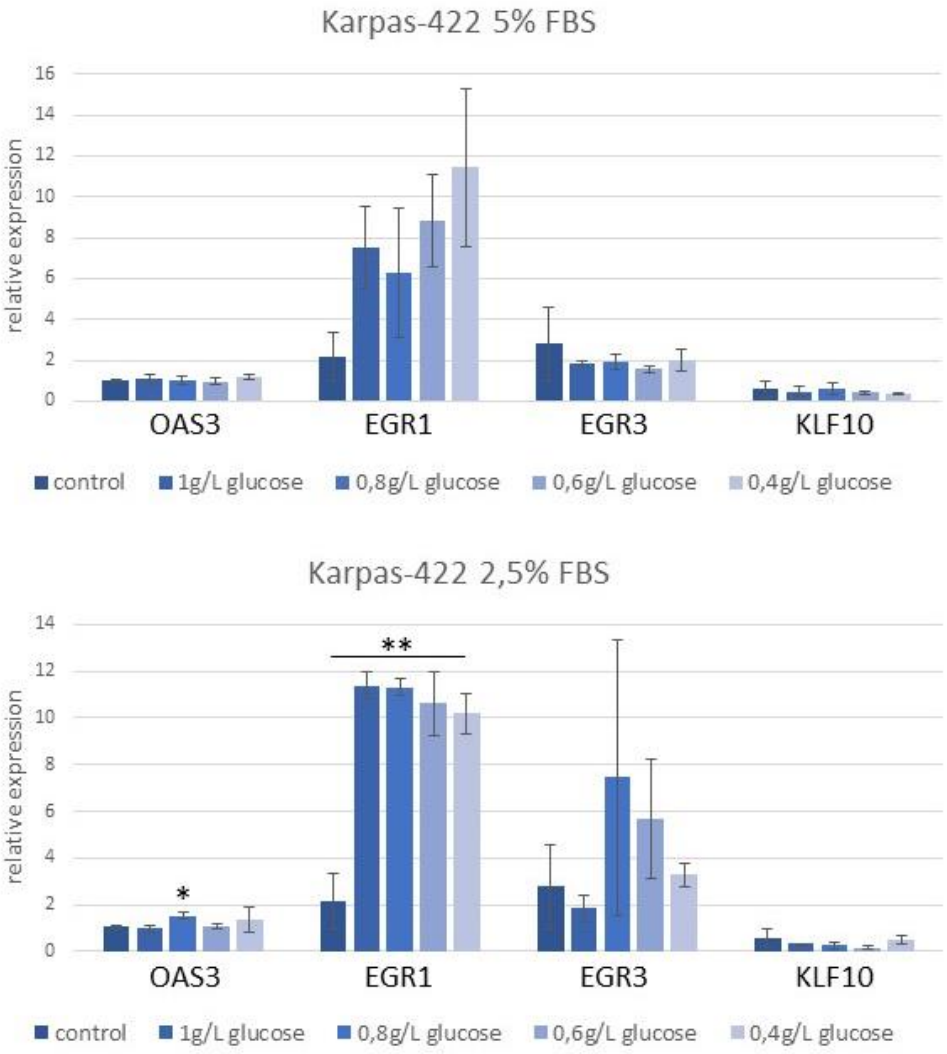

Figure 29 Analysis of significant upregulated target genes (*OAS3, EGR1, EGR3* and *KLF10*) of the MAPK pathway under fasting conditions in the GCB-DLBCL Karpas-422.
Each bar represents the mean median of the relative mRNA expression plus/minus standard error of the mean. The glucose and protein fasted samples were compared with the untreated controls (10% FBS; 2g/L glucose). * = p-value < 0.1; ** = p-value < 0.05; *** = p-value < 0.01. The different colours indicate different glucose fasting conditions (0.4; 0.6; 0.8; 1g/L glucose). In addition, the % in the title define the FBS concentration (either 2.5% or 5% FBS).

Similar to the GCB-DLBCL SuDHL4 in the Burkitt lymphoma Raji mRNA levels of *OAS3, EGR1* and *EGR3* revealed no affection to the double fasting conditions. The only exception was *KLF10,* where an upregulation (2.6-fold, $p < 0.05$) but also a downregulation (5-fold, $p < 0.05$) occurred (figure 30).

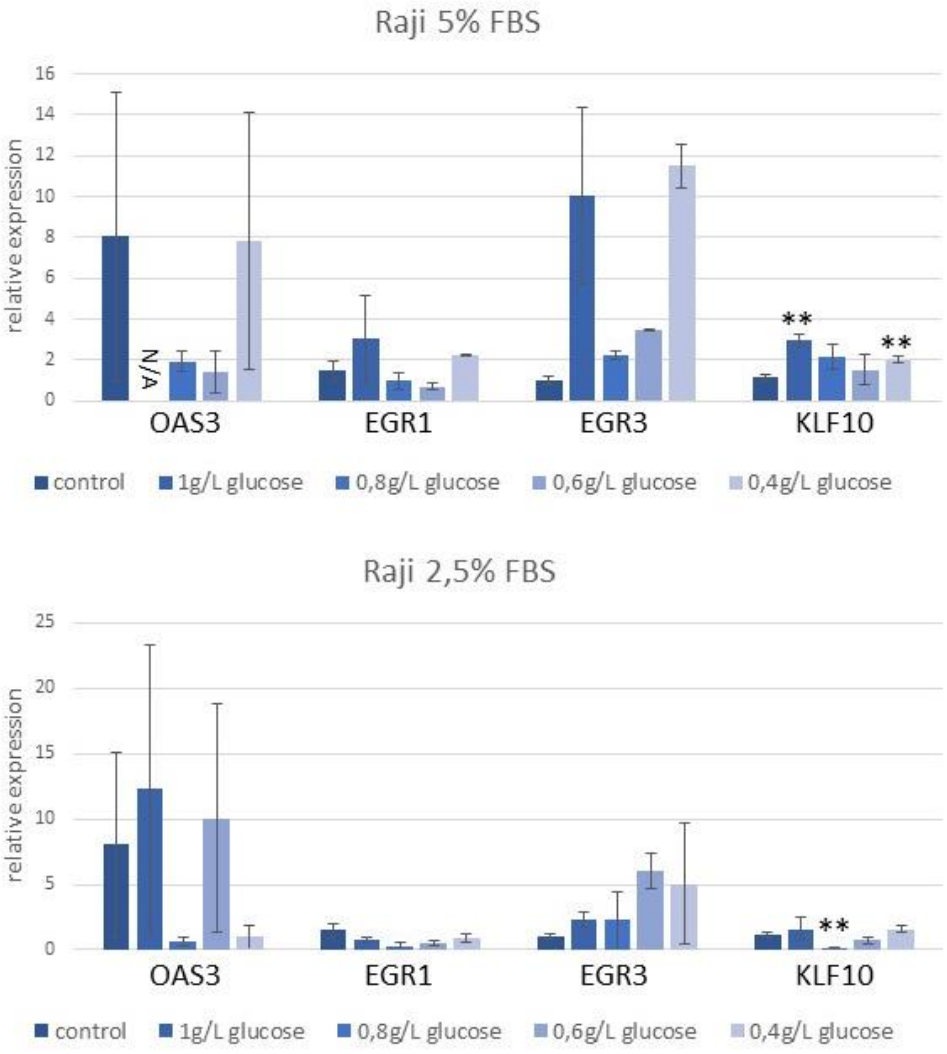

Figure 30 Analysis of significant upregulated target genes (*OAS3, EGR1, EGR3* and *KLF10*) of the MAPK pathway under fasting conditions in the Burkitt lymphoma Raji.
Each bar represents the mean median of the relative mRNA expression plus/minus standard error of the mean. The glucose and protein fasted samples were compared with the untreated controls (10% FBS; 2g/L glucose). * = p-value < 0.1; ** = p-value < 0.05; *** = p-value < 0.01. The different colours indicate different glucose fasting conditions (0.4; 0.6; 0.8; 1g/L glucose). In addition, the % in the title define the FBS concentration (either 2.5% or 5% FBS). N/A indicates concentrations under the detection level.

In contrast to the Raji cell line the Burkitt lymphoma BL-2 revealed upregulation in three of four genes under FBS and glucose restriction. *OAS3* (3.1-fold, $p < 0.01$) *EGR1* (9.8-fold, $p < 0.1$) and *KLF10* (2.8-fold, $p < 0.01$) were upregulated. *EGR3* (2-fold, $p < 0.05$) had a decreased mRNA expression caused by double fasting (figure 31).

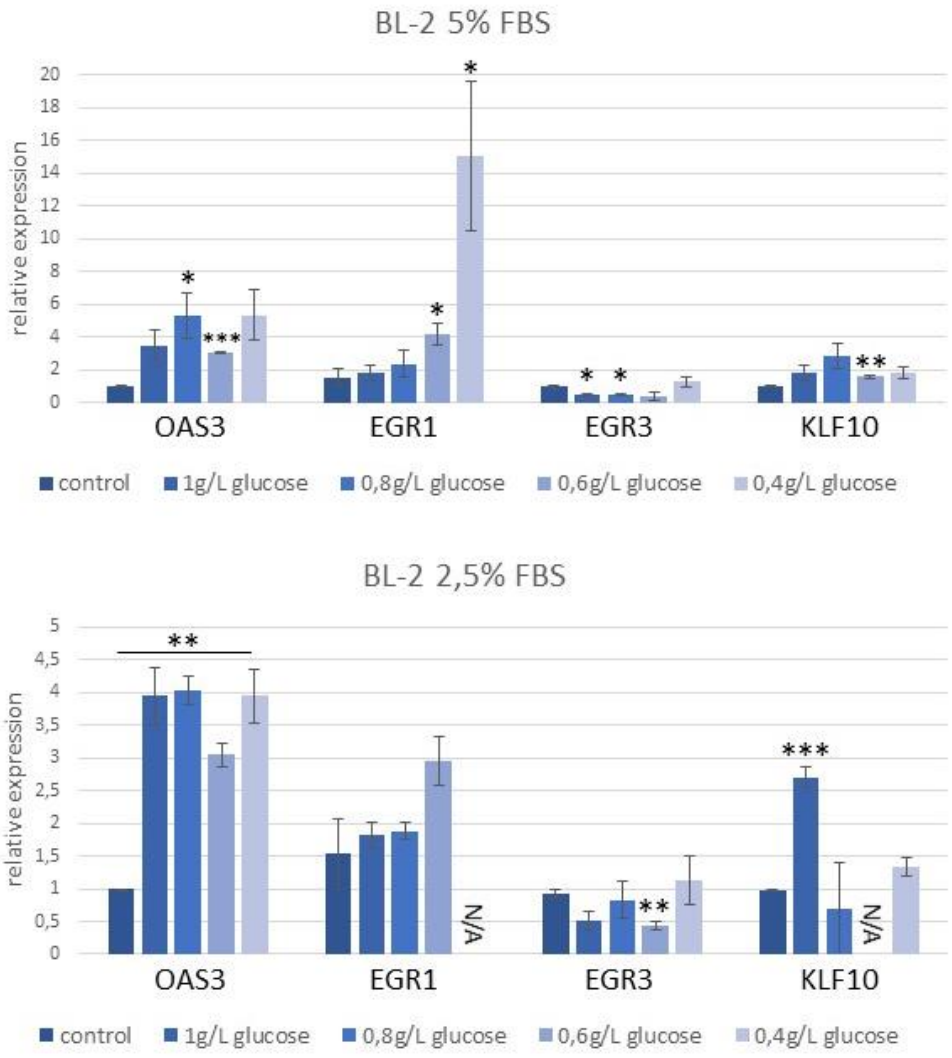

Figure 31 Analysis of significant upregulated target genes (*OAS3, EGR1, EGR3* and *KLF10*) of the MAPK pathway under fasting conditions in the Burkitt lymphoma BL-2.
Each bar represents the mean median of the relative mRNA expression plus/minus standard error of the mean. The glucose and protein fasted samples were compared with the untreated controls (10% FBS; 2g/L glucose). * = p-value < 0.1; ** = p-value < 0.05; *** = p-value < 0.01. The different colours indicate different glucose fasting conditions (0.4; 0.6; 0.8; 1g/L glucose). In addition, the % in the title define the FBS concentration (either 2.5% or 5% FBS). N/A indicates concentrations under the detection level.

4.5.3. PI3-Kinase/Akt pathway

The ABC-DLBCL RI-1 revealed upregulations in six of the eight genes under double fasting conditions, as there were *cFOS* (1.8-fold, $p < 0.01$), *MxD1* (2.5-fold, $p < 0.01$), *JunB* (3.9-fold, $p < 0.05$), *JunC* (3.4-fold, $p < 0.1$), *DUSP1* (3.1-fold, $p < 0.1$) and *ETV5* (7.2-fold, $p < 0.01$). Bub1 was not affected by the fasting conditions and *CCND2* had no concentrations over the detection level in RI-1 cells (figure 32).

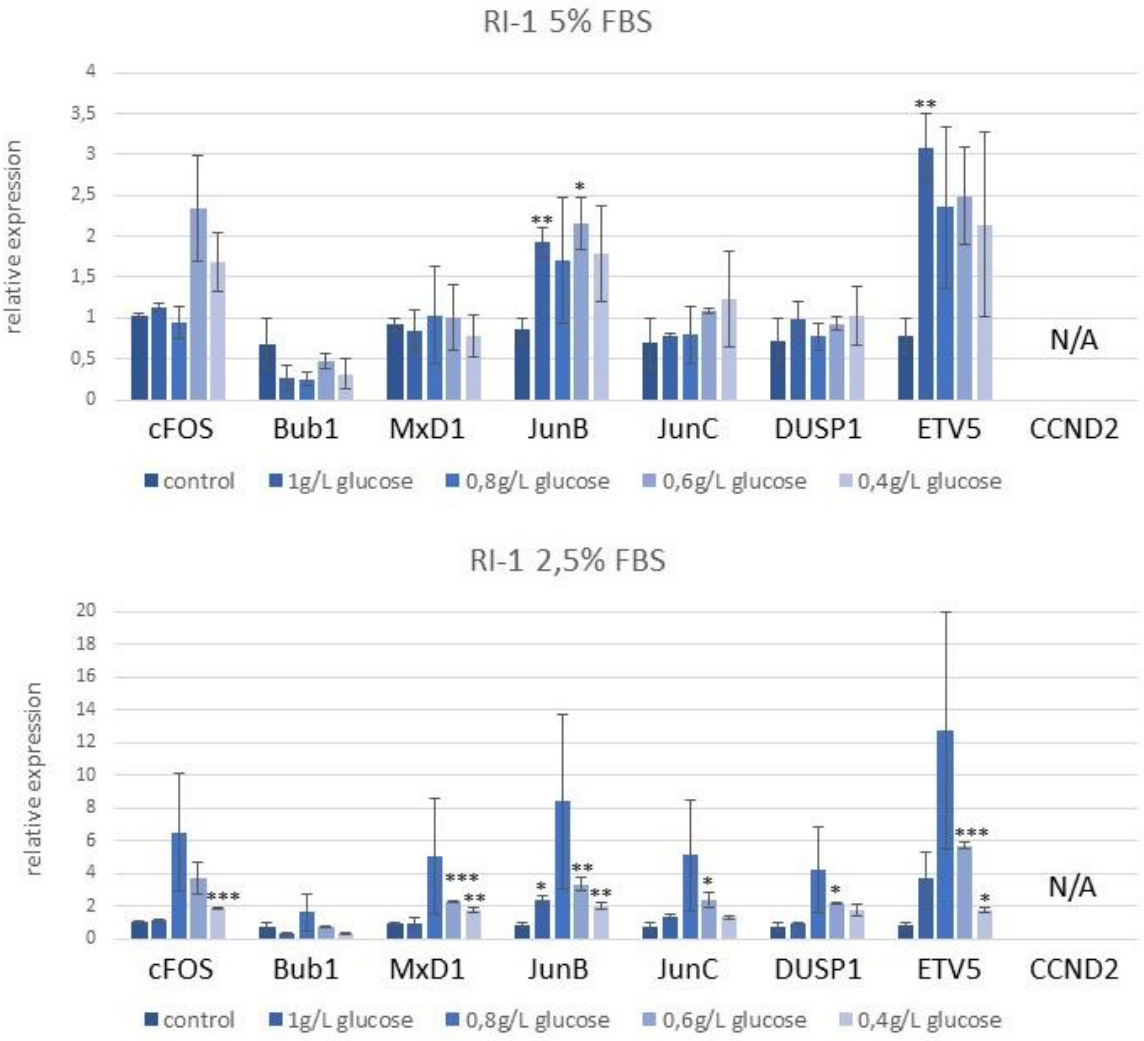

Figure 32 Analysis of significant upregulated target genes (*cFOS, Bub1, MxD1, JunB, JunC, DUSP1, ETV5 and CCND2*) of the PI3K/Akt pathway under fasting conditions in the ABC-DLBCL RI-1.
Each bar represents the mean median of the relative mRNA expression plus/minus standard error of the mean. The glucose and protein fasted samples were compared with the untreated controls (10% FBS; 2g/L glucose). * = p-value < 0.1; ** = p-value < 0.05; *** = p-value < 0.01. The different colours indicate different glucose fasting conditions (0.4; 0.6; 0.8; 1g/L glucose). In addition, the % in the title define the FBS concentration (either 2.5% or 5% FBS). N/A indicates concentrations under the detection level.

In the U2932 – the second ABC-DLBCL – *cFOS* (2.0-fold, $p < 0.05$), *JunC* (3.3-fold, $p < 0.05$) and *DUSP1* (11.2-fold, $p < 0.05$) revealed higher mRNA levels under glucose and FBS restriction. *Bub1* (2.5-fold, $p < 0.1$) was downregulated, while *MxD1, JunB* and *CCND2* had no significant deregulation under these conditions (figure 33).

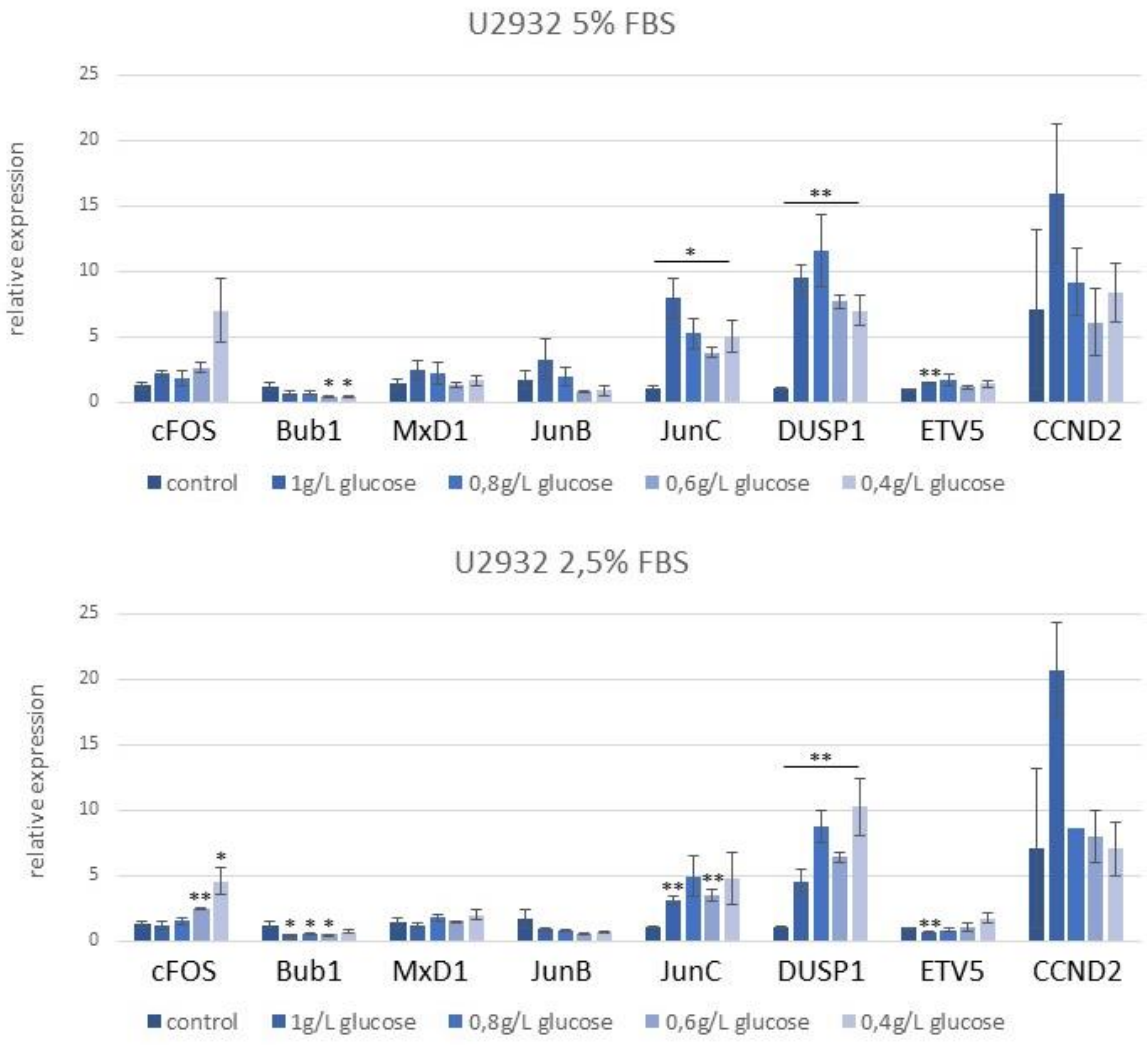

Figure 33 Analysis of significant upregulated target genes (*cFOS, Bub1, MxD1, JunB, JunC, DUSP1, ETV5 and CCND2*) of the PI3K/Akt pathway under fasting conditions in the ABC-DLBCL U2932.
Each bar represents the mean median of the relative mRNA expression plus/minus standard error of the mean. The glucose and protein fasted samples were compared with the untreated controls (10% FBS; 2g/L glucose). * = p-value < 0.1; ** = p-value < 0.05; *** = p-value < 0.01. The different colours indicate different glucose fasting conditions (0.4; 0.6; 0.8; 1g/L glucose). In addition, the % in the title define the FBS concentration (either 2.5% or 5% FBS).

In the GCB-DLBCL SuDHL4 combined fasting conditions led to upregulation of five out of the eight genes – *JunB* (1.9-fold, $p < 0.1$), *JunC* (2.8-fold, $p < 0.05$), *DUSP1* (5.0-fold, $p < 0.01$), *ETV5* (14.5-fold, $p < 0.01$) and *CCND2* (3.4-fold, $p < 0.05$). Expression levels of *MxD1* were under the detectable concentrations under double fasting conditions while *cFOS* and *Bub1* were not affected (figure 34).

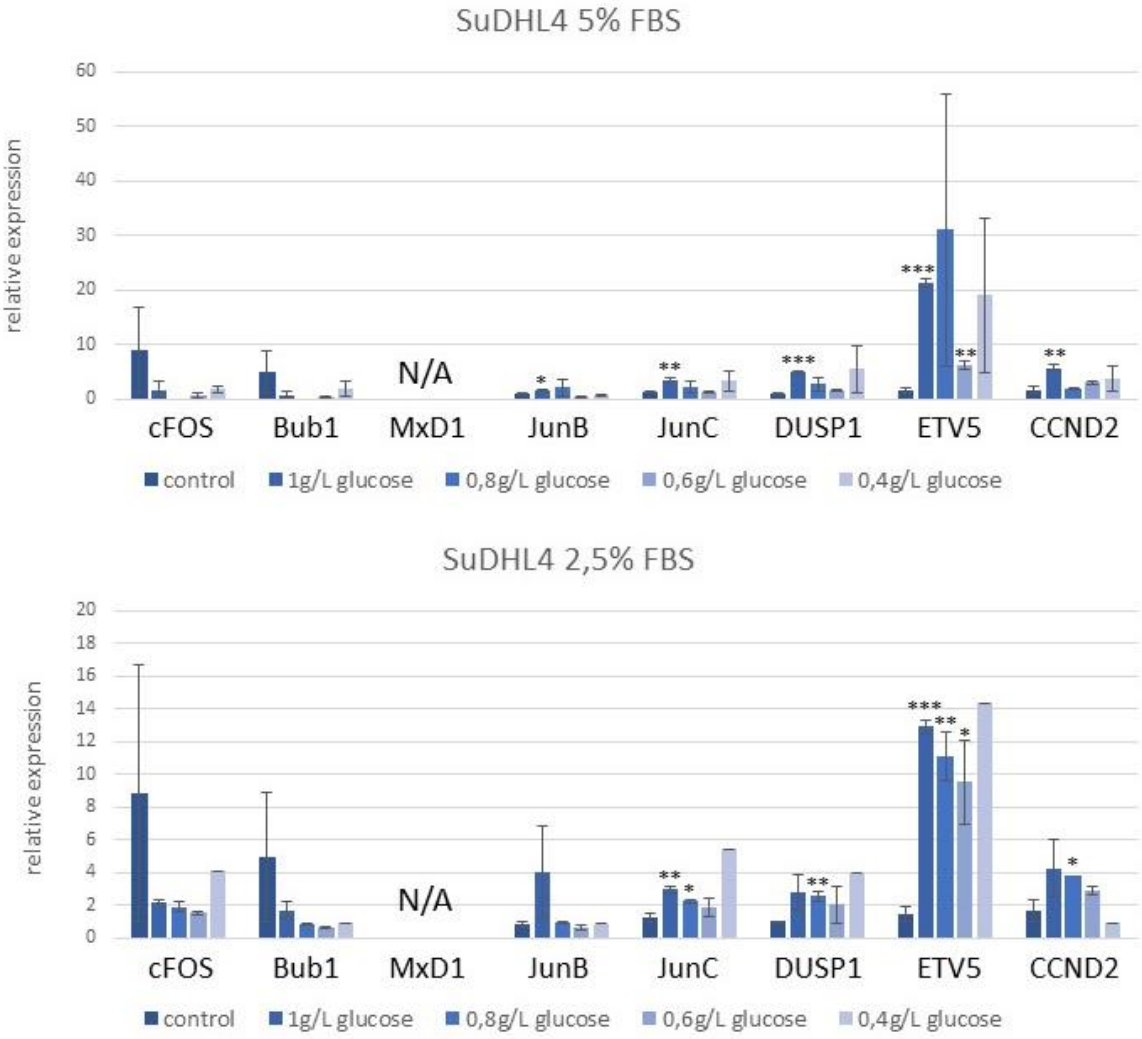

Figure 34 Analysis of significant upregulated target genes (*cFOS, Bub1, MxD1, JunB, JunC, DUSP1, ETV5 and CCND2*) of the PI3K/Akt pathway under fasting conditions in the GCB-DLBCL SuDHL4.
Each bar represents the mean median of the relative mRNA expression plus/minus standard error of the mean. The glucose and protein fasted samples were compared with the untreated controls (10% FBS; 2g/L glucose). * = p-value < 0.1; ** = p-value < 0.05; *** = p-value < 0.01. The different colours indicate different glucose fasting conditions (0.4; 0.6; 0.8; 1g/L glucose). In addition, the % in the title define the FBS concentration (either 2.5% or 5% FBS). N/A indicates concentrations under the detection level.

The GCB-DLBCL Karpas-422 cell line revealed similar effects under double fasting conditions. Here six out of eight target genes were upregulated – *cFOS* (3.1-fold, $p < 0.05$), *Bub1* (1.8-fold, $p < 0.05$), *MxD1* (2.7-fold, $p < 0.05$), *JunB* (5.3-fold, $p < 0.05$), *JunC* (3.4-fold, $p < 0.05$) and *DUSP1* (1.7-fold, $p < 0.1$; figure 35).

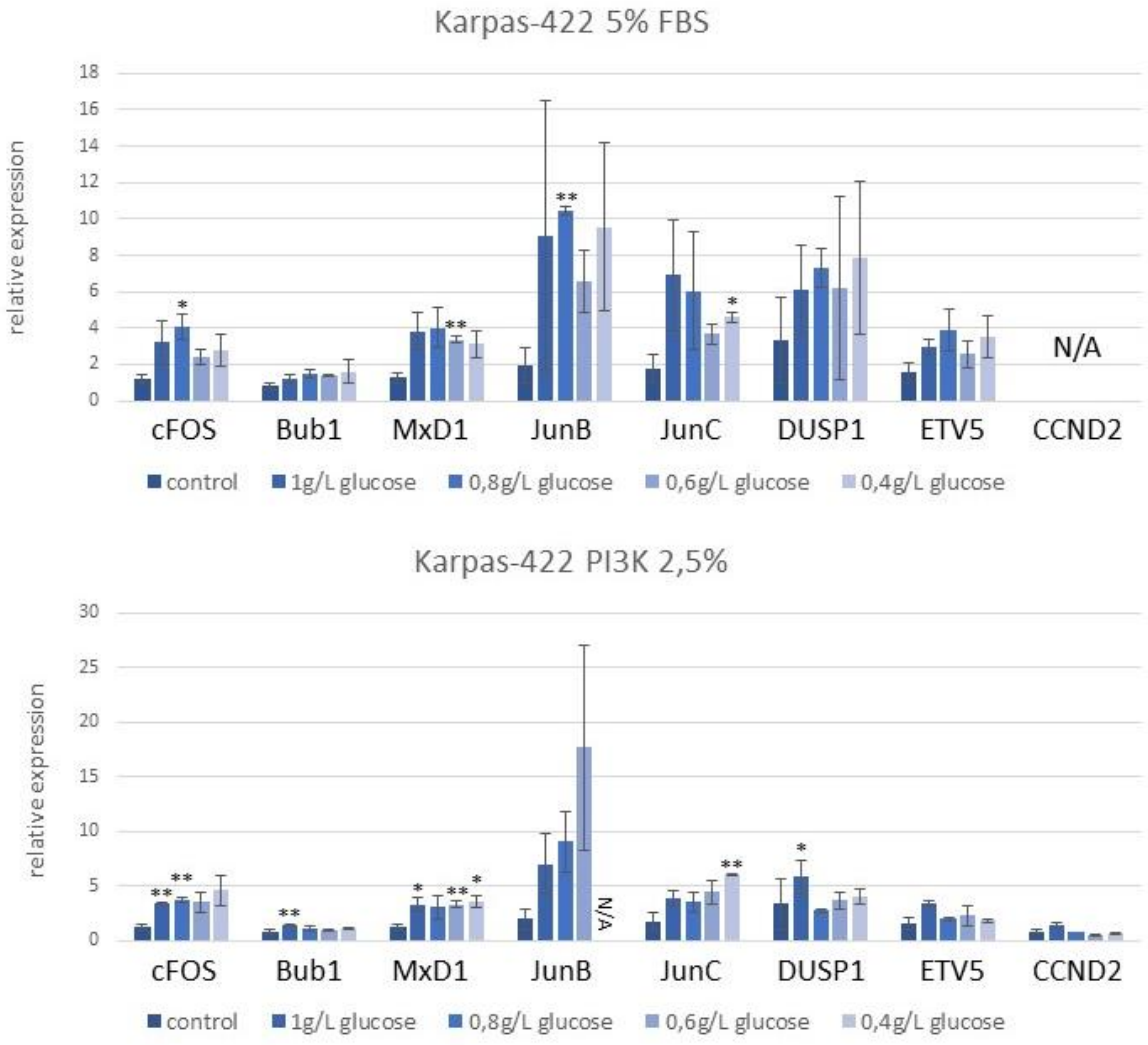

Figure 35 Analysis of significant upregulated target genes (*cFOS, Bub1, MxD1, JunB, JunC, DUSP1, ETV5 and CCND2*) of the PI3K/Akt pathway under fasting conditions in the GCB-DLBCL Karpas-422.
Each bar represents the mean median of the relative mRNA expression plus/minus standard error of the mean. The glucose and protein fasted samples were compared with the untreated controls (10% FBS; 2g/L glucose). * = p-value < 0.1; ** = p-value < 0.05; *** = p-value < 0.01. The different colours indicate different glucose fasting conditions (0.4; 0.6; 0.8; 1g/L glucose). In addition, the % in the title define the FBS concentration (either 2.5% or 5% FBS). N/A indicates concentrations under the detection level.

In the Burkitt lymphoma Raji the reduction of FBS and glucose led to nearly no deregulation at a significant level. The only exception was an upregulation of *CCND2* (7.7-fold, $p < 0.05$; figure 36).

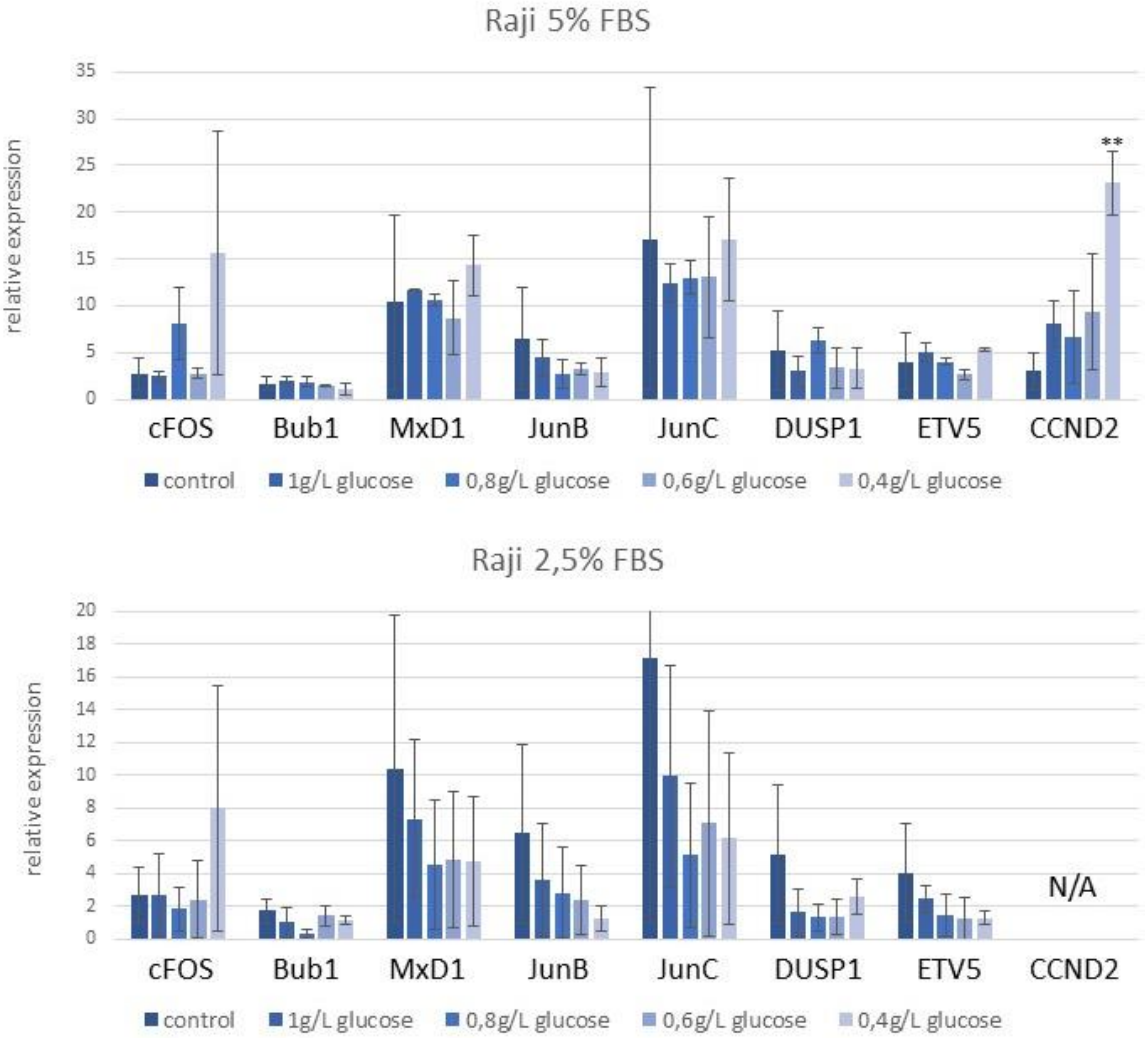

Figure 36 Analysis of significant upregulated target genes (*cFOS, Bub1, MxD1, JunB, JunC, DUSP1, ETV5 and CCND2*) of the PI3K/Akt pathway under fasting conditions in the Burkitt lymphoma Raji.
Each bar represents the mean median of the relative mRNA expression plus/minus standard error of the mean. The glucose and protein fasted samples were compared with the untreated controls (10% FBS; 2g/L glucose). * = p-value < 0.1; ** = p-value < 0.05; *** = p-value < 0.01. The different colours indicate different glucose fasting conditions (0.4; 0.6; 0.8; 1g/L glucose). In addition, the % in the title define the FBS concentration (either 2.5% or 5% FBS). N/A indicates concentrations under the detection level.

Contrary to the Raji cell line the second Burkitt lymphoma cell line BL-2 revealed upregulations in nearly all eight target genes. While *cFOS* (7.4-fold, $p < 0.01$), *Bub1* (2.1-fold, $p < 0.01$), *MxD1* (10.7-fold, $p < 0.01$), *JunB* (4.7-fold, $p < 0.01$), *JunC* (15.9-fold, $p < 0.01$), *DUSP1* (9.3-fold, $p < 0.01$) and *ETV5* (20.8-fold, $p < 0.05$) revealed upregulations under double fasting conditions, *CCND2* had no mRNA concentrations over the detection level (figure 37).

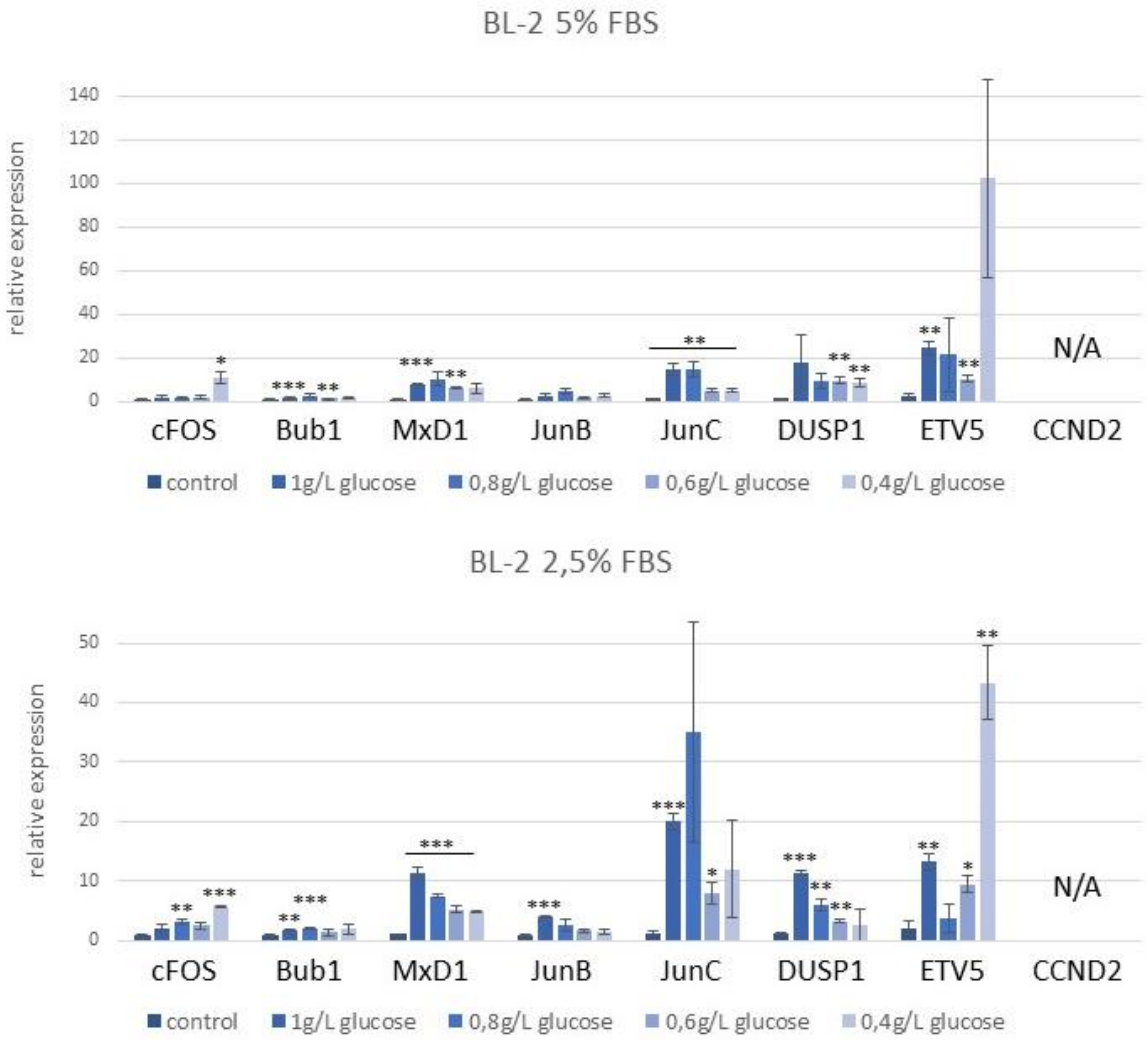

Figure 37 Analysis of significant upregulated target genes (*cFOS, Bub1, MxD1, JunB, JunC, DUSP1, ETV5 and CCND2*) of the PI3K/Akt pathway under fasting conditions in the Burkitt lymphoma BL-2.
Each bar represents the mean median of the relative mRNA expression plus/minus standard error of the mean. The glucose and protein fasted samples were compared with the untreated controls (10% FBS; 2g/L glucose). * = p-value < 0.1; ** = p-value < 0.05; *** = p-value < 0.01. The different colours indicate different glucose fasting conditions (0.4; 0.6; 0.8; 1g/L glucose). In addition, the % in the title define the FBS concentration (either 2.5% or 5% FBS). N/A indicates concentrations under the detection level.

4.6. Quantitative analysis of the NF-κB pathway via western blot

To further investigate the effects of fasting on the activity of the NF-κB pathway, protein levels of three members of NF-κB genes (p100, p65, NIK) and their active forms (phosphorylated p100 and phosphorylated p65) were tested using Western blot analysis. In addition, p53 protein levels were tested. p53 is an intensively studied tumour suppressor gene with pro-apoptotic function and a well-known marker for apoptosis and the apoptotic pathways. For this purpose, all lymphoma cell lines (RI-1, U2932, SuDHL4, Karpas-422, Raji, BL-2) were fasted with 0.4g/L glucose and 5% FBS for 24 hours. GAPDH was used as a loading control.

p100 and p65 as well as the phosphorylated pp100 proteins were higher expressed in the fasted cell lines compared to the unfasted control. In addition, p53 was also induced by fasting as shown in figure 38. The Karpas-422 cell line showed overall low expression levels of the NF- κB proteins – except pp100 were the protein was higher expressed in the fasted cell line. Table 7 contains the ratio between the intensity of fasted and unfasted samples. Western blot analysis of NIK and pp65 revealed that these two antibodies did not work.

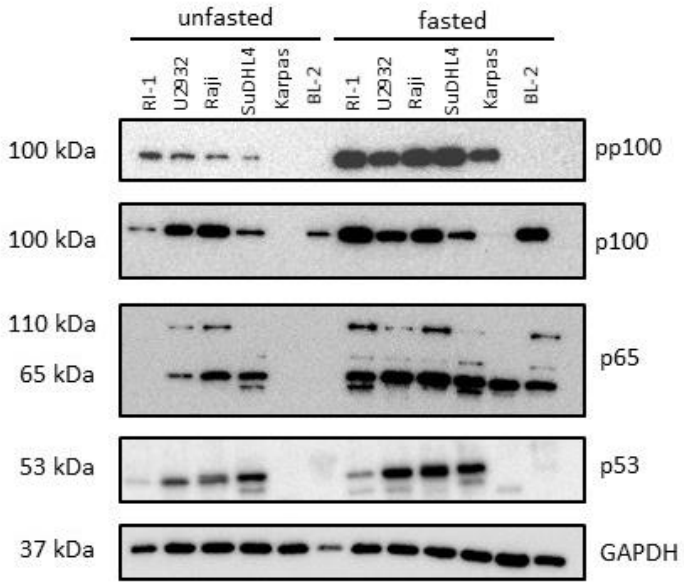

Figure 38 Western blot of members of the NF-κB pathway (p100 and its phosphorylated form pp100, p65) and p53 in fasted and unfasted cell lines.
GAPDH served as an constitutive housekeeping gene. All six cell lines ABC-DLBCL (RI-1, U2932), GCB (SuDHL4, Karpas-422) and Burkitt lymphoma (Raji, BL-2) were tested under fasted and unfasted condition.

Table 7 Western blot ratio
The ratio was calculated by dividing the intensity of four genes (phosphotylated p100, p100, p65 and p53) of the fasted samples by the unfasted ones. N/A data occurs on the one hand caused by no signal in both samples or on the other hand by a singal that only appears in the fasted cell samples (green coloured). The green coloured fields indicate an occurring signal under fasting conditions, however there was no signal in the unfasted ones, therefore no ratio could be done.

	pp100	p100	p65	p53
RI-1	4,888	11,40	N/A	1,966
U2932	10,08	1,383	17,03	3,782
SuDHL4	88,00	1,938	3,403	1,687
Karpas-422	N/A	N/A	N/A	N/A
Raji	39,61	1,689	5,280	7,969
BL-2	N/A	1,556	N/A	N/A

5. Discussion

This master thesis was designed to comprehensively study the effects fasting on enhanced anti-cancer activity of Ibrutinib and on oncogenic pathways in aggressive lymphomas. For solid cancer it has been demonstrated that fasting potentiates the anticancer activity of tyrosine kinase inhibitors [80] but has not been investigated in aggressive lymphomas so far.

We clearly demonstrated that Ibrutinib possesses growth inhibitory effects on ABC-DLBCL, GCB-DLCBL and Burkitt lymphomas cell lines as well on the Jurkat T cell lymphoma cell line. Ibrutinib is an oral inhibitor of BTK [81], which is activated by BCR signalling [54] and is constitutively activated in many B cell receptor malignancies, i.e. DLBCL - especially ABC-DLCBL, CLL, MCL and Burkitt lymphoma [59,60,81]. Our observed growth inhibitory effects of Ibrutinib on ABC-DLCBL, GCB-DLCBL and Burkitt lymphoma cell lines confirmed data of already published studies [82] and demonstrate that the growth of these lymphoma entities significantly dependents on constitutively activated BCR signalling. Additionally, inhibitory effects of Ibrutinib on interleukin-2-inducible T-cell kinase (ITK) and limited anti-lymphoma effects of it against T cell lymphoma have been described explaining the observed growth inhibitory effects of Ibrutinib on the Jurkat lymphoma cell line [83].

We observed that the growth inhibitory effect of Ibrutinib is enhanced by protein fasting. In a non-malignant condition and fasting it inhibits cell proliferation and protein synthesis and activates energy generating processes [84]. However, in cancer cells like lymphoma some protein kinase like the BTK are constitutively activated causing stress for the malignant cells, therefore sensitizing them for anti-cancer agents. Our observation that the growth inhibitory effects of Ibrutinib are enhanced under protein and glucose fasting condition indicates that the anti-lymphoma effects are significantly influenced by fasting conditions and that they might be potentiated by harsher situations. Furthermore, we also demonstrate that a higher percentage of lymphoma cells stained positive for Annexin V under Ibrutinib and fasting conditions indicating their apoptotic effects.

Our gene expression analysis of NF-κB target genes and Western blot analysis of NF-κB members revealed that the expression levels of most of the target genes and NF-κB members were induced by fasting. Furthermore, we also observed that under this condition a higher amount of the NF-κB member p100 was phosphorylated. Taking altogether this data suggests that NF-κB is activated by fasting in aggressive lymphoma cells. This correlates with earlier studies, where the activation of this pathway by fasting has been described in muscle cells [85]. As the NF-κB pathway is the major activated pathway by BCR signalling, it appears that it plays an essential role in lymphoma cell survival [86]. Furthermore, the expression analysis of PI3K and MAPK pathways demonstrated that the targets genes of both pathways were induced by the combined glucose and protein fasting. These two pathways also play an important role in lymphoma genesis and impact on lymphoma growth and cell proliferation [87].

Based on these findings, it might be speculated that the fasted lymphoma cells activate these pathways in order to adapt their metabolism to the nutrient's deprivation.

Our Western blot analysis also revealed that glucose and protein fasting induced p53 protein content in aggressive lymphoma cells. Since p53 is able to induce apoptosis [88], it is possible this function also significantly impacts lymphomagenesis. However, we tested and optimized the fasting condition in a way that the cell growth was not influenced, therefor it is very unlikely that under this optimized fasting condition the induced p53 possesses any pro-apoptotic function in aggressive lymphoma cells. Based on the observation that p53 is stabilized by fasting and required for amino acid catabolism and gluconeogenesis in liver cells [89], it might be speculated that p53 also possesses some metabolic function in fasted aggressive lymphoma cells.

For further research the limitations of these tests must be defined as these findings can only be confirmed on molecular level and in cancer cells. Therefore, its necessary to conduct experiments with non-cancer controls. The combination and interaction of fasting and chemotherapy on a human scale could be different, caused by a variety of glucose regulatory mechanism and compensatory effects.

In conclusion, our data demonstrates that glucose and protein fasting sensitizes aggressive lymphoma cell lines to Ibrutinib and potentiate its anticancer activity. Furthermore, on molecular levels it seems that fasting activates NF-κB, PI3K and MAPK pathways and therefore potentially making lymphoma cells more vulnerable to specific inhibitors. As for the future fasting seems to function as a well-fitting tool in combination with specific therapeutics like Ibrutinib or other TKI´s, but therefore it is necessary to further investigate the effect of fasting in combination therapies especially on non-molecular levels, like clinical try-outs.

References

[1] Hoffman, William; Lakkis, Fadi G.; Chalasani, Geetha (2016): B Cells, Antibodies, and More. In: Clinical journal of the American Society of Nephrology: CJASN 11 (1), S. 137–154.

[2] Eibel, Hermann; Kraus, Helene; Sic, Heiko; Kienzler, Anne-Kathrin; Rizzi, Marta (2014): B cell biology: an overview. In: Current allergy and asthma reports 14 (5), S. 434.

[3] Pieper, Kathrin; Grimbacher, Bodo; Eibel, Hermann (2013): B-cell biology and development. In: The Journal of allergy and clinical immunology 131 (4), S. 959–971.

[4] Ichii, Michiko; Oritani, Kenji; Kanakura, Yuzuru (2014): Early B lymphocyte development: Similarities and differences in human and mouse. In: World journal of stem cells 6 (4), S. 421–431.

[5] Hardy, R. R.; Hayakawa, K. (2001): B cell development pathways. In: Annual review of immunology 19, S. 595–621.

[6] Busslinger, Meinrad (2004): Transcriptional control of early B cell development. In: Annual review of immunology 22, S. 55–79.

[7] Kuo, Tracy C.; Schlissel, Mark S. (2009): Mechanisms controlling expression of the RAG locus during lymphocyte development. In: Current opinion in immunology 21 (2), S. 173–178.

[8] Dong, Yanying; Wu, Caijun; Zhao, Xiaohui; Zhang, Ping; Zhang, Hua; Zheng, Mingzhe et al. (2017): Epigenetic modifications of the VH region after DJH recombination in Pro-B cells. In: Immunology 152 (2), S. 218–231.

[9] Hagman, James; Lukin, Kara (2006): Transcription factors drive B cell development. In: Current opinion in immunology 18 (2), S. 127–134.

[10] Lu, Runqing (2008): Interferon regulatory factor 4 and 8 in B-cell development. In: Trends in immunology 29 (10), S. 487–492.

[11] Kranich, Jan; Krautler, Nike Julia (2016): How Follicular Dendritic Cells Shape the B-Cell Antigenome. In: Frontiers in immunology 7, S. 225.

[12] Silva, Nilushi S. de; Klein, Ulf (2015): Dynamics of B cells in germinal centres. In: Nature reviews. Immunology 15 (3), S. 137–148.

[13] Basso, Katia; Dalla-Favera, Riccardo (2015): Germinal centres and B cell lymphomagenesis. In: Nature reviews. Immunology 15 (3), S. 172–184.

[14] W. Böcker; H. Denk; U. Heitz (2008): Pathologie 4.Auflage S.564-574.

[15] Tamaru, Jun-Ichi (2017): 2016 revision of the WHO classification of lymphoid neoplasms. In: [Rinsho ketsueki] The Japanese journal of clinical hematology 58 (10), S. 2188–2193.

[16] Jaffe, Elaine S.; Pittaluga, Stefania (2011): Aggressive B-cell lymphomas: a review of new and old entities in the WHO classification. In: Hematology. American Society of Hematology. Education Program 2011, S. 506–514.

[17] Pasqualucci, Laura (2013): The genetic basis of diffuse large B-cell lymphoma. In: Current opinion in hematology 20 (4), S. 336–344.

[18] Zhao, Ying; Wang, Hong; Jin, Song; Zheng, Jiajia; Huang, Man; Tang, Yaqiong et al. (2017): Prognostic analysis of DLBCL patients and the role of upfront ASCT in high-intermediate and high-risk patients. In: Oncotarget 8 (42), S. 73168–73176.

[19] Li, Shaoying; Young, Ken H.; Medeiros, L. Jeffrey (2018): Diffuse large B-cell lymphoma. In: Pathology 50 (1), S. 74–87.

[20] Nowakowski, Grzegorz S.; Czuczman, Myron S. (2015): ABC, GCB, and Double-Hit Diffuse Large B-Cell Lymphoma: Does Subtype Make a Difference in Therapy Selection? In: American Society of Clinical Oncology educational book. American Society of Clinical Oncology. Annual Meeting, e449-57.

[21] Gatter, Kevin; Brown, David (2006): Bone marrow diagnosis. An illustrated guide. 2nd ed. Malden, MA, Oxford: Blackwell Pub.

[22] Molyneux, Elizabeth M.; Rochford, Rosemary; Griffin, Beverly; Newton, Robert; Jackson, Graham; Menon, Geetha et al. (2012): Burkitt's lymphoma. In: The Lancet 379 (9822), S. 1234–1244.

[23] Dozzo, Massimo; Carobolante, Francesca; Donisi, Pietro Maria; Scattolin, Annamaria; Maino, Elena; Sancetta, Rosaria et al. (2017): Burkitt lymphoma in adolescents and young adults: management challenges. In: Adolescent health, medicine and therapeutics 8, S. 11–29.

[24] Oren, M. (2003): Decision making by p53: life, death and cancer. In: Cell death and differentiation 10 (4), S. 431–442.

[25] Ozaki, Toshinori; Nakagawara, Akira (2011): Role of p53 in Cell Death and Human Cancers. In: Cancers 3 (1), S. 994–1013.

[26] Jin, Shufang; Yang, Xi; Li, Jiayi; Yang, Wenyi; Ma, Hailong; Zhang, Zhiyuan (2019): p53-targeted lincRNA-p21 acts as a tumor suppressor by inhibiting JAK2/STAT3 signalling pathways in head and neck squamous cell carcinoma. In: Molecular cancer 18 (1), S. 38.

[27] Chen, Yifan; Pan, Kewu; Wang, Pingzhang; Cao, Zhengyi; Wang, Weibin; Wang, Shuya et al. (2016): HBP1-mediated Regulation of p21 Protein through the Mdm2/p53 and TCF4/EZH2 Pathways and Its Impact on Cell Senescence and Tumorigenesis. In: The Journal of biological chemistry 291 (24), S. 12688–12705.

[28] Jin, S.; Levine, A. J. (2001): The p53 functional circuit. In: Journal of cell science 114 (Pt 23), S. 4139–4140.

[29] Harris, Sandra L.; Levine, Arnold J. (2005): The p53 pathway: positive and negative feedback loops. In: Oncogene 24 (17), S. 2899–2908.

[30] Carr, Michael I.; Jones, Stephen N. (2016): Regulation of the Mdm2-p53 signalling axis in the DNA damage response and tumorigenesis. In: Translational cancer research 5 (6), S. 707–724.

[31] Malkin, D.; Li, F. P.; Strong, L. C.; Fraumeni, J. F.; Nelson, C. E.; Kim, D. H. et al. (1990): Germ line p53 mutations in a familial syndrome of breast cancer, sarcomas, and other neoplasms. In: Science (New York, N.Y.) 250 (4985), S. 1233–1238.

[32] Zilfou, Jack T.; Lowe, Scott W. (2009): Tumor suppressive functions of p53. In: Cold Spring Harbor perspectives in biology 1 (5), a001883.

[33] Fan, Yongjun; Dutta, Jui; Gupta, Nupur; Fan, Gaofeng; Gélinas, Céline (2008): Regulation of programmed cell death by NF-kappaB and its role in tumorigenesis and therapy. In: Advances in experimental medicine and biology 615, S. 223–250.

[34] Oeckinghaus, Andrea; Ghosh, Sankar (2009): The NF-kappaB family of transcription factors and its regulation. In: Cold Spring Harbor perspectives in biology 1 (4).

[35] Hayden, Matthew S.; Ghosh, Sankar (2004): Signalling to NF-kappaB. In: Genes & development 18 (18), S. 2195–2224.

[36] Grimm, S.; Baeuerle, P. A. (1993): The inducible transcription factor NF-kappa B: structure-function relationship of its protein subunits. In: The Biochemical journal 290 (Pt 2), S. 297–308.

[37] Oeckinghaus, Andrea; Ghosh, Sankar (2009): The NF-kappaB family of transcription factors and its regulation. In: Cold Spring Harbor perspectives in biology 1 (4),

[38] Sun, Shao-Cong (2017): The non-canonical NF-κB pathway in immunity and inflammation. In: Nature reviews. Immunology 17 (9), S. 545–558.

[39] Gilmore, T. D. (2006): Introduction to NF-kappaB: players, pathways, perspectives. In: Oncogene 25 (51), S. 6680–6684.

[40] Demchenko, Yulia N.; Kuehl, W. Michael (2010): A critical role for the NFkB pathway in multiple myeloma. In: Oncotarget 1 (1), S. 59–68.

[41] Balaji, Swathi; Ahmed, Makhdum; Lorence, Elizabeth; Yan, Fangfang; Nomie, Krystle; Wang, Michael (2018): NF-κB signalling and its relevance to the treatment of mantle cell lymphoma. In: Journal of hematology & oncology 11 (1), S. 83.

[42] Courtois, G.; Gilmore, T. D. (2006): Mutations in the NF-kappaB signalling pathway: implications for human disease. In: Oncogene 25 (51), S. 6831–6843.

[43] Jana, Arundhati; Krett, Nancy L.; Guzman, Grace; Khalid, Ahmer; Ozden, Ozkan; Staudacher, Jonas J. et al. (2017): NFkB is essential for activin-induced colorectal cancer migration via upregulation of PI3K-MDM2 pathway. In: Oncotarget 8 (23), S. 37377–37393.

[44] Morrison, Deborah K. (2012): MAP kinase pathways. In: Cold Spring Harbor perspectives in biology 4 (11).

[45] Shaul, Yoav D.; Seger, Rony (2007): The MEK/ERK cascade: from signalling specificity to diverse functions. In: Biochimica et biophysica acta 1773 (8), S. 1213–1226.

[46] Keshet, Yonat; Seger, Rony (2010): The MAP kinase signalling cascades: a system of hundreds of components regulates a diverse array of physiological functions. In: Methods in molecular biology (Clifton, N.J.) 661, S. 3–38.

[47] Tanoue, Takuji; Nishida, Eisuke (2003): Molecular recognitions in the MAP kinase cascades. In: Cellular signalling 15 (5), S. 455–462.

[48] Boulton, T. G.; Nye, S. H.; Robbins, D. J.; Ip, N. Y.; Radziejewska, E.; Morgenbesser, S. D. et al. (1991): ERKs: a family of protein-serine/threonine kinases that are activated and tyrosine phosphorylated in response to insulin and NGF. In: Cell 65 (4), S. 663–675.

[49] Kyriakis, J. M.; Banerjee, P.; Nikolakaki, E.; Dai, T.; Rubie, E. A.; Ahmad, M. F. et al. (1994): The stress-activated protein kinase subfamily of c-Jun kinases. In: Nature 369 (6476), S. 156–160.

[50] Freshney, N. W.; Rawlinson, L.; Guesdon, F.; Jones, E.; Cowley, S.; Hsuan, J.; Saklatvala, J. (1994): Interleukin-1 activates a novel protein kinase cascade that results in the phosphorylation of Hsp27. In: Cell 78 (6), S. 1039–1049.

[51] Huang, Gonghua; Shi, Lewis Zhichang; Chi, Hongbo (2009): Regulation of JNK and p38 MAPK in the immune system: signal integration, propagation and termination. In: Cytokine 48 (3), S. 161–169.

[52] Dal Porto, Joseph M.; Gauld, Stephen B.; Merrell, Kevin T.; Mills, David; Pugh-Bernard, Aimee E.; Cambier, John (2004): B cell antigen receptor signalling 101. In: Molecular immunology 41 (6-7), S. 599–613.

[53] Gauld, Stephen B.; Dal Porto, Joseph M.; Cambier, John C. (2002): B cell antigen receptor signalling: roles in cell development and disease. In: Science (New York, N.Y.) 296 (5573), S. 1641–1642.

[54] Laurie O.Beitz; David A. Fruman; Tomohiro Kurosaki; Lewis C. Cantley; Andrew M. Scharenberg (1999): SYK Is Upstream of Phosphoinositide 3-Kinase in B Cell Receptor Signalling. In: Journal of Biological Chemistry 274 No. 46, S. 32662-32666.

[55] Buhl, A. M.; Cambier, J. C. (1999): Phosphorylation of CD19 Y484 and Y515, and linked activation of phosphatidylinositol 3-kinase, are required for B cell antigen receptor-mediated activation of Bruton's tyrosine kinase. In: Journal of immunology (Baltimore, Md: 1950) 162 (8), S. 4438–4446.

[56] Aagaard-Tillery, K. M.; Jelinek, D. F. (1996): Phosphatidylinositol 3-kinase activation in normal human B lymphocytes. In: Journal of immunology (Baltimore, Md: 1950) 156 (12), S. 4543–4554.

[57] Buhl, A. M.; Pleiman, C. M.; Rickert, R. C.; Cambier, J. C. (1997): Qualitative regulation of B cell antigen receptor signalling by CD19: selective requirement for PI3-kinase activation, inositol-1,4,5-trisphosphate production and Ca2+ mobilization. In: The Journal of experimental medicine 186 (11), S. 1897–1910.

[58] Wang, Yue; Brooks, Stephen R.; Li, Xiaoli; Anzelon, Amy N.; Rickert, Robert C.; Carter, Robert H. (2002): The physiologic role of CD19 cytoplasmic tyrosines. In: Immunity 17 (4), S. 501–514.

[59] Young, Ryan M.; Shaffer, Arthur L.; Phelan, James D.; Staudt, Louis M. (2015): B-cell receptor signalling in diffuse large B-cell lymphoma. In: Seminars in hematology 52 (2), S. 77–85.

[60] Herishanu, Yair; Pérez-Galán, Patricia; Liu, Delong; Biancotto, Angélique; Pittaluga, Stefania; Vire, Berengere et al. (2011): The lymph node microenvironment promotes B-cell receptor signalling, NF-kappaB activation, and tumor proliferation in chronic lymphocytic leukemia. In: Blood 117 (2), S. 563–574.

[61] Davids, Matthew S.; Brown, Jennifer R. (2014): Ibrutinib: a first in class covalent inhibitor of Bruton's tyrosine kinase. In: Future oncology (London, England) 10 (6), S. 957–967

[62] Pal Singh, Simar; Dammeijer, Floris; Hendriks, Rudi W. (2018): Role of Bruton's tyrosine kinase in B cells and malignancies. In: Molecular cancer 17 (1), S. 57.

[63] Wilson, Wyndham H.; Young, Ryan M.; Schmitz, Roland; Yang, Yandan; Pittaluga, Stefania; Wright, George et al. (2015): Targeting B cell receptor signalling with ibrutinib in diffuse large B cell lymphoma. In: Nature medicine 21 (8), S. 922–926.

[64] Jain, Nitin; O'Brien, Susan (2013): Ibrutinib (PCI-32765) in chronic lymphocytic leukemia. In: Hematology/oncology clinics of North America 27 (4), 851-60.

[65] Parmar, Sapna; Patel, Khilna; Pinilla-Ibarz, Javier (2014): Ibrutinib (imbruvica): a novel targeted therapy for chronic lymphocytic leukemia. In: P & T: a peer-reviewed journal for formulary management 39 (7), S. 483–519.

[66] Maffei, Rossana; Fiorcari, Stefania; Martinelli, Silvia; Potenza, Leonardo; Luppi, Mario; Marasca, Roberto (2015): Targeting neoplastic B cells and harnessing microenvironment: the "double face" of ibrutinib and idelalisib. In: Journal of hematology & oncology 8, S. 60.

[67] Winter, Allison M.; Landsburg, Daniel J.; Mato, Anthony R.; Isaac, Krista; Hernandez-Ilizaliturri, Francisco J.; Reddy, Nishitha et al. (2017): A multi-institutional outcomes analysis of patients with relapsed or refractory DLBCL treated with ibrutinib. In: Blood.

[68] Sivina, Mariela; Kreitman, Robert J.; Arons, Evgeny; Ravandi, Farhad; Burger, Jan A. (2014): The bruton tyrosine kinase inhibitor ibrutinib (PCI-32765) blocks hairy cell leukaemia survival, proliferation and B cell receptor signalling: a new therapeutic approach. In: British journal of haematology 166 (2), S. 177–188.

[69] Caccialanza, Riccardo; Cereda, Emanuele; Lorenzo, Francesco de; Farina, Gabriella; Pedrazzoli, Paolo (2018): To fast, or not to fast before chemotherapy, that is the question. In: BMC cancer 18 (1), S. 337.

[70] Nencioni, Alessio; Caffa, Irene; Cortellino, Salvatore; Longo, Valter D. (2018): Fasting and cancer: molecular mechanisms and clinical application. In: Nature reviews. Cancer 18 (11), S. 707–719.

[71] Hanahan, Douglas; Weinberg, Robert A. (2011): Hallmarks of cancer: the next generation. In: Cell 144 (5), S. 646–674.

[72] Longo, Valter D.; Mattson, Mark P. (2014): Fasting: Molecular Mechanisms and Clinical Applications. In: Cell metabolism 19 (2), S. 181–192.

[73] Brandhorst, Sebastian; Longo, Valter D. (2016): Fasting and Caloric Restriction in Cancer Prevention and Treatment. In: Recent results in cancer research. Fortschritte der Krebsforschung. Progres dans les recherches sur le cancer 207, S. 241–266.

[74] Cheng, Chia-Wei; Adams, Gregor B.; Perin, Laura; Wei, Min; Zhou, Xiaoying; Lam, Ben S. et al. (2014): Prolonged fasting reduces IGF-1/PKA to promote hematopoietic-stem-cell-based regeneration and reverse immunosuppression. In: Cell stem cell 14 (6), S. 810–823.

[75] Safdie, Fernando M.; Dorff, Tanya; Quinn, David; Fontana, Luigi; Wei, Min; Lee, Changhan et al. (2009): Fasting and cancer treatment in humans: A case series report. In: Aging 1 (12), S. 988–1007.

[76] Shi, Yandong; Felley-Bosco, Emanuela; Marti, Thomas M.; Orlowski, Katrin; Pruschy, Martin; Stahel, Rolf A. (2012): Starvation-induced activation of ATM/Chk2/p53 signalling sensitizes cancer cells to cisplatin. In: BMC cancer 12, S. 571.

[77] Laviano, Alessandro; Rossi Fanelli, Filippo (2012): Toxicity in chemotherapy--when less is more. In: The New England journal of medicine 366 (24), S. 2319–2320.

[78] Lee, Changhan; Raffaghello, Lizzia; Brandhorst, Sebastian; Safdie, Fernando M.; Bianchi, Giovanna; Martin-Montalvo, Alejandro et al. (2012): Fasting cycles retard growth of tumors and sensitize a range of cancer cell types to chemotherapy. In: Science translational medicine 4 (124).

[79] Di Biase, S.; Longo, V. D. (2016): Fasting-induced differential stress sensitization in cancer treatment. In: Molecular & cellular oncology 3 (3).

[80] Caffa, Irene; D'Agostino, Vito; Damonte, Patrizia; Soncini, Debora; Cea, Michele; Monacelli, Fiammetta et al. (2015): Fasting potentiates the anticancer activity of tyrosine kinase inhibitors by strengthening MAPK signalling inhibition. In: Oncotarget 6 (14), S. 11820–11832.

[81] Wilson, Wyndham H.; Young, Ryan M.; Schmitz, Roland; Yang, Yandan; Pittaluga, Stefania; Wright, George et al. (2015): Targeting B cell receptor signaling with ibrutinib in diffuse large B cell lymphoma. In: Nature medicine 21 (8), S. 922–926.

[82] Chu, Yaya; Lee, Sanghoon; Shah, Tishi; Yin, Changhong; Barth, Matthew; Miles, Rodney R. et al. (2019): Ibrutinib significantly inhibited Bruton's tyrosine kinase (BTK) phosphorylation,in-vitro proliferation and enhanced overall survival in a preclinical Burkitt lymphoma (BL) model. In: Oncoimmunology 8 (1), e1512455.

[83] Dubovsky JA, Beckwith KA, Natarajan G, et al. (2015): Ibrutinib is an irreversible molecular inhibitor of ITK driving a Th1-selective pressure in T lymphocytes. Blood.; 122(15):2539-2549.

[84] Mihaylova MM, Shaw RJ. (2011): The AMPK signalling pathway coordinates cell growth, autophagy and metabolism. Nat Cell Biol.;13(9):1016–1023.

[85] Lee, Donghoon; Goldberg, Alfred L. (2015): Muscle Wasting in Fasting Requires Activation of NF-κB and Inhibition of AKT/Mechanistic Target of Rapamycin (mTOR) by the Protein Acetylase, GCN5. In: The Journal of biological chemistry 290 (51), S. 30269–30279.

[86] Schulze-Luehrmann, Jan; Ghosh, Sankar (2006): Antigen-receptor signaling to nuclear factor kappa B. In: Immunity 25 (5), S. 701–715.

[87] Westin, Jason R. (2014): Status of PI3K/Akt/mTOR pathway inhibitors in lymphoma. In: Clinical lymphoma, myeloma & leukemia 14 (5), S. 335–342.

[88] Aubrey, Brandon J.; Kelly, Gemma L.; Janic, Ana; Herold, Marco J.; Strasser, Andreas (2018): How does p53 induce apoptosis and how does this relate to p53-mediated tumour suppression? In: Cell death and differentiation 25 (1), S. 104–113.

[89] Prokesch, Andreas; Graef, Franziska A.; Madl, Tobias; Kahlhofer, Jennifer; Heidenreich, Steffi; Schumann, Anne et al. (2017): Liver p53 is stabilized upon starvation and required for amino acid catabolism and gluconeogenesis. In: FASEB journal: official publication of the Federation of American Societies for Experimental Biology 31 (2), S. 732–742.

Attachment

Additional data to chapter “4.2. Ibrutinib-treatment under protein fasting conditions”

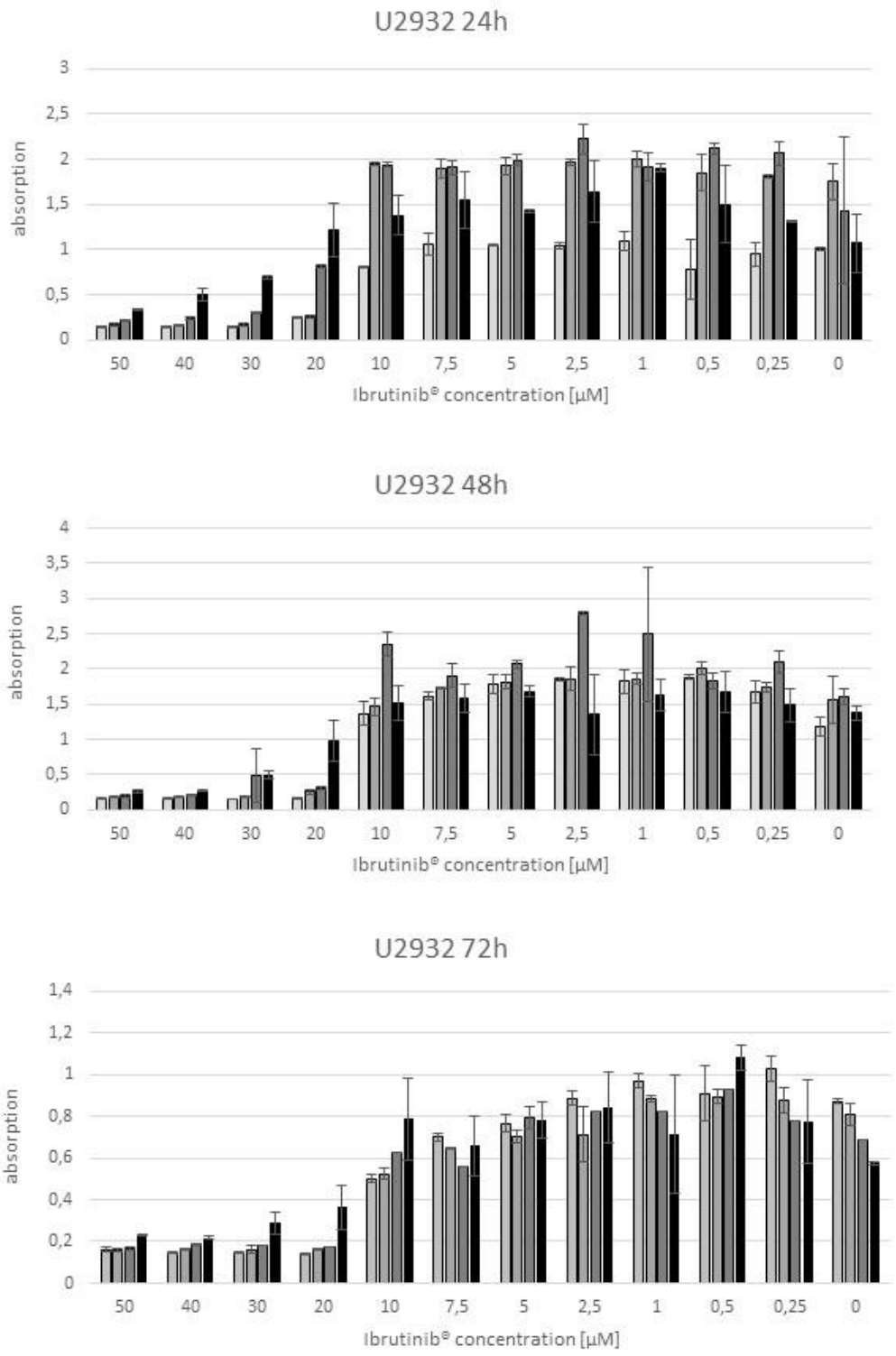

Cell growth of ABC-DLBCL cell line U2932 under Ibrutinib and protein fasting conditions.
Cell growth of U2932 (as ABC-DLBCL model) cell line under different FBS fasting conditions (1; 2.5; 5; 10% FBS) and Ibrutinib treatment (0; 0.25; 0.5; 1; 2.5; 5; 7.5; 10; 20; 30; 40; 50 µM) as determined by the EZ4U proliferation assay and depicted as absorption at 492nm after 24, 48 and 72 hours. Each bar represents the mean ± standard of the mean.

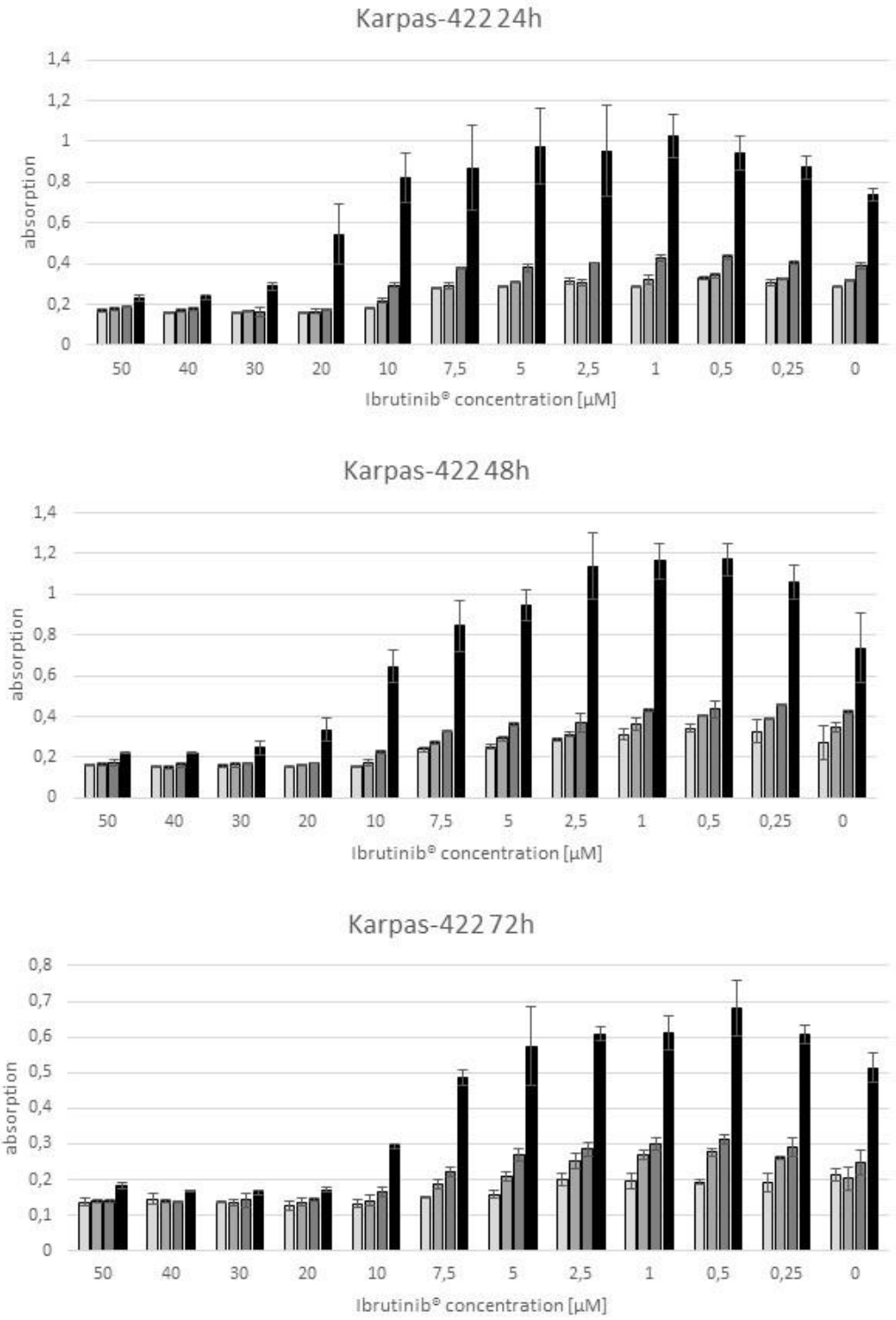

Cell growth of GCB-DLBCL cell line Karpas-422 under Ibrutinib and protein fasting conditions.
Cell growth of Karpas-44 (as GCB-DLBCL model) cell line under different FBS fasting conditions (1; 2.5; 5; 10% FBS) and Ibrutinib treatment (0; 0.25; 0.5; 1; 2.5; 5; 7.5; 10; 20; 30; 40; 50 µM) as determined by the EZ4U proliferation assay and depicted as absorption at 492nm after 24, 48 and 72 hours. Each bar represents the mean ± standard of the mean.

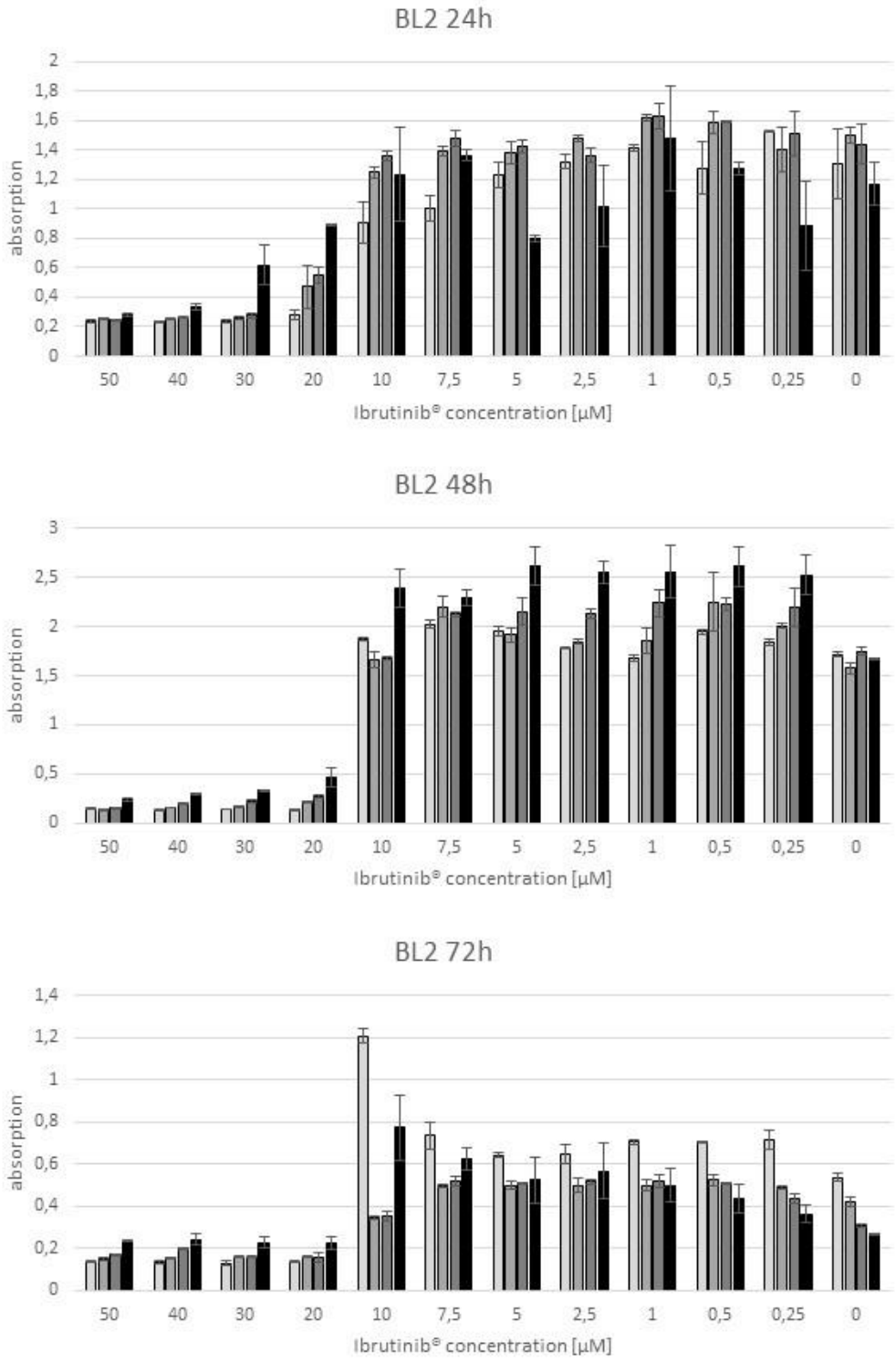

Cell growth of Burkitt lymphoma cell line BL-2 under Ibrutinib and protein fasting conditions.
Cell growth of BL-2 (as Burkitt lymphoma model) cell line under different FBS fasting conditions (1; 2.5; 5; 10% FBS) and Ibrutinib treatment (0; 0.25; 0.5; 1; 2.5; 5; 7.5; 10; 20; 30; 40; 50 µM) as determined by the EZ4U proliferation assay and depicted as absorption at 492nm after 24, 48 and 72 hours. Each bar represents the mean ± standard of the mean.